

Inflaton Decay and Heavy Particle Production with Negative Coupling

Brian R. Greene*

Departments of Physics and Mathematics, Columbia University, New York, NY 10027

Tomislav Prokopec[†] and Thomas G. Roos[‡]

F. R. Newman Laboratory of Nuclear Studies, Cornell University, Ithaca, NY 14853

(May 19, 1997)

Abstract

We study the decay of the inflaton in a general $\mathcal{Z}_2 \times \mathcal{Z}_2$ symmetric two scalar theory. Since the dynamics of the system is dominated by states with large occupation numbers which admit a semiclassical description, the decay can be studied by solving the classical equations of motion on the lattice. Of particular interest is the case when the cross-coupling between the inflaton and the second scalar field is negative, which is naturally allowed in many realistic models. While the inflaton decays *via* parametric resonance in the positive coupling case we find that for negative coupling there is a new mechanism of particle production which we call *negative coupling instability*. Due to this new mechanism the variances of the fields grow significantly larger before the production is shut off by the backreaction of the created particles, which could have important consequences for symmetry restoration by non-thermal phase transitions. We also find that heavy particles are produced much more efficiently with negative coupling, which is of prime importance for GUT baryogenesis. Using a simple toy model for baryogenesis and the results of our lattice simulations we show that for natural values of the cross-coupling enough 10^{14} GeV bosons are created to produce a baryon to entropy ratio consistent with observation. This is to be contrasted with the situation for positive coupling, where the value of the cross-coupling required to produce such massive particles is unnaturally large. In addition to our numerical

*On leave from: F. R. Newman Laboratory of Nuclear Studies, Cornell University, Ithaca, NY 14853. E-mail: greene@math.columbia.edu

[†]E-mail: tomislav@mail.lns.cornell.edu

[‡]E-mail: roost@mail.lns.cornell.edu

results we obtain analytical estimates for the maximum variances of the fields in an expanding universe for all cases of interest: massive and massless inflaton, positive and negative cross-coupling, with and without significant self interactions for the second field.

I. INTRODUCTION

It has recently been realized [1,2] that an oscillating scalar field can transfer its energy efficiently to other bosonic degrees of freedom [3] via a process analogous to the classical phenomenon of parametric resonance. The most important application of this mechanism is to reheating after inflation. When the inflationary stage terminates the universe is essentially devoid of matter and the inflaton field oscillates with large amplitude about the minimum of its potential. Its coupling to other bosonic fields can then lead to explosive particle production via the non-perturbative resonance mechanism. This is sometimes called *preheating* in the literature because the produced particles are far from thermal equilibrium. The simplest model for studying this phenomenon is a theory with two real scalar fields and effective potential

$$V(\phi, \chi) = \frac{1}{2}m_\phi^2\phi^2 + \frac{1}{2}m_\chi^2\chi^2 + \frac{\lambda_\phi}{4}\phi^4 + \frac{\lambda_\chi}{4}\chi^4 + \frac{g}{2}\phi^2\chi^2. \quad (1)$$

Such models exhibit chaotic inflation when one of the fields, called the *inflaton*, acquires a large expectation value (compared to the Planck mass) [4]. The energy density of the universe then becomes dominated by the potential energy of the inflaton and the universe starts inflating. This continues until the amplitude of the inflaton expectation value becomes of order the Planck mass. At this point the inflationary stage terminates and the inflaton starts oscillating.

An intuitive picture of the parametric resonance mechanism emerges by assuming that the inflation field ϕ oscillates sinusoidally about its minimum [5]. With $\phi(\vec{x}, t) \rightarrow \Phi_0 \cos(\omega_\phi^0 t)$ and neglecting the λ_χ term, the mode equations for the χ field can be written as the Mathieu equation

$$\frac{d^2\chi_k}{dz^2} + [A_0(k) - 2q_0 \cos(2z)]\chi_k = 0, \quad (2)$$

$$A_0(k) = \frac{\omega_\chi(k)^2}{(\omega_\phi^0)^2} + 2q_0, \quad q_0 = \frac{g\Phi_0^2}{4(\omega_\phi^0)^2} \quad (3)$$

where $z = \omega_\phi^0 t$ and $\omega_\chi(k)^2 = k^2 + m_\chi^2$ is the frequency squared of χ_k . It is well known that the Mathieu equation possesses unstable solutions for which the modes grow as $\chi_k \propto \exp[\mu_k \omega_\phi^0 t]$. This corresponds to exponentially growing occupation numbers $n_\chi(k) \propto \exp[2\mu_k \omega_\phi^0 t]$ and is interpreted as particle production. The most important features of the solutions to Eq. (2) are readily understood from the stability chart depicted in figures 1(a) and (b). The $\mu = 0$ curves divide the chart into stable (dark) and unstable (light) regions. Some curves of constant positive μ are also shown. For clarity figure 1(a) contains only a limited range of A_0 and q_0 , although the physically interesting values are $|q_0| \gg 1$ [2,12]. The $q_0 \gg 1$ regime is called “broad resonance” in the literature. Figure 1(b) shows a piece of the instability chart for large $|q_0|$ around the line $A_0 = 2q_0$. Notice that, if one makes the usual assumption $g > 0$, then for $m_\chi^2 \geq 0$ the allowed A_0 lie above the line $A_0 = 2q_0$ (*cf.* Eq. (3)). As a consequence the regions of large μ are excluded, and the maximum value μ reaches is $\lesssim 1$, attained for $A_0 \approx 2q_0$ and $q_0 \gtrsim 1$. Above $A_0 = 2q_0$, μ is a rapidly decreasing function of A_0 . Since the separation between neighboring instability bands for large q_0 is of order $q_0^{1/2}$, this implies that the dominant production of χ particles occurs for $k \sim k_{\text{res}} \simeq q_0^{1/4} \omega_\phi^0$. It

is important to note that the inflaton also decays into its own fluctuations *via* parametric resonance [2]. However, the value of μ corresponding to this decay channel is typically a few times smaller than the value of μ for decay into χ fluctuations as long as q_0 is large. Hence, unless the decay into χ particles is somehow shut off, the decay into ϕ particles is subdominant.

While the above picture is simple and intuitive, in reality the situation is much more complex. First of all, the equations of motion (EOM), and hence the dynamics, are strongly modified in an expanding universe. In particular, the amplitude of the inflaton oscillations decreases even in the absence of particle production. Secondly, as the inflaton decays, the backreaction of created particles alters the parameters in the Mathieu equation. The amplitude decreases as energy is drained away and the masses get contributions of the form $\delta m_\phi^2 = g\langle(\delta\chi)^2\rangle + 3\lambda_\phi\langle(\delta\phi)^2\rangle$, $\delta m_\chi^2 = g\langle(\delta\phi)^2\rangle + 3\lambda_\chi\langle(\delta\chi)^2\rangle$, with $\langle(\delta\phi)^2\rangle = \langle\phi^2\rangle - \langle\phi\rangle^2$ and $\langle(\delta\chi)^2\rangle = \langle\chi^2\rangle - \langle\chi\rangle^2$ denoting the variances of the fields. One can still gain insight into the decay by replacing the initial values A_0 and q_0 in Eq. (2) by time dependent parameters

$$A(k) = \frac{k^2 + m_{\chi\text{ eff}}^2}{\omega_{\phi\text{ eff}}^2} + 2q, \quad q = \frac{g\Phi^2}{4\omega_{\phi\text{ eff}}^2} \quad (4)$$

where

$$\begin{aligned} m_{\chi\text{ eff}}^2 &= m_\chi^2 + g\langle(\delta\phi)^2\rangle + 3\lambda_\chi\langle(\delta\chi)^2\rangle, \\ \omega_{\phi\text{ eff}}^2 &= \omega_\phi^2 + g\langle(\delta\chi)^2\rangle + 3\lambda_\phi\langle(\delta\phi)^2\rangle. \end{aligned} \quad (5)$$

Here Φ is the slowly varying amplitude of the oscillating inflaton expectation value $\phi_0(t) \equiv \langle\phi(\vec{x}, t)\rangle$, and ω_ϕ is the frequency of $\phi_0(t)$ in the absence of backreaction. We distinguish ω_ϕ from its initial value ω_ϕ^0 because due to the ϕ^4 term in Eq. (1) the frequency is time dependent even without decay in an expanding universe. The reason it is useful to think about the decay in terms of the parameters defined in Eq. (5) is that the basic features of the resonance mechanism are extremely robust. The amplification of the modes depends only on the fact that one is dealing with oscillators with a time dependent frequency, and in what follows we will only make use of the most prominent features of the stability chart when obtaining analytical estimates. For large q these are independent of the details of the potential and the exact time dependence of the parameters. The description in terms of an equation of the form of Eq. (2) finally breaks down completely when the resonant mode amplitudes grow large. For then the nonlinear terms in the EOM become important and scatterings become fast. The result is a slowly evolving “scattering regime” characterized by smooth power spectra [11–13]. The resonant decay of the inflaton has been treated in various approximations by many authors [1,2,6–10]. The full nonlinear problem has been studied in detail using lattice simulations. The idea is that one can evolve the system using the classical equations of motion because the dynamics is dominated by states with large occupation numbers which admit a semiclassical description. This approach was pioneered in [11], where it was applied to the decay of a massless field into its own fluctuations. The decay into a second massless field with and without self-coupling was treated in [12], and the decay of a massive inflaton was discussed in [13].

Our main interest in this paper is to investigate what happens when the coupling g in Eq. (1) is negative, which has not been previously studied. The point is that parameters

like g that couple two or more scalar fields appear in almost all extensions of the standard model, and that there is generally no reason whatsoever that these parameters should be positive. Of course the effective potential should be bounded from below in order to ensure the existence of a sensible vacuum. For the potential given in Eq. (1) this requires

$$r \equiv \frac{\lambda_\phi \lambda_\chi}{g^2} > 1. \quad (6)$$

We will assume that this stability bound is satisfied.

Naively, as one can see from figure 1(a), the negative g case is dramatically different from the positive g case. The resonant momenta are now limited to the region above the line $A_0 = -2|q_0|$, instead of above the line $A_0 = 2|q_0|$. When $2|q_0| \geq |A_0| \gg 1$ [14]

$$\begin{aligned} \cosh 2\pi\mu &= \cosh \Im \left[\int_0^{2\pi} dz (A_0 - 2q_0 \cos(2z))^{\frac{1}{2}} \right] \\ &\times \cos \Re \left[\int_0^{2\pi} dz (A_0 - 2q_0 \cos(2z))^{\frac{1}{2}} \right]. \end{aligned} \quad (7)$$

Along $A_0 = -2|q_0|$ this evaluates to $\mu = (4/\pi)|q_0|^{1/2}$ (see also [15]). For large $|q_0|$ this is easily orders of magnitude larger than the corresponding positive g value, which is always $\lesssim 1$. Since the decay time is proportional to μ^{-1} one might hence expect that particle production and consequently inflaton decay is much faster for negative g .

This conclusion, however, is premature since we have implicitly assumed that initially the expectation value $\chi_0 \equiv \langle \chi(\vec{x}, t) \rangle = 0$. To see whether this is the case one has to examine the EOM for the fields during inflation. Note that the large expectation value $\phi_0(t)$ of the inflaton induces a ϕ_0 -dependent minimum in the potential for the second field:

$$\tilde{\chi}_0^2 = \begin{cases} \frac{-m_\chi^2 - g\phi_0^2}{\lambda_\chi} & \text{for } m_\chi^2 + g\phi_0^2 < 0 \\ 0 & \text{otherwise} \end{cases} \quad (8)$$

It is not hard to see analytically that if $\chi_0 \approx \tilde{\chi}_0$ initially, then it remains so during inflation, as long as $|g|/\lambda_\phi \gg 1/2$ and m_χ is not too large [17]. Our numerical simulations show that even if χ_0 is not close to $\tilde{\chi}_0$ initially, it will become so by the end of inflation, provided the above conditions are satisfied. Since the physically important broad resonance case with $\lambda_\phi \ll |g|$ is our main concern, this means that the correct initial condition for the oscillatory regime is given by Eq. (8).

To illustrate the effect of $\chi_0 \neq 0$, consider the linearized mode equation for $\delta\chi_k$, the Fourier transform of $\chi - \chi_0$. Neglecting the expansion of the Universe we obtain

$$\frac{d^2\delta\chi_k}{d^2t} + \left(k^2 + m_\chi^2 + 3\lambda_\chi\chi_0^2 + g\phi_0^2 \right) \delta\chi_k + 2g\phi_0\chi_0\delta\phi_k = 0 \quad (9)$$

where ϕ_0 is the oscillating expectation value of the inflaton field. Note that if $\chi_0 \approx \tilde{\chi}_0$ even during the oscillatory regime, then the term in parentheses of (9) is positive (*cf.* (8)). This would mean that the evolution of $\delta\chi_k$ resembles that of a positive g case. Neglecting the last term for the moment, we see that in the simple case when $m_\chi = 0$ and $\chi_0 = \tilde{\chi}_0$, Eq. (9) reduces to Eq. (2) with $A_0 = (k^2/(\omega_\phi^0)^2) + 2q_0$ and $q_0 = 2|g|\Phi_0^2/(2\omega_\phi^0)^2$. In the case $m_\chi \neq 0$ there is no such simple correspondence, but the effective q is still positive. Note

that the effect of the last term in Eq. (9) is that it produces resonant growth of $\delta\chi_k$ when the amplitude of $\delta\phi_k$ is large and $\chi_0 \neq 0$. Since most of the time $\delta\chi_k \gg \delta\phi_k$ for the resonant modes, the effect of this term will be small. The analogous term in the mode equation for $\delta\phi_k$ speeds up its growth when $\delta\chi_k$ is large.

We have just seen that if χ_0 follows its instantaneous equilibrium value $\tilde{\chi}_0$ the fact that g is negative should not make much difference. The situation changes drastically if χ_0 is not “enslaved” by ϕ_0 in this way: there is then a portion of the period for which the term in parentheses of (9) is negative. During this time the $\delta\chi_k$ are unstable and are expected to grow exponentially with large μ , just as in the naive negative g picture discussed initially (*cf.* also [15]). The physics hence depends crucially on the detailed dynamics of the field expectation values. This dynamics is very complicated due to the interactions with the nonzero modes, especially once their amplitudes become large due to the resonance. To fully investigate the negative g case one must hence resort to lattice simulations, and this is the subject we turn to next.

In section II we will discuss massless fields, followed by a detailed study of massive fields in section III. The relevance of our results for grand unified theory (GUT) baryogenesis are discussed in section IV. Finally, our conclusions are presented in section V.

Before diving into the analysis we should point out that most of our numerical calculations and analytical estimates will be concerned with obtaining the maximum variances attained by the fields during preheating. There are two reasons for focusing on these quantities: first, the maximum variances determine the symmetry restoration “power” relevant to the occurrence of so-called nonthermal phase transitions [18,19]. Second, for very massive particles such as the bosons needed for GUT baryogenesis the variance is directly proportional to the energy and particle number densities. This will be discussed in more detail in sections III and V.

II. MASSLESS FIELDS

A. Numerical Results

We begin our investigation by studying massless fields, which is convenient for two reasons. First, the positive g massless case has been studied extensively on the lattice in [12], allowing for a detailed comparison of the positive and negative g cases. Second, massless fields ($m_\chi = m_\phi = 0$) are the simplest to treat numerically because in this case the EOM in a Friedman-Robertson-Walker (FRW) universe are conformally equivalent to those in Minkowski space. By this we mean the following: in terms of the variables $\tau = \int dt/a(t)$, $\bar{\phi} = \phi a(\tau)/a(0)$, and $\bar{\chi} = \chi a(\tau)/a(0)$, where $a(\tau)$ is the scale factor, the expanding universe EOM reduce to those of two interacting scalar fields in static space-time [11,12]. This is true provided the energy density behaves as radiation dominated, which is indeed the case for a massless inflaton in the oscillatory regime [6]. Since it is less time consuming to do simulations in Minkowski space our numerics for the massless fields were done in terms of the barred variables defined above, and our lattice time was τ . The conversion of lattice quantities to physical quantities will be discussed in detail below.

The computational techniques involved are described in detail in [12]. In short we evolve the classical EOM on a three dimensional lattice starting from certain random initial con-

dition for the inhomogeneous modes [16]. The initial conditions for the zero modes (field expectation values) are given by the values at the breakdown of the slow roll inflationary stage: $\Phi_0 = \Phi(t=0) \sim M_{\text{P}}$, where $M_{\text{P}} \equiv (8\pi G)^{-1/2} \simeq 2.4 \times 10^{18} \text{GeV}$ is the reduced Planck mass, and $\chi_0 = \tilde{\chi}_0$ as in Eq. (8). The results presented in this section were obtained on 128^3 lattices.

We begin by comparing the dynamics of two theories with opposite signs of g but otherwise identical parameters. The chosen values are $\lambda_\phi = 10^{-12}$, $\lambda_\chi = 10^{-7}$, and $|g| = 10^{-10}$. For a massless inflaton the zero mode ϕ_0 oscillates with frequency $\omega_\phi = c\lambda_\phi^{1/2}\Phi$, where $c \approx 0.85$. Hence these couplings correspond to $q_0 \simeq 35$ and $r = 10$ (*cf.* Eqs. (4), (6)). The evolution of the expectation values ϕ_0 and χ_0 for the negative and positive g cases are shown in figures 2 and 3, respectively. The corresponding variances are shown in figures 4 and 5. Since the energy density in the inflaton zeromode is proportional to Φ^4 we see from figure 2 that in the negative g case 40% of the initial energy is in fluctuations by the time $\tau \approx 3 \times 10^8 \Phi_0^{-1}$. Notice also that χ_0 follows ϕ_0 faithfully (*i.e.* $\chi_0 \approx \tilde{\chi}_0$) until $\tau \approx 8 \times 10^7 \Phi_0^{-1}$. After this the two expectation values are no longer in phase, even though the dynamics of χ_0 is clearly still strongly influenced by ϕ_0 . Figure 3 shows that it takes until $\tau \approx 4.5 \times 10^8 \Phi_0^{-1}$ for 40% of the energy to decay in the positive g case, and in contrast to the situation for $g < 0$ here almost all of the decayed energy goes into ϕ fluctuations. After $\tau \approx 4.5 \times 10^8 \Phi_0^{-1}$ the decay rate becomes very small, a fact that is also reflected in the variances (figure 5), which are both changing very slowly beyond this point. Similarly we see in figure 4 that for negative g the variances level off at $\tau \sim 9 \times 10^7 \Phi_0^{-1}$, although the ϕ variance is still growing slowly until $\tau \sim 2.2 \times 10^8 \Phi_0^{-1}$. We will explain all of these features, and give estimates for the magnitudes of the relevant quantities, in section II B.

Before doing so let us briefly discuss the conversion of lattice quantities to physical quantities. As discussed at the beginning of this section, the lattice fields are rescaled by a factor $a(\tau)$, where τ is the conformal time (for convenience we define $t = \tau = 0$ to correspond to the beginning of our simulation (*i.e.* the end of slow roll inflation) and choose $a(0) = 1$). This means that one must simply divide lattice quantities such as energy densities and variances by the appropriate powers of $a(\tau)$ to get the physical values. For example, $\langle \delta\chi^2 \rangle = \langle \delta\tilde{\chi}^2 \rangle / a(\tau)^2$. In the oscillatory regime of a massless inflaton the scale factor behaves as in a radiation dominated universe, so we can write $a(\tau) = (1 + H_0\tau)$ where $H_0 = (\rho(0)/3)^{1/2} M_{\text{P}}^{-1}$ is the Hubble constant at the end of inflation. It is easy to show that at the end of slow roll $\Phi_0 \approx 1.8M_{\text{P}}$ and the kinetic energy density is about half the potential energy density [20]. Using the fact that $\rho_{\text{PE}} = \lambda_\phi \Phi_0^4 / 4$ for $g > 0$ and $\rho_{\text{PE}} = (1 - 1/r)\lambda_\phi \Phi_0^4 / 4$ for $g < 0$ we thus obtain $H_0 \approx \sqrt{\lambda_\phi} M_{\text{P}}$ for $g > 0$ and $H_0 \approx (\lambda_\phi(1 - 1/r))^{1/2} M_{\text{P}}$ for $g < 0$.

With these estimates, and recalling that our lattice time is τ , it is simple to convert from lattice to physical quantities. This was done in obtaining figure 6(b) from figure 6(a): figure 6(a) shows the maximum lattice variances for negative g as a function of q_0 for two values of r . The corresponding physical variances are shown in figure 6(b). Since the variances are fluctuating significantly (see, for example, figure 4), both peak and valley values are given. These curves, too, will be explained in section II B. Here we simply note that when the lattice variances behave as shown in figures 4 and 5 it is easy to obtain the maximum physical variances: since we must divide by $a(\tau)^2$ to obtain the latter from the former, the maximum occurs at the time when the slowly varying state sets in. After that the slow increase cannot keep up with the decrease due to the expansion.

B. Discussion and Analytical Estimates

The most striking feature of figures 2–5 is the fact that after an initial period of rapid exponential decay the system reaches a slowly evolving state during which the rate of energy transfer from the inflaton zeromode to the fluctuations is quite small. This effect has been studied in detail in [12], where it is shown that for large q_0 or r backreaction and scattering limits the maximum amplitudes of the variances and essentially shuts down the resonance. Throughout this paper we will refer to the slowly evolving state as the *scattering regime* [21]. The variances of the physical fields at the time the scattering regime begins are of central interest since they are the maximum variances of the fields reached during preheating. The reason that the decay of the inflaton shuts off for large q_0 or r while most of the energy is still in the oscillating zeromode is the backreaction of the created particles on the EOM. In particular the effective masses of the fields get contributions of the form $\delta m_\phi^2 = g\langle(\delta\chi)^2\rangle + 3\lambda_\phi\langle(\delta\phi)^2\rangle$, $\delta m_\chi^2 = g\langle(\delta\phi)^2\rangle + 3\lambda_\chi\langle(\delta\chi)^2\rangle$. As was explained in the introduction, the instability index μ_k is a rapidly decreasing function of A above the line $A = 2|q|$ [22] (see also figure 1). In fact the decay due to the second band above this line is already very slow. Now the backreaction terms add a contribution $\delta A = \delta m_\chi^2/\omega_\phi^2$ to A , and for large q the distance between the first two bands above $A = 2|q|$ is about $|q|^{1/2}$ (cf. figure 1(b)). Hence when the shift in A becomes so large that

$$A(k=0) + \delta A \geq 2|q| + |q|^{\frac{1}{2}} \quad (10)$$

the first band above $A = 2|q|$ is rendered ineffective and the decay slows down dramatically [23]. From this condition one can obtain estimates of the variances at the beginning of the slowly varying scattering regime. As explained in [12], the (lattice) variances are then kept roughly constant at these maximum values by a feedback mechanism. It is important to point out that scattering plays a crucial part in the shut off mechanism. For example, we will see below that when λ_χ is small the resonance is shut off by the $g\langle(\delta\phi)^2\rangle$ term. This term grows large due to scattering of resonant χ particles off the ϕ zeromode, an effect that is completely lost in the Hartree type approximations often used to study preheating. The fact that the ϕ variance is responsible for shutting off the resonance for small λ_χ was first realized in [12].

Before deriving estimates for the variances based on Eq. (10) we wish to point out that there is always a substantial “intrinsic” uncertainty associated with such estimates. By this we mean that physical quantities such as maximum variances, energies, *et cetera*, are extremely sensitive functions of the parameters in the model. For example, we have seen above that for large q a shift of order $|q|^{1/2}$ is enough to move the initial position of the first resonant momentum above $A = 2|q|$ from $k^2 \approx 0$ to $k^2 \approx |q|^{1/2}\omega_\phi^2$. Since μ_k is a rapidly decreasing function of k [22] such a shift can have a substantial effect on the early evolution of the system. The upshot is that for a small change $\delta g/g = \delta q/q \sim |q|^{-1/2} \ll 1$, the time at which the scattering regime sets in changes by a factor of a few. As a consequence the maximum physical variances reached vary by about an order of magnitude. In this context we point out that the maximum lattice variances reached are much less sensitive to small changes in the parameters. The reason is simply that the lattice variances do not decrease due to the expansion, so the time it takes to reach the scattering regime is immaterial. This observation explains why the curves in figure 6(a) are relatively smooth compared to those

in figure 6(b). The sensitivity to small changes in parameter values has also been observed in [7].

We will now estimate the maximum variances in the massless case based on Eq. (10). Positive and negative coupling – **Cases I** and **II** – will be treated separately. As explained above, the maximum physical variances are reached at the beginning of the slowly evolving scattering regime. Since the variances fluctuate we distinguish between peak values and valley values. Estimates obtained from Eq. (10) correspond to peak values since Eq. (10) is the condition for shutting off the resonance. This condition must be met during those parts of the period of the inflaton zero mode when the resonance is active, but in between the variances can drop to smaller (valley) values. The formulae below will be given in terms of the quantity Φ_s , which is the amplitude of oscillations at the time the maximum variances are reached [24]. We will discuss how to estimate Φ_s after deriving the expressions for the variances. Note that Eq. (10) involves the time dependent parameter q rather than the initial value q_0 . Recalling from section II A that in the massless case $\omega_\phi = c\lambda_\phi^{1/2}\Phi$, with $c \approx 0.85$, a glance at Eqs. (4) and (5) reveals that both the numerator and the denominator of q scale as $a(t)^{-2}$. Hence, while q may change significantly due to the decay of the inflaton, it does *not* change due to the expansion in the massless case.

Case I. For $g > 0$, Eq. (10) reduces to

$$\delta A \equiv \frac{m_{\chi \text{ eff}}^2}{\omega_{\phi \text{ eff}}^2} \simeq q^{\frac{1}{2}}, \quad (11)$$

with $m_{\chi \text{ eff}}^2$ and $\omega_{\phi \text{ eff}}^2$ given by Eq. (5). When the self-coupling λ_χ is small, in the sense that the $3\lambda_\chi \langle (\delta\chi)^2 \rangle$ term in $m_{\chi \text{ eff}}^2$ may be neglected compared to $g \langle (\delta\phi)^2 \rangle$, Eq. (11) yields an estimate for the ϕ field variance:

$$\langle (\delta\phi)^2 \rangle_{\text{peak}} \simeq \frac{1}{2} g^{-\frac{1}{2}} \Phi_s \omega_{\phi \text{ eff}} = \frac{1}{4} q^{-\frac{1}{2}} \Phi_s^2. \quad (12)$$

This can be turned into an estimate for $\langle (\delta\chi)^2 \rangle$ by assuming approximate equipartition of energy between the fluctuations of the two fields. In [12] we have argued that this is reasonable because the transfer of energy between the two fields is efficient in the scattering regime. We thus obtain

$$\langle (\delta\chi)^2 \rangle_{\text{peak}} \simeq \frac{\omega_\phi^2}{4g} = \frac{1}{16} q^{-1} \Phi_s^2. \quad (13)$$

Our original assumption that λ_χ was small can be translated into the constraint

$$\langle (\delta\chi)^2 \rangle < \frac{1}{48c^2} q^{-\frac{3}{2}} r^{-1} \Phi_s^2. \quad (14)$$

Hence Eqs. (12) and (13) are valid provided that $r < (3c^2 q^{1/2})^{-1}$. This condition defines what is meant by “small λ_χ ”. Note that it translates roughly into $\lambda_\chi < g^{3/2}/\lambda_\phi^{1/2}$. None of the runs presented in this paper satisfy this condition, and the above estimates are included here only for completeness. The “small λ_χ ” case was treated in detail in [12].

For “large λ_χ ”, *i.e.* $r q^{1/2} > (3c^2)^{-1}$, Eq. (11) immediately yields an estimate for the χ field variance:

$$\langle(\delta\chi)^2\rangle_{\text{peak}} \simeq \frac{1}{6} \frac{g^{\frac{1}{2}} \Phi_s \omega_\phi}{\lambda_\chi} \quad (15)$$

$$= \frac{1}{48c^2} q^{-\frac{3}{2}} r^{-1} \Phi_s^2. \quad (16)$$

This is obtained using $\omega_{\phi \text{ eff}}^2 \approx \omega_\phi^2$, which is true because here $r > (12c^2 q^{1/2})^{-1}$. The run shown in figures 3 and 5 belongs in the large λ_χ , positive g category. To see how well Eq. (16) works in this case note that we can replace $(\delta\chi)^2$ with the lattice quantity $(\delta\bar{\chi})^2$ on the left hand side if we do the same with Φ_s on the right hand side. From figure 3, $\bar{\Phi}_s \approx \Phi_0$, so Eq. (16) predicts $\langle(\delta\bar{\chi})^2\rangle_{\text{peak}} = 1.4 \times 10^{-5} \Phi_0^2$. From figure 5 we see that this is in good agreement with the first peak $\langle(\delta\bar{\chi})^2\rangle_{\text{peak}} \simeq 1 \times 10^{-5} \Phi_0^2$ at $\tau \approx 0.65 \times 10^8 \Phi_0^{-1}$. To test the q_0 dependence in Eq. (16) we ran our code for several values of q_0 ranging from 3.5 to 1000. A power law fit to the data gives $\langle(\delta\chi)^2\rangle_{\text{peak}} \propto q_0^{-1.41}$, in reasonable agreement with the prediction.

Figure 5 also illustrates nicely that the inflaton decays into its own fluctuations via parametric resonance, as discussed in the introduction. Once the χ resonance is shut off this usually subdominant process becomes important and the ϕ variance continues to grow. After $\tau = 2 \times 10^8 \Phi_0^{-1}$ the growth is clearly exponential, and during this stage the inflaton decays essentially as if it were not coupled to the χ field at all. The decay finally stops when the ϕ field variance reaches its scattering value $\langle(\delta\phi)^2\rangle_{\text{peak}} \sim 10^{-1} \Phi^2(\tau_s^\phi) \sim 10^{-6} M_{\text{P}}^2$ [25]. This is discussed in more detail in [12], as is the amount of energy in the χ fluctuations at the beginning of scattering regime [26].

Case II. When $g < 0$, Eq. (10) reduces to

$$\delta A \equiv \frac{m_{\chi \text{ eff}}^2}{\omega_{\phi \text{ eff}}^2} \simeq 4|g|. \quad (17)$$

Since we must now allow for the possibility that χ_0 has an appreciable amplitude, Eq. (5) for $m_{\chi \text{ eff}}^2$ and $\omega_{\phi \text{ eff}}^2$ should really be modified to

$$\begin{aligned} m_{\chi \text{ eff}}^2 &= g \langle(\delta\phi)^2\rangle + 3\lambda_\chi \left(\langle(\delta\chi)^2\rangle + \chi_0^2 \right), \\ \omega_{\phi \text{ eff}}^2 &= \omega_\phi^2 + g \left(\langle(\delta\chi)^2\rangle + \chi_0^2 \right) + 3\lambda_\phi \langle(\delta\phi)^2\rangle. \end{aligned} \quad (18)$$

In this analysis, however, we set χ_0 to *zero*. The reason is simply that we are interested in obtaining an estimate of the *peak* variance. Once $\langle(\delta\chi)^2\rangle$ becomes appreciable χ_0 no longer follows $\tilde{\chi}_0$ of Eq. (8) [27], and there are certainly times when χ_0 is small (*cf.* figure 2). These times are precisely the times during which $\langle(\delta\chi)^2\rangle$ reaches its maximum value, as can be seen from Eqs. (17) and (18), as well as figure 4.

With $\chi_0 = 0$ Eq. (17) simply says

$$m_{\chi \text{ eff}}^2 \simeq |g| \Phi_s^2, \quad (19)$$

independent on ω_ϕ . Assuming that $\langle(\delta\chi)^2\rangle$ dominates $m_{\chi \text{ eff}}^2$ [28] we obtain

$$\langle(\delta\chi)^2\rangle_{\text{peak}} \simeq \frac{|g|}{3\lambda_\chi} \Phi_s^2 = \frac{1}{12c^2} |q|^{-1} r^{-1} \Phi_s^2. \quad (20)$$

This is a factor $4|q|^{1/2}$ times larger than the corresponding positive g value Eq. (16). The difference between positive and negative g is nicely illustrated in figure 1. In order to shut off the fast exponential growth in the $g > 0$ case, it is sufficient that the first instability band above $A = 2|q|$ is rendered ineffective, *i.e.* $\delta A \sim q^{1/2}$. In the negative g case, on the other hand, the instability is shut off only when A is shifted all the way from $A = -2|q|$ to above the line $A = 2|q|$, *i.e.* $\delta A \sim 4|q|$. After $\langle(\delta\chi)^2\rangle_{\text{peak}}$ is reached, $\langle(\delta\phi)^2\rangle$ wants to grow to its one field scattering value $\simeq 0.1\Phi^2(\tau_s^\phi)$ [25], just as in the positive g case. However, due to the large χ occupation numbers scatterings become fast before the ϕ variance can grow this large, and it is cut off at a somewhat smaller value. If one assumes that, because of the efficient scattering, equipartition is reasonably well satisfied, one obtains the estimate [29]

$$\langle(\delta\phi)^2\rangle_{\text{peak}} \simeq \frac{|g|^{3/2}}{3\lambda_\chi} \frac{\Phi_s^3}{\omega_{\phi\text{eff}}} = \frac{1}{6c^2} |q|^{-1/2} r^{-1} \Phi_s^2. \quad (21)$$

Here we have taken the appropriate value of Φ to be Φ_s even though the ϕ variance really peaks somewhat later than the χ variance. To get an order of magnitude estimate the difference should not matter as long as scatterings terminate the ϕ resonance soon after $\langle(\delta\chi)^2\rangle$ reaches its maximum. While our simulations indicate that this formula holds fairly well for moderate values of q ($\lesssim 100$) we are at present unsure how well it extrapolates to very large q or r . The reason is that we cannot reliably capture both the ϕ and χ resonances simultaneously if q is too large [30]. We should point out that we expect Eq. (21) to fail for very large r (*i.e.* large λ_χ). The reason is simply that in this case the χ resonance shuts off for relatively small occupation numbers, so that $\phi \leftrightarrow \chi$ scatterings should not affect the ϕ resonance very much, and hence $\langle(\delta\phi)^2\rangle$ should reach its one field value.

Note that the variances in Eqs. (20) and (21) do not significantly change ω_ϕ at the time the scattering regime is reached since $g\langle(\delta\chi)^2\rangle_{\text{peak}}, 3\lambda_\phi\langle(\delta\phi)^2\rangle_{\text{peak}} < \omega_\phi^2$ is satisfied for $|q|, r > 1$. We can now compare the predictions of Eqs. (20) and (21) with the numerical results shown in figure 4. Recall that we can turn the above estimates for physical variances into estimates for lattice variables by replacing the fields on both sides of the equation with the barred lattice fields. Then noting that $\bar{\Phi}_s \approx \Phi_0$ we read from figure 4: $\langle(\delta\bar{\chi})^2\rangle_{\text{peak}} \simeq 1 \times 10^{-3}\Phi_0^2$ and $\langle(\delta\bar{\phi})^2\rangle_{\text{peak}} \simeq 5 \times 10^{-3}\Phi_0^2$. Eqs. (20) and (21) predict $\langle(\delta\bar{\chi})^2\rangle_{\text{peak}} = 0.33 \times 10^{-3}\Phi_0^2$ and $\langle(\delta\bar{\phi})^2\rangle_{\text{peak}} = 4 \times 10^{-3}\Phi_0^2$, so that the agreement is quite good.

We will now address the question how to estimate the quantity Φ_s in terms of which our expressions for the variances, Eqs. (12), (13), (15), (16), (20), and (21), are given. Recall that Φ_s is the amplitude of ϕ_0 at the time when the scattering regime is reached and the variances peak in the expanding universe. The first thing to note is that in the *absence* of expansion the amplitude of the ϕ zeromode does not decrease significantly by the time the scattering regime is reached. This can be observed in figures 2 and 3. The reason is simply that the energy density is proportional to Φ^4 , so that even a substantial loss of energy corresponds to a rather small change in amplitude. To obtain an estimate for Φ_s we can thus take the decrease to be due to the expansion alone. Then

$$\Phi_s = \frac{\Phi_0}{a(\tau_s)}, \quad (22)$$

where τ_s is the beginning of the scattering regime. As already pointed out at the beginning of this section, τ_s depends sensitively on the initial position of the resonance and is consequently

difficult to estimate accurately. Since the occupation numbers grow as $n = n_0 \exp(2\mu\omega_\phi^0\tau)$ we find

$$\tau_s = \frac{1}{2\mu\omega_\phi^0} \ln \left(\frac{n_{\text{scatt}}}{n_0} \right), \quad (23)$$

where n_{scatt} is the occupation number of the resonant modes at the beginning of the scattering regime. Our initial conditions correspond to “ n_0 ” $\sim 1/2$ [12], and n_{scatt} is roughly g^{-1} for the small λ_χ , $g > 0$ case, and $10/\lambda_\chi$ for the large λ_χ , $g > 0$ and $g < 0$ cases [31]. The difference arises because in the first case $\langle(\delta\phi)^2\rangle$ is responsible for shutting off the resonance while in the latter two cases the growth of $\langle(\delta\chi)^2\rangle$ terminates the exponential regime (see also [12]). This leaves us with the question what value to take for μ . From figure 1 we see that $\mu \sim 0.2$ is reasonable for the positive g case, where we are limited to the region above $A = 2|q|$. This is also correct in the negative g case: it is not hard to show that $\chi_0 \approx \tilde{\chi}_0$ until $\langle(\delta\chi)^2\rangle \sim (12c^2r|q|^{3/2})^{-1}\Phi^2$ ([32]), which is already larger than the positive g value given in Eq. (16). As discussed in the introduction, the negative g case is equivalent to positive g as long as $\chi_0 \approx \tilde{\chi}_0$, so during this initial period the positive g value for μ is appropriate. Once χ_0 stops following $\tilde{\chi}_0$ the variance rises rapidly to its negative g peak, in a time interval negligible compared to the already elapsed time. Hence we can estimate τ_s using the positive g value for μ [33]. For example, for the runs in figures 2–5 we obtain $\tau_s \sim 1 \times 10^8 \Phi_0^{-1}$, in reasonable agreement with the numerical results. Eqs. (22) and (23), together with the formula $a(\tau) = (1 + H_0\tau) \approx (1 + [\lambda_\phi(1 - 1/r)]^{1/2} M_P \tau)$ given in section II A, complete our estimate of Φ_s .

The final task of this section will be to explain the evolution of the variances in more detail. A closer look at figures 4 and 5 reveals a rather complex behavior of the variances. The first prominent feature is a slow modulation of the maximum ϕ variance. A simple explanation of this phenomenon can be gotten by assuming that the infrared (IR) modes oscillate in phase and can be modeled by one oscillator of a definite frequency $\omega^2 = k^2 + \omega_{\phi \text{ eff}}^2$. For $k \ll \omega_{\phi \text{ eff}}$ we then have two weakly coupled oscillators, the IR mode and the zero mode, with the same natural frequency. These modes will transfer energy back and forth much like two pendulums coupled by a spring. As can be seen in figures 3 and 5, the maxima of the variance envelope correspond to minima of the zeromode envelope, and vice versa. Note that no such modulation occurs for the χ field since no dominant χ zeromode develops in the scattering regime.

The second prominent feature of the variances is that in the scattering regime they fluctuate between “peak” and “valley” values with frequency $2\omega_{\phi \text{ eff}}$. Understanding this behavior is potentially important for applications where precise values of the variances are required, such as nonthermal phase transitions and baryogenesis. A first estimate of the amplitude of these fluctuations has been given in Ref. [13]. Here we will present an alternative derivation, leading to somewhat different results. We will attempt to explain the origin of the variance *fluctuations* using a simple toy model which contains some generic features of the resonant growth, and also teaches us something about the slowly varying scattering regime. We will illustrate our model on the χ field and first treat the case $g > 0$. After neglecting the non-linear (scattering) terms, the equation of motion for a field mode $X = \chi_k$ can be written as

$$\ddot{X} + \omega_X^2 X = 0, \quad (24)$$

where

$$\omega_X^2 = k^2 + g\phi_0^2(t) + g\langle(\delta\phi)^2\rangle + 3\lambda_\chi\langle(\delta\chi)^2\rangle. \quad (25)$$

Since we are interested in IR modes that contribute significantly to the variance we can neglect the momentum dependence of the frequency. Using Eq. (11) we then find that in the scattering regime ω_X^2 varies between $\omega_{\max}^2 \simeq g\Phi^2 \simeq 4q\omega_\phi^2$ and $\omega_{\min}^2 \simeq 3\lambda_\chi\langle(\delta\chi)^2\rangle + g\langle(\delta\phi)^2\rangle \sim q^{1/2}\omega_\phi^2$. Dropping k^2 in Eq. (25) hence amounts to assuming that the variance is dominated by modes with $k^2 \leq k_{\text{res}}^2 \sim q^{1/2}\omega_\phi$. Consider now the solution to Eq. (24) if $\omega_X = \omega_0$ for $t < 0$ and $\omega_X = \omega_1$ for $t > 0$:

$$\begin{aligned} X &= X_0 \cos \omega_0 t + \frac{\dot{X}_0}{\omega_0} \sin \omega_0 t, & \text{for } t < 0 \\ X &= X_0 \cos \omega_1 t + \frac{\dot{X}_0}{\omega_1} \sin \omega_1 t, & \text{for } t > 0. \end{aligned} \quad (26)$$

The important feature of Eq. (26) is that for $\omega_0 > \omega_1$ the amplitude of the "kinetic term" \dot{X}_0/ω_1 at $t > 0$ is amplified by ω_0/ω_1 in comparison to the kinetic term at $t < 0$. This amplification captures the essence of the amplitude growth mechanism, and it may be used to explain the variance fluctuations in the scattering regime, as follows. Consider a sequence of N matchings as in Eq. (26), with $\omega_n/\omega_{n+1} = e^\epsilon$. Assuming that at each matching the solution of the previous time interval has a random phase [34] one obtains an amplification $X_N/X_0 = [(1 + e^{2\epsilon})/2]^{N/2}$. Using the fact that $\omega_0/\omega_N \equiv \omega_{\max}/\omega_{\min} = e^{N\epsilon}$ we find for ϵ small that $X_N/X_0 \approx (\omega_{\max}/\omega_{\min})^{1/2}$. Since these are the modes that dominate the variance, this translates into $\langle(\delta\chi)^2\rangle_{\text{peak}}/\langle(\delta\chi)^2\rangle_{\text{valley}} \sim X_N^2/X_0^2 \sim \omega_{\max}/\omega_{\min}$. Plugging in the values for the frequencies obtained below Eq. (25) yields

$$\frac{\langle(\delta\chi)^2\rangle_{\text{peak}}}{\langle(\delta\chi)^2\rangle_{\text{valley}}} \sim \frac{\omega_{\chi \max}}{\omega_{\chi \min}} \approx q^{1/4} \quad (g > 0). \quad (27)$$

This estimate agrees well with figure 5 after $\tau \approx 4.5 \times 10^8 \Phi_0^2$. Before that the oscillations are somewhat larger. Eq. (27) also agrees well with the large q runs presented in [12].

For negative g the fluctuations in the variance are of different origin. For one thing, the peaks in $\langle(\delta\chi)^2\rangle$ now occur when ϕ_0 is *maximum*, in contrast to the positive g case just discussed. As already pointed out following Eq. (18), the largest peaks occur when $\chi_0 \approx 0$ and ϕ_0 is large. The reason for this is simply that when χ_0 gets out of phase with $\tilde{\chi}_0$, the negative $g\phi_0^2$ contribution to the χ mass tends to destabilize the system. To compensate, the positive $3\lambda_\chi\langle(\delta\chi)^2\rangle_{\text{peak}}$ term must acquire a magnitude $3\lambda_\chi\tilde{\chi}_0^2$, since, as shown in the introduction, this is the value required to stabilize the mode equations. We have argued above that χ_0 falls out of phase with $\tilde{\chi}_0$ when $\langle(\delta\chi)^2\rangle \sim (12c^2r|q|^{3/2})^{-1}\Phi^2$ [32]. For example, in figure 2 this occurs at $\tau \approx 9 \times 10^7 \Phi_0^{-1}$. Figure 4 shows that the largest variance is reached a quarter of an oscillation later, when ϕ_0 reaches its maximum. During this first half-period after χ_0 stops following $\tilde{\chi}_0$ there is genuine instability, causing the variance to grow. At later times the IR modes have sufficient amplitude to compensate the negative mass term without growing exponentially: they simply get pulled by ϕ_0 and keep the effective mass positive at all times. When ϕ_0 passes through zero the variance returns to its previous "valley" value.

We can estimate the ratio of peak to valley variances by again appealing to our toy model of matching oscillatory solutions with different frequencies, as in Eq. (26). There are, however, significant differences between the case at hand and the positive g case discussed earlier. For negative g the maximum frequency of an infrared χ mode that contributes significantly to the variance occurs when ϕ_0 passes through zero and is approximately given by $\omega_{\max}^2 \simeq 3\lambda_\chi \langle (\delta\chi)^2 \rangle_{\text{valley}}$. This frequency holds only for a small fraction of the oscillation: as soon as $|g|\phi_0^2 \geq 3\lambda_\chi \langle (\delta\chi)^2 \rangle_{\text{valley}}$ the χ mode gets dragged along with the ϕ zeromode and its frequency changes to $\omega_{\min} \simeq \omega_{\phi \text{ eff}}$. Hence there is no continuous change in frequency as in the positive g case, and consequently only one matching of solutions *à la* Eq. (26). The single matching gives $X_{\max}/X_{\min} \approx \omega_{\max}/\omega_{\min}$, where we assumed that after the matching the kinetic term dominates. This is the case unless $\dot{X}_0/\omega_0 \ll X_0$ in Eq. (26). Next we use $\langle (\delta\chi)^2 \rangle_{\text{peak}} \sim \tilde{\chi}_0^2 \approx |g|\Phi^2/\lambda_\chi$ to obtain

$$\frac{\langle (\delta\chi)^2 \rangle_{\text{peak}}}{\langle (\delta\chi)^2 \rangle_{\text{valley}}} \sim \left(\frac{\omega_{\chi \text{ max}}}{\omega_{\chi \text{ min}}} \right)^2 \approx |q|^{\frac{1}{2}} \quad (g < 0). \quad (28)$$

This prediction can be compared to the numerical results presented in figure 6. As explained previously, the maximum lattice variances are much smoother functions of the parameters than the physical variances, and we will thus concentrate on figure 6(a). Note that even though we have presented $|q_0| = 0.35$ runs in figure 6, these runs just barely reach the scattering regime, especially for $r = 2$ (*cf.* [21]). After discarding the $|q| = 0.35$ runs we obtain as a best fit $\langle (\delta\bar{\chi})^2 \rangle_{\text{peak}} \simeq 0.16|q|^{-0.92}r^{-0.82}\bar{\Phi}^2$ and $\langle (\delta\bar{\chi})^2 \rangle_{\text{valley}} \simeq 0.1|q|^{-1.46}r^{-0.77}\bar{\Phi}^2$, and hence $\langle (\delta\bar{\chi})^2 \rangle_{\text{peak}}/\langle (\delta\bar{\chi})^2 \rangle_{\text{valley}} \simeq 1.6|q|^{0.54}r^{-0.05}$. This agrees reasonably well with Eqs. (20) and (28). Note that the slopes in figure 6(a) are increasing with $|q|$, which may indicate that at $|q_0| = 3.5$ the variances still have not reached the full scattering regime values. This could be the explanation of the somewhat low slopes quoted above. Unfortunately we cannot test our estimates reliably for $|q_0| > 350$ since this would require enormous computing resources. The problem is essentially that as g and λ_χ get large the particles scatter readily into high momentum states and one needs an enormous ultraviolet cutoff in order to accommodate the decayed energy. This must be combined with good IR resolution in order not to miss scatterings such as $\chi(k_{\text{res}})\phi(k=0) \rightarrow \chi(k)\phi(k)$ which involve very IR momenta. The upshot is that we have found negative g simulations with $|q_0| \gtrsim 500$ to be unreliable even on 128^3 lattices (in the massless case).

III. MASSIVE FIELDS

A. Numerical Results

For massive fields the expansion of the universe cannot be taken into account by a simple rescaling as was done for massless fields in section II A. The equations of motion in a FRW universe are

$$\begin{aligned} \frac{\partial^2 \phi(\vec{x}, t)}{\partial t^2} + 3H \frac{\partial \phi(\vec{x}, t)}{\partial t} + \left[m_\phi^2 - \frac{\nabla^2}{a(t)^2} + g\chi^2(\vec{x}, t) + \lambda_\phi \phi^2(\vec{x}, t) \right] \phi(\vec{x}, t) &= 0, \\ \frac{\partial^2 \chi(\vec{x}, t)}{\partial t^2} + 3H \frac{\partial \chi(\vec{x}, t)}{\partial t} + \left[m_\chi^2 - \frac{\nabla^2}{a(t)^2} + g\phi^2(\vec{x}, t) + \lambda_\chi \chi^2(\vec{x}, t) \right] \chi(\vec{x}, t) &= 0, \end{aligned} \quad (29)$$

where

$$H(t) = \frac{\dot{a}(t)}{a(t)} = \sqrt{\frac{\rho}{3M_{\text{P}}^2}}, \quad (30)$$

and ρ is the total energy density. This set of partial differential equations was solved without approximation on the lattice. The initial conditions for the fields were chosen as follows: the ϕ zeromode ϕ_0 was set equal to $2M_{\text{P}}$. As explained in section II A, this corresponds to a time slightly before the end of inflation. χ_0 was set equal to $\tilde{\chi}_0$ as given in Eq. (8), and the velocities $\dot{\phi}_0$ and $\dot{\chi}_0$ were set equal to their slow roll values. The initial conditions for the inhomogeneous modes were chosen as described in [12] and [16].

Here we will present a brief survey of our main numerical results for massive fields. In section III B below we will discuss the figures in detail and give analytical estimates for various quantities of interest. We should mention that throughout this paper we have chosen parameters that are “realistic” within the context of chaotic inflation. In particular we use $\Phi_0 \sim M_{\text{P}}$, $\lambda_\phi \sim 10^{-12}$, and $m_\phi \sim 10^{13}\text{GeV}$. The latter two values are determined by the observed anisotropies in the microwave background, as measured by the cosmic background explorer (COBE) [35].

All of the numerical results presented are for $g < 0$. In figure 7(a) we show the maximum χ variances produced in the expanding universe for a massless inflaton as a function of m_χ for various values of $|q_0|$. Figure 7(b) is a blow-up of the $|q_0| = 350$ curve. The important feature to observe is the extremely *spiky* nature of the curve, with huge jumps in production for small changes in the parameters. We have already discussed in section II B that the maximum variances are not smooth functions of the parameters, but the variation here is more extreme and of a different origin. It will be explained in section III B. Figures 8(a) and (b) show the variances and occupation numbers [36] for a set of parameters for which there is very little growth, *i.e.* a point corresponding to one of the valleys in figure 7 [37]. In figure 9 we show the same quantities for parameters where significant production does occur.

Figure 10 shows the maximum peak and valley χ variances produced in the expanding universe for a massive inflaton as a function of m_χ for $|q_0| = 350$. Again we observe extreme sensitivity to small changes in the parameters. In figures 11(a) and (b) we show the variances and χ field zeromode as a function of time for three runs with just slightly different values of m_χ . As can be seen in figure 11(a) the maximum variances reached differ by several orders of magnitude. In section III B we will explain how the growth of the variance depends on the dynamics of the χ zeromode, which is illustrated in figure 11(b).

An important point which will be discussed in detail in section III B is that a theory with negative coupling can produce massive particles for much smaller values of $|q_0|$. In fact we will see that for most of the parameter range in figures 7 and 10 there would be no particle production at all for $g > 0$. As will be explained in section IV, the fact that massive particles are produced more readily with negative g is crucial in constructing GUT baryogenesis models with “natural” coupling constants. This will be illustrated by figures 12(a) and (b), where we show the maximum peak and valley variances reached for $m_\chi = 10^{14}\text{GeV}$ as a function of $|g|$. For the range of couplings shown in the figures it is impossible to produce such heavy particles with $g > 0$.

B. Discussion and analytical estimates

In this section we explain the main features of inflaton decay into massive particles, with particular emphasis on the resonant growth and its subsequent shut-off. We will also give analytical estimates for various quantities of interest. The physics of the shut-off mechanism is rather simple. For positive g parametric resonance produces particles with *physical* momenta of order $k_{\text{res}}^{\text{phys}} \sim q^{1/4}\omega_\phi$, so that $k_{\text{res}}^{\text{phys}} \gg \omega_\phi$ when $q \gg 1$. When the particles mass exceeds the resonant momenta, the production shuts off. For comparison we note that perturbative decays are kinematically forbidden if the total mass of the decay products is greater than the energy of the decaying particles. As a consequence, parametric resonance can produce much heavier particles ($m_\chi \sim q^{1/4}\omega_\phi$) than perturbative decays ($m_\chi \sim \omega_\phi$). (When $q \ll 1$ the resonant and perturbative scales coincide.) This observation could have important consequences in that parametric resonance provides a mechanism to produce the heavy gauge and Higgs bosons necessary for GUT baryogenesis. This will be discussed in some detail in section IV. Before presenting our results regarding the production of massive particles we wish to point out that from the outset one might expect the sign of the coupling g to play an important role in this context. The reason is that in the negative g case the maximum resonant momenta are of order $k_{\text{res}}^{\text{phys}} \sim 2|q|^{1/2}\omega_\phi$, which is by a factor $2|q|^{1/4}$ larger than in the positive g case. Therefore, one expects that with negative g the resonance is much more effective in producing massive particles. This expectation is confirmed below.

For completeness we will study all cases of interest: massless and massive inflaton, positive and negative cross-coupling g . We will then compare our estimates for positive g with the numerical results of [7], and for negative g with figures 7–12. The estimates we obtain in this section will be used in section IV to estimate baryon production. In connection with this we remark that very massive particles are created only marginally relativistic and quickly become nonrelativistic due to redshifting. In this situation the variance is simply related to the number density of particles n and energy density ρ of the field: $n_\chi \approx m_\chi \langle (\delta\chi)^2 \rangle$ and $\rho_\chi \approx m_\chi^2 \langle (\delta\chi)^2 \rangle$.

Based on Eq. (10) one can make a quantitative estimate of when the resonance shuts off. Indeed, when A becomes larger than about $2|q| + |q|^{1/2}$ the inflaton decay slows down dramatically, essentially because the instability exponent μ decreases rapidly above the $A = 2|q|$ line (*cf.* figure 1). If the increase in A is mostly due to the (tree level) mass m_χ , we say that the resonance is shut off by the χ mass. If, on the other hand, the growth of A can be attributed mainly to the backreaction effects (the contribution of the growing variances to the effective mass), the situation resembles the massless case in the sense that the variances reach their scattering regime values of section II B and a slowly varying state sets in. Before we begin studying the details of each of the cases mentioned above, we point out that the Universe expansion is crucial in shutting off the inflaton decay. This is so in essence because the inflaton amplitude decreases as the Universe expands, while the tree level mass stays constant. More concretely, the resonance shuts off when the mass becomes greater than the typical physical resonant momentum, which scales as $k_{\text{res}}^{\text{phys}} \propto a^{-1}$ for a massless inflaton and $k_{\text{res}}^{\text{phys}} \propto a^{-3/4}$ for a massive inflaton. This means that, as the Universe expands, the (physical) scale on which particles are produced redshifts and hence the relative importance of the χ mass increases, leading eventually to the termination of particle production. Once the resonance is shut off, the only energy exchange mechanism that remains active is the

perturbative scatterings. We now turn to discuss the details of each of the cases mentioned above.

1. Massless inflaton, $g > 0$

For positive g and a *massless* inflaton the criterion for the χ resonance shut-off is (*cf.* Eq. (11))

$$m_{\chi \text{ eff}}^2 \gtrsim q^{\frac{1}{2}} \omega_{\phi \text{ eff}}^2 \simeq q_0^{\frac{1}{2}} (\omega_{\phi}^0)^2 \left(\frac{a_0}{a} \right)^2, \quad (31)$$

where $m_{\chi \text{ eff}}^2 = m_{\chi}^2 + g \langle (\delta\phi)^2 \rangle + 3\lambda_{\chi} \langle (\delta\chi)^2 \rangle$. Here we have explicitly written the dependence on the scale parameter a , used the fact that $\Phi \propto a^{-1}$ for a massless inflaton, and assumed $\omega_{\phi \text{ eff}} \simeq \omega_{\phi}$. For massless fields the maximum variances reached were given in Eqs. (12) and (13) for “small” λ_{χ} ($r q^{1/2} < (3c^2)^{-1}$) and in Eqs. (15) and (16) for “large” λ_{χ} . It is clear that these estimates still hold for a massive χ field if, by the *conformal* time τ_s at which the scattering regime is reached, $m_{\chi}^2 < q^{1/2} (\omega_{\phi}^0)^2 (a_0/a(\tau_s))^2$ is satisfied. Masses that satisfy this condition are small in the sense that the resonance is shut off by the variance rather than the mass term in the lagrangian, and the maximum variances reached are hence the same as in the massless case. If, on the other hand, the resonance is shut off by the χ mass before the scattering regime sets in, the maximum variances reached are smaller by a factor $\exp[-2\mu\omega_{\phi}^0(\tau_s - \tau_m)]$, where τ_m , the conformal time at which the mass term kills the resonance, is defined by $m_{\chi}^2 = q_0^{1/2} (\omega_{\phi}^0)^2 (a_0/a(\tau_m))^2$. The borderline case is the maximum χ mass for which the scattering regime is still reached:

$$m_{\chi} \simeq q_0^{\frac{1}{4}} \omega_{\phi}^0 \frac{a_0}{a(\tau_s)}, \quad (\text{massless inflaton}). \quad (32)$$

This can be rewritten as an estimate for the minimum initial value of q required to reach the scattering regime for a given value of m_{χ} . Using

$$a_0 \tau_s \simeq \frac{1}{2\omega_{\phi}^0 \mu} \ln \frac{n_{\text{scatt}}^{\chi}}{n_0^{\chi}}, \quad (33)$$

and

$$\frac{a}{a_0} = 1 + H_0 a_0 \tau, \quad H_0 \approx \frac{1}{2\sqrt{2}c} \omega_{\phi}^0 \frac{\Phi_0}{M_{\text{P}}}, \quad (34)$$

where H_0 is the Hubble parameter at the beginning of the oscillatory stage, one obtains

$$q_0^{\text{min}} \simeq \left(\frac{m_{\chi}}{\omega_{\phi}^0} \frac{a}{a_0} \right)^4 \simeq \left(\frac{1}{4c\sqrt{2}} \frac{m_{\chi}}{\omega_{\phi}^0} \frac{\Phi_0}{M_{\text{P}}} \frac{1}{\mu} \ln \frac{n_{\text{scatt}}^{\chi}}{n_0^{\chi}} \right)^4, \quad (35)$$

where $n_0^{\chi} \approx 1/2$, and $n_{\text{scatt}}^{\chi} \sim g^{-1}$ for small λ_{χ} and $\sim 10/\lambda_{\chi}$ for large λ_{χ} [31]. For $q_0 \geq q_0^{\text{min}}$ the variances peak at their scattering regime values. For a typical choice of parameters $\Phi_0/M_{\text{P}} = 1.8$, $\mu = 0.1$, and taking $\lambda_{\chi} = 0$, Eq. (35) yields $q_0^{\text{min}} \sim 2 \times 10^6$ for $m_{\chi} = \omega_{\phi}^0$, and $q_0^{\text{min}} \sim 8 \times 10^8$ for $m_{\chi} = 10\omega_{\phi}^0$ [38]. This is roughly in agreement with Ref. [7], where the

authors estimate that no significant resonant production occurs for $q_0 \leq 10^6$ if $m_\chi \leq \omega_\phi^0$. Of course the choice of μ introduces significant uncertainty into the estimates: using $\mu = 0.2$, for example, lowers the values of q_0^{\min} by a factor of 5–10. To test the validity of Eq. (35) we ran our code with $m_\chi = 1.07\omega_\phi^0$, $\lambda_\chi = 0$, and $q_0 = 3.65 \times 10^6$ and found that the scattering regime is marginally reached when the resonance shuts off at $t \sim 1.5 \times 10^8 M_P^{-1}$. The peak and valley values of the χ variance are $\langle(\delta\chi)^2\rangle_{\text{peak}} \approx 4 \times 10^{-10} M_P^2$ and $\langle(\delta\chi)^2\rangle_{\text{valley}} \approx 6 \times 10^{-12} M_P^2$. This is in good agreement with the prediction for the scattering regime peak and valley values of Eqs. (13) and (27): $\langle(\delta\chi)^2\rangle_{\text{peak}} \approx 4 \times 10^{-10} M_P^2$ and $\langle(\delta\chi)^2\rangle_{\text{valley}} \approx 1.3 \times 10^{-11} M_P^2$, where we used for $\Phi_s = \Phi_0(a_0/a(\tau_s)) \simeq 0.08 M_P$. Note that even though these variances are rather small the scattering regime is reached since large q corresponds to large g . For $q_0 = 10^5$ we find that the resonant growth shuts off well before the scattering regime is reached. The χ variance grows to about 1% of its scattering regime values (13) and (27).

2. Massive inflaton, $g > 0$

Before discussing the effect of the χ field mass on the resonance shut off we will discuss briefly the simpler situation with $m_\chi = 0$ but massive inflaton. Since for a *massive* inflaton $\Phi \propto a^{-3/2}$, we find that $q = q_0(a_0/a(t))^3$. There are then two possible mechanisms for terminating the resonance: either the resonance is shut off as usual by the variances, or q becomes $\ll 1$ due to the expansion before this happens. In the former case the maximum variances can be estimated as usual from Eq. (10). Hence Eqs. (12) and (13) for “small” λ_χ ($rq^{1/2} < (3c^2)^{-1}$) and Eq. (15) for “large” λ_χ apply *also in the massive inflaton case* if the variances shut off the resonance, *i.e.* if the scattering regime is reached [39]. The difference is that Φ_s is *not* obtained from Eq. (22). Instead one must use

$$\Phi_s = \Phi_0 \left[\frac{a_0}{a(t_s)} \right]^{3/2} \quad (\text{massive inflaton}) \quad (36)$$

where

$$\frac{a(t)}{a_0} = \left(1 + \frac{3}{2} H_0 t \right)^{\frac{2}{3}}, \quad H_0 \approx \frac{1}{2} \frac{\Phi_0}{M_P} m_\phi, \quad t_s \simeq \frac{1}{2m_\phi\mu} \ln \frac{n_{\text{scatt}}^\chi}{n_0^\chi}, \quad (37)$$

and t_s is the *physical* time at the beginning of the scattering regime. The estimates for the n_{scatt}^χ and n_0^χ are given below Eq. (35).

On the other hand, if $q \ll 1$ before the variances reach the values obtained from the above estimates then the resonance shuts off simply because there is no strong instability for small q (*cf.* figure 1(a)). The regime with $q \ll 1$ is often called “narrow resonance” in the literature because the width of the instability bands goes to zero as q becomes small. Using the fact that $q \propto a^{-3}$ and the estimate for t_s above it is easy to find the minimum initial value of q such that $q(t_s) \gtrsim 1$. One obtains

$$q_0^{\min} \approx \left(\frac{3}{8} \frac{\Phi_0}{M_P} \frac{1}{\mu} \ln \frac{n_{\text{scatt}}}{n_0} \right)^2, \quad (m_\chi^2 = 0). \quad (38)$$

For typical values $\Phi_0 = 1.8 M_P$ and $\mu \sim 0.1$ this evaluates to $q_0^{\min} \approx 10^4$ in the small λ_χ case and $q_0^{\min} \approx 46 \ln^2(\frac{8\pi}{\lambda_\chi})$ in the large λ_χ case. If $q_0 \ll q_0^{\min}$ then only a small fraction

of the inflaton energy decays before $q(t) \ll 1$ and the fast decay shuts off because $\mu \ll 1$. However, if $q_0 \approx q_0^{\min}$ then the inflaton can decay almost completely before entering either the scattering regime or the narrow resonance regime. This is the situation for which the variances of the fields reach their maximum possible values.

When the χ field is massive, one requires larger values of q_0 for the variances to reach their scattering regime values. The minimum value of q_0 for which the estimates of section II B, together with Eqs. (36) and (37), apply can be found as in the previous section by requiring $m_\chi^2 < q^{1/2}(t_s)m_\phi^2 = q_0^{1/2}(a_0/a(t_s))^{3/2}m_\phi^2$. The result is

$$q_0^{\min} \simeq \left(\frac{m_\chi}{m_\phi}\right)^4 \left(\frac{a}{a_0}\right)^3 \simeq \left(\frac{m_\chi}{m_\phi}\right)^4 \left(\frac{3}{8} \frac{\Phi_0}{M_{\text{P}}} \frac{1}{\mu} \ln \frac{n_{\text{scatt}}^\chi}{n_0^\chi}\right)^2. \quad (39)$$

If q_0 is larger than this, the resonance is terminated by the variance. Taking the same parameter values as in the massless inflaton case of section III B 1 we obtain $q_0^{\min} \sim 10^4$ for $m_\chi = m_\phi$ and $q_0^{\min} \sim 3 \times 10^7$ for $m_\chi = 10m_\phi$. Hence we conclude that for a massive inflaton the values of q_0^{\min} are typically *one to two* orders of magnitude smaller than in the massless inflaton case. A comparison of Eqs. (35) and (39) leads to $q_{\text{massive}}/q_{\text{massless}}^{1/2} \simeq (9c^2/2)(m_\chi/\omega_\phi^0)^2$, where we assumed equal occupation numbers, μ 's, χ masses, Φ_0 's, and $\omega_\phi^0 = m_\phi$. We should point out that for a massive inflaton the slow roll ends somewhat earlier and that hence the appropriate values of Φ_0 are perhaps 20% larger than in the massless case. To summarize, the main reason why the massive inflaton is more efficient in producing massive particles is that the typical resonant momenta redshift slower. This gives the resonance more time to create particles before it is shut off.

It is interesting to compare our analytical formula for the maximum variance reached with the estimate given in [13]. As explained above, the expressions given in section II B apply as long as q_0 is large enough so that the scattering regime is reached. For small λ_χ the appropriate formula is then Eq. (13), which is particularly easy to apply for a massive inflaton since the combination $\Phi(t)^2/q(t) = 4m_\phi^2/g$ does not redshift due to the expansion. Hence $\langle(\delta\chi)^2\rangle_{\text{peak}} \approx \Phi_0^2/16q_0$. For $q_0 = 10^8$, which as shown above is sufficient to reach the scattering regime even when $m_\chi/m_\phi = 10$, we thus obtain $\langle(\delta\chi)^2\rangle_{\text{peak}} \approx 10^{-9}M_{\text{P}}^2$. This is in good agreement with [13], where the authors find $\langle(\delta\chi)^2\rangle_{\text{peak}} \sim 10^{-9}M_{\text{P}}^2$ [40]. Note, however, that the parametric dependence of the estimate for $\langle(\delta\chi)^2\rangle_{\text{peak}}$ given in [13] seems to be different from our Eq. (13).

3. Negative Coupling

The case of inflaton decay into massive χ particles with a negative cross-coupling g is significantly more complex than the positive g case. We hence begin by discussing the main characteristics of the process.

The first notable feature is that the resonance is shut off by the χ mass only when

$$m_\chi^2 \gtrsim |g|\Phi^2 \approx 4|q|\omega_\phi^2, \quad (40)$$

which should be compared to the positive g criterion $m_\chi^2 \gtrsim q^{1/2}\omega_\phi^2$. Eq. (40) is simply Eq. (10) for $A(k=0) = -2|q| + m_\chi^2/\omega_\phi^2$ and $\delta A/A \ll 1$, $q \gg 1$. Hence in order to get

significant resonant production, one requires $m_\chi^2 \ll |g|\Phi_0^2$, which is a much weaker condition than for positive g . Since Φ scales with the expansion of the Universe (as $\propto a^{-1}$ for a massless inflaton and $\propto a^{-3/2}$ for a massive inflaton), there is then a time interval during which resonant production is possible. The growth mechanism is quite different from the positive g case, and we will describe its main features below. However, a complete analytical understanding is extremely difficult to achieve. The reason is the extremely “chaotic” nature of the process, which we have already pointed out when describing the figures in section III A.

It turns out that the positive g resonant scale $k_{\text{res}}^{\text{phys}} = |q|^{1/4}\omega_\phi$ plays an important role in understanding the dynamics. While $m_\chi^2 \ll |q|^{1/2}\omega_\phi^2$, the dynamics is equivalent to a positive g case with $q_{\text{eff}} = 2|q|$ and $\mu_{\text{eff}} \sim 0.1$, essentially because χ_0 evolves according to Eq. (8) (with $m_\chi \approx 0$). Once $m_\chi > k_{\text{res}}^{\text{phys}}$, which always occurs sooner or later since $k_{\text{res}}^{\text{phys}}$ redshifts with the expansion of the Universe, the ‘positive g resonance’ shuts off completely. This does not mean that production stops altogether. There is another effect which we refer to as the *negative coupling instability*.

We now give a heuristic explanation of this new effect. In some sense we already discussed it in section II B, where we argued that once the variances get so large that $\delta m_\chi \sim |q|^{1/4}\omega_\phi$, χ_0 falls out of phase with $\tilde{\chi}_0$ (*cf.* also [32]). The difference is that for massive χ the “falling out of phase” can occur without the need for large variances. The reason is the following. After ϕ_0 passes through zero and starts growing, it tries to pull χ_0 along, attempting to keep it equal to $\tilde{\chi}_0$ prescribed in Eq. (8). However, if m_χ is large enough so that χ_0 has time to oscillate while ϕ_0 is small, then a phase mismatch can occur and prevent χ_0 from growing and following $\tilde{\chi}_0$. This will be illustrated with a simple model below. When such a mismatch occurs the infrared χ modes grow very fast since for these modes the frequency squared is negative, and their potential corresponds to an inverted harmonic oscillator. The growth exponent $\mu_{\text{eff}} = \chi_k^{-1}d\chi_k/dt$ may be as large as $\sim |q|^{1/2}\omega_\phi$, and the range of momenta which grow can be as broad as $\Delta k_{\text{phys}}^2 \sim |g|\Phi^2$. A dramatic effect indeed, compared to the usual positive coupling parametric resonance. This is what we mean by *negative coupling instability*. The explosive growth ends once χ_0 grows sufficiently large to catch up with $\tilde{\chi}_0$, at which point the infrared modes resume their normal oscillatory behavior. An example of this effect is presented in figure 11(a). For $m_\chi^2 = 5.4 \times 10^{-11}M_{\text{P}}^2$ the variance grows with an exponent of order $\mu_{\text{eff}} \approx 14 \approx 2|q|^{1/2}m_\phi$.

A quantity which is clearly of interest is the probability that for a given set of parameters a negative coupling instability, and the huge particle production associated with it, occurs. As explained above, the instability can occur if there is a phase mismatch between χ_0 and ϕ_0 at the moment when χ_0 should stop oscillating about the origin according to Eq. (8). Specifically, the instability can occur at the instant when the curvature of the χ potential $V(\chi)$ at the origin changes sign, which happens when ϕ_0 becomes larger than $m_\chi^2/|g|$. This observation can be used to estimate the *a priori* probability for an instability to occur, based on the assumption that the phase of χ_0 is random at the instant the curvature changes sign. We stress that this assumption is reasonable only when $m_\chi^2 \gtrsim |q|^{1/2}\omega_\phi^2$. If this condition is not satisfied χ_0 does not have time to oscillate while ϕ_0 is small, and hence no phase mismatch can occur. In this case χ_0 simply follows $\tilde{\chi}_0$, just as in the first part of the evolution shown in figure 2.

One might guess that the *a priori* probability for the mode amplitudes to grow by a factor G ought to be of order G^{-1} . This estimate is supported by the following toy model.

Let us take the time at which the curvature of $V(\chi)$ at the origin changes sign to be $t = 0$. Assume that, while $\phi_0 \simeq 0$, $X = \chi_0$ satisfies

$$X = X_0 \cos m_\chi t + \frac{\dot{X}_0}{m_\chi} \sin m_\chi t, \quad \text{for } t < 0. \quad (41)$$

When ϕ_0 becomes larger than $m_\chi^2/|g|$ at $t = 0$, χ_0 finds itself, at least momentarily, in the potential of an upside down oscillator. Hence we have

$$X = \frac{1}{2} \left(X_0 - \frac{\dot{X}_0}{\nu} \right) e^{-\nu t} + \frac{1}{2} \left(X_0 + \frac{\dot{X}_0}{\nu} \right) e^{\nu t}, \quad \text{for } t > 0, \quad (42)$$

where $\nu \equiv \mu\omega_\phi \approx |q|^{1/2}\omega_\phi$. We are interested in the possibility of a phase mismatch, by which we mean that X matches mostly onto the decaying solution and hence the amplitude of the growing mode at $t = 0$ is small, *i.e.*

$$\frac{1}{2} \left(X_0 + \frac{\dot{X}_0}{\nu} \right) = \epsilon A_0, \quad \text{where } A_0^2 = X_0^2 + \left(\frac{\dot{X}_0}{m_\chi} \right)^2, \quad \epsilon \ll 1. \quad (43)$$

To recover its original amplitude A_0 , and catch up with $\tilde{\chi}_0$, X has to grow by a factor $\exp \nu t \sim \epsilon^{-1} \gg 1$. During this time period the infrared modes are unstable, and the χ variance may grow by a factor as large as $\sim \epsilon^{-2} \approx G^2$. The question we want to answer is, how likely is such an event? As mentioned above, the estimate we are about to present is based on the assumption that χ_0 has a uniform random phase at $t = 0$, which should not be a bad approximation for $m_\chi > |q|^{1/4}\omega_\phi$. The appropriate probability distribution is then the uniform distribution on the circle of phases:

$$d\mathcal{P} = \frac{d\varphi}{2\pi}, \quad X_0 = A_0 \cos \varphi, \quad \frac{\dot{X}_0}{m_\chi} = A_0 \sin \varphi. \quad (44)$$

After some simple algebra we obtain the desired probability

$$\mathcal{P}_\epsilon \equiv \mathcal{P} \left(\left| \frac{1}{2A_0} \left[X_0 + \frac{\dot{X}_0}{\nu} \right] \right| \leq \epsilon \right) \approx \frac{4}{\pi} \frac{\epsilon}{\left[1 + (m_\chi/\nu)^2 \right]^{1/2}}, \quad \epsilon \ll 1 \quad (45)$$

The probability that the variance grows by a factor $\langle (\delta\chi)^2 \rangle / \langle (\delta\chi)^2 \rangle_0 \sim G^2$ is then $\mathcal{P}_\epsilon \simeq (2/\pi)G^{-1} \sim G^{-1}$, as anticipated above. Here we used $G \approx \epsilon^{-1}$ for the amplitude growth factor and the fact that production becomes impossible when $m_\chi^2 \gtrsim |g|\Phi^2$ (*cf.* Eq. (40)), so Eq. (45) applies only when $\nu \sim |q|^{1/2}\omega_\phi \gtrsim m_\chi$. In figure 11(a) we present a run with $m_\chi^2 = 5.4 \times 10^{-11} M_{\text{P}}^2 = 75m_\phi^2$ in which the χ variance grows by a factor 3×10^4 in the interval $t \in [2.21, 3.16] \times 10^6 M_{\text{P}}^{-1}$. According to our estimate the probability for such a large growth to occur is about 0.8%. Figure 11(b) shows χ_0 *vs.* time for three slightly different χ masses to illustrate the dramatic effect of a phase mismatch at the instant when the curvature of the χ potential at the origin changes sign. The $m_\chi^2 = 5.4 \times 10^{-11} M_{\text{P}}^2$ run matches almost entirely on the decaying mode, so in that case χ_0 spends a long time near the origin and the variance grows by a huge factor. As can be seen in figures 11(a) and (b), a tiny (1%) change in the χ mass causes a different matching and changes the resulting variances by

several orders of magnitude [41]. This explains the spiky nature of the curves in figures 7 and 10. The high sensitivity of the growth to small changes in the parameters can be also seen in figure 12. Note that because of the chaotic nature of the production mechanism one should not take the fact that we have connected our data points in these figures with line segments too seriously - for all but the most closely spaced points there could be numerous peaks and valleys in between.

The probability \mathcal{P}_ϵ in Eq. (45) is essentially the probability *per inflaton half-period* that the variance grows by a factor ϵ^{-2} , provided that $q^{1/4}\omega_{\phi\text{ eff}} \lesssim m_{\chi\text{ eff}} \lesssim q^{1/2}\omega_{\phi\text{ eff}}$. Note that, since the χ variance contributes to $m_{\chi\text{ eff}}^2$, the last inequality also determines the maximum growth that can be achieved. This will be discussed in detail below. Here we want to emphasize that the probability is *per inflaton half-period* because a phase mismatch can occur twice per period when the curvature of $V(\chi)$ at the origin changes sign from positive to negative. This means that to obtain the total probability for a negative coupling instability to occur for a given set of parameters one must multiply \mathcal{P}_ϵ by twice the number of inflaton oscillations that take place while $q^{1/4}\omega_{\phi\text{ eff}} \lesssim m_{\chi\text{ eff}} \lesssim q^{1/2}\omega_{\phi\text{ eff}}$ is satisfied [42]. Since we are mostly interested in very heavy particles that could not be produced with $g > 0$, we will assume that the first part of the inequality is satisfied from the start. It is then easy to calculate how large $|g|$ needs to be in order to have n chances for instability before $q^{1/2} < m_{\chi\text{ eff}}/\omega_{\phi\text{ eff}}$ and all production shuts off. The minimum $|g|$ for n chances is

$$|g_n| = \frac{m_\chi^2}{\Phi_0^2} \left(1 + \beta n \frac{\Phi_0}{M_{\text{P}}} \right)^2, \quad (46)$$

where $\beta \approx 3\pi/4$ for a massive inflaton and $\beta \approx \pi/2\sqrt{2}c$ for a massless inflaton. Since Φ_0 is also slightly larger in the massive case we see that one requires somewhat smaller values of $|g|$ in the massless case.

We will now briefly discuss the ratio of “peak” to “valley” variances in the scattering regime for massive particles. This was discussed for massless particles at the end of section IIB, where we found distinctly different behaviors for positive and negative g . If the χ field is massive the situation is more complex. For $g > 0$ the ratio $\langle(\delta\chi)^2\rangle_{\text{peak}}/\langle(\delta\chi)^2\rangle_{\text{valley}}$ is still given by $\omega_{\text{max}}/\omega_{\text{min}} \sim q^{1/4}$. Of course this is only valid if the scattering regime is reached. For $g < 0$ two kinds of behaviors are possible. If the resonance is shut off by the χ mass, *i.e.* the scattering regime is not reached, then the curvature at the origin of the χ potential remains positive after resonance shut off and the oscillating $\phi_0(t)$ simply modulates the frequency of the χ oscillations. In this case the frequency of the χ field changes continuously, so the “random phase” approximation discussed at the end of section IIB applies, and the ratio is again $\langle(\delta\chi)^2\rangle_{\text{peak}}/\langle(\delta\chi)^2\rangle_{\text{valley}} \sim \omega_{\text{max}}/\omega_{\text{min}}$. The difference is that now $\omega_{\text{max}}^2 = m_\chi^2 + 3\lambda_\chi\langle(\delta\chi)^2\rangle_{\text{valley}} \approx m_\chi^2$, and $\omega_{\text{min}}^2 = m_\chi^2 - |g|\Phi^2 + 3\lambda_\chi\langle(\delta\chi)^2\rangle_{\text{peak}} \approx m_\chi^2 - |g|\Phi^2$. If, on the other hand, the scattering regime is reached when $m_\chi^2 \ll |g|\Phi^2$, then the infrared χ modes can be dragged along by ϕ_0 just as in the massless negative g case, and hence

$$\frac{\langle(\delta\chi)^2\rangle_{\text{peak}}}{\langle(\delta\chi)^2\rangle_{\text{valley}}} \sim \left(\frac{\omega_{\text{max}}}{\omega_{\text{min}}} \right)^2 \sim \frac{m_\chi^2 + 3\lambda_\chi\langle(\delta\chi)^2\rangle_{\text{valley}}}{\omega_\phi^2}, \quad (47)$$

which reduces to $\sim (m_\chi/\omega_\phi)^2$ when $m_\chi^2 > 3\lambda_\chi\langle(\delta\chi)^2\rangle_{\text{valley}}$, and to $\sim |g|^{1/2}\Phi/\omega_\phi$ when $m_\chi^2 < 3\lambda_\chi\langle(\delta\chi)^2\rangle_{\text{valley}}$. Here we used $3\lambda_\chi\langle(\delta\chi)^2\rangle_{\text{peak}} \sim |g|\Phi^2$. Note that eventually the expansion of

the universe always reduces Φ sufficiently so that the condition $m_\chi^2 < |g|\Phi^2$ becomes violated and this case turns into the one discussed above Eq. (47).

We are now ready to discuss the specifics of the massless and massive inflaton cases.

4. Massless Inflaton, $g < 0$

In figure 7(a) we show the peak variances reached as a function of m_χ^2 for various values of $|q_0|$. Figure 7(b) is a blow-up of the $|q_0| = 350$ curve. For these runs $\omega_\phi^0 = c\sqrt{\lambda_\phi}\Phi_0 \approx 1.5 \times 10^{-6}M_{\text{P}}$, so the horizontal range in figure 7(a) corresponds to $m_\chi/\omega_\phi^0 \approx 0.63 - 66$. The range in figure 7(b) corresponds to $m_\chi/\omega_\phi^0 \approx 1.84 - 8$. As discussed in section III B 1, for positive g the scattering regime would never be reached for these mass ratios with $q_0 = 350$. Even more dramatic is the fact that for $m_\chi^2/M_{\text{P}}^2 \gtrsim 2 \times 10^{-11}$, there would be no production at all for the chosen parameters if g were positive [43]. This illustrates in concrete terms the power of negative coupling to produce massive particles.

The spiky nature of the curves was already explained in the previous section. In figures 8(a) and (b) we show the variances and occupation numbers [36] of a run with a χ field mass for which there happen to be no phase mismatches and hence no negative coupling instability. In figures 9(a) and (b) we show the same quantities for a case where the instability does occur. Note that m_χ is actually larger for the run in figure 9.

The minimum value of $|q_0|$ for which there is any chance of production can be immediately obtained from Eq. (46) with $n = 1$:

$$|q_0^{\text{min}}| = \left(\frac{m_\chi}{2\omega_\phi^0}\right)^2 \left(1 + \frac{\pi}{2\sqrt{2}c} \frac{\Phi_0}{M_{\text{P}}}\right)^2. \quad (48)$$

With $\Phi_0 = 1.8M_{\text{P}}$ this evaluates to $|q_0^{\text{min}}| = 2.8$ for $m_\chi/\omega_\phi^0 = 1$ and $|q_0^{\text{min}}| = 280$ for $m_\chi/\omega_\phi^0 = 10$. These values are orders of magnitude less than the corresponding positive g values derived in section III B 1.

The maximum variance which can be reached is determined by Eq. (40) (with $m_\chi^2 \rightarrow m_{\chi \text{ eff}}^2$) to be

$$\langle(\delta\chi)^2\rangle_{\text{max}} = \frac{|g|\Phi^2 - m_\chi^2}{3\lambda_\chi}. \quad (49)$$

The appropriate value of Φ depends on exactly when the growth occurs. If a phase mismatch and the associated negative coupling instability occurs very early on (right after the first zero crossing, say) Φ can be as large as $0.5M_{\text{P}}$.

5. Massive inflaton, $g < 0$

When discussing the massive inflaton case with negative coupling it is important to keep in mind that the stability bound $r > 1$ always requires the presence of a $\lambda_\phi\phi^4$ (or higher order) term in the effective potential. For the runs in this section we have chosen the inflaton mass such that $m_\phi^2 \lesssim 3\lambda_\phi\Phi_0^2$ at the end of slow roll. This clearly corresponds to mild fine tuning as there is no a priori reason that these quantities should be of the same order.

If one chooses $\lambda_\phi \ll m_\phi^2/M_{\text{P}}^2$ it becomes more difficult to satisfy $r > 1$ and the available parameter space is somewhat limited. For these reasons we believe that with negative g the more natural situation is the one with $m_\phi^2 \ll 3\lambda_\phi\Phi_0^2$, in which case the analysis of the previous section applies. Nevertheless it is interesting to study the situation where the inflaton dynamics is dominated by the mass term during the oscillatory stage, and we do so below.

Figure 10 shows the maximum peak and valley variances reached during preheating *vs.* m_χ^2 for $|q_0| \approx 350$ (the exact parameters are given in the caption). The horizontal range corresponds to $2.4 < m_\chi/m_\phi < 12$. According to the analysis of section III B 2 the scattering regime is never reached for the same parameter values with $g > 0$. Moreover, for $m_\chi^2/M_{\text{P}}^2 \gtrsim 10^{-11}$ there is no production at all for the chosen value of $|g|$ if $g > 0$ [43].

As in the massless inflaton case the minimum value of $|q_0|$ for which there is any chance of heavy particle production is obtained from Eq. (46) with $n = 1$:

$$|q_0^{\text{min}}| = \left(\frac{m_\chi}{2m_\phi}\right)^2 \left(1 + \frac{3\pi}{4} \frac{\Phi_0}{M_{\text{P}}}\right)^2. \quad (50)$$

For $m_\chi/m_\phi = 1$ this evaluates to $|q_0^{\text{min}}| = 6.9$, and for $m_\chi/m_\phi = 10$ one obtains $|q_0^{\text{min}}| = 690$ (here we have taken $\Phi_0 = 1.8M_{\text{P}}$). Comparison with the results of section III B 2 shows that once again the required values are orders of magnitude less for negative coupling than for positive coupling. On the other hand comparison with section III B 4 shows that for negative coupling the massless inflaton is actually somewhat more effective in producing massive particles than the massive inflaton. This is opposite to the positive coupling situation, although it should be noted that for the present case the difference arises only from a numerical factor; the parametric dependence is the same. Finally we point out that the maximum possible variance is given by Eq. (49) also for the massive inflaton since Eq. (40) holds in both cases.

IV. BARYOGENESIS

It is well known that grand unified theories generically predict the existence of baryon number (B) violating interactions. Much effort has gone into converting this fact into a viable mechanism for baryogenesis [44]. In the standard scenario, B violating gauge or Higgs bosons fall out of thermal equilibrium as the temperature of the universe drops below their mass and subsequently decay, creating net B in the process. This B must then be protected from being wiped out by sphalerons, electroweak B violating processes. Fortunately sphaleron transitions conserve B–L, where L is lepton number, so that any GUT that creates a non vanishing B–L remains a viable candidate. Examples are $SO(10)$ and E_6 .

According to the old theory of reheating [45], based on perturbative decay of the inflaton, GUT baryogenesis seems rather difficult to implement [46]. The reason is simply that the heavy B violating gauge or Higgs bosons cannot be produced efficiently. The gauge bosons are expected to have masses of order the GUT scale (10^{16}GeV), while the Higgs bosons may have masses as low as 10^{14}GeV . Since the mass of the inflaton m_ϕ cannot be larger than about 10^{13}GeV in order not to be in conflict with the measured anisotropy in the microwave background [35], direct perturbative production of GUT bosons is kinematically forbidden.

In addition, the weak coupling of the inflaton to other fields causes the reheat temperature, as obtained in perturbation theory, to be so low that thermal production is also ineffective [47].

Clearly GUT baryogenesis after inflation is resurrected by parametric resonance. Not only can bosons with masses larger than the inflaton be produced directly. They are automatically far from thermal equilibrium, thus satisfying one of the prerequisites for baryogenesis. The first model following the baryon asymmetry from the end of preheating to the final decay of the inflaton is presented in [48]. The authors assume that during the resonance stage a fraction of the initial inflaton energy is rapidly transferred to GUT bosons with mass $10m_\phi$. These bosons then decay in a CP violating manner, producing net baryon number in the process.

While the results of the toy model in [48] are very encouraging, it has a rather unpleasant feature. As shown in [7] as well as sections III B 1 and III B 2, for $g > 0$ it is quite difficult to produce particles as massive as $10m_\phi$ during preheating. Specifically, production of such particles requires a massive inflaton and $q_0 \gtrsim 10^8$. Since $m_\phi \approx 10^{13}\text{GeV}$ this corresponds to $g \gtrsim 10^{-3}$, which leads to a fine tuning problem: in order to reproduce the anisotropies in the microwave background the quartic self coupling of the inflaton is constrained to be $\lambda_\phi \lesssim 10^{-12}$, which is unnatural because λ_ϕ receives contributions of order g^2 at the one-loop level. As mentioned in [48] this problem does not arise if the value of λ_ϕ is protected by a supersymmetric non-renormalization theorem. However, so far no such model has been constructed, and in any case it is interesting to explore other solutions to the naturalness problem.

In light of these considerations our investigation of massive particle production in section III is particularly important for baryogenesis. We have shown that with $g < 0$ large amounts of heavy particles are produced even for moderate values of q_0 . In particular the naturalness condition $g^2 \lesssim \lambda_\phi$ is easily satisfied even for $m_\chi \sim 10^{14}\text{GeV}$ or more. Additionally, the production of the heavy particles is extremely rapid, so that it is not affected by competing decay channels. In fact, as explained in section III B, for $g < 0$ the decay into massive particles is much faster than the decay into light particles provided the mass is such that χ_0 and $\tilde{\chi}_0$ quickly fall out of phase. Finally, in contrast to the positive g case, with $g < 0$ heavy particles are produced by both massive and massless inflaton fields. For these reasons we feel that negative coupling baryogenesis after preheating is an exciting possibility.

In order to illustrate how this baryogenesis mechanism works we adopt the toy model presented in [48], with some minor modifications. Before doing so let us briefly mention two potential problems with the GUT baryogenesis scenario in general. First, there is the possibility that GUT symmetry is restored after inflation by a thermal or nonthermal [18,19] phase transition. This could lead to the production of cosmologically dangerous topological defects. Fortunately it seems unlikely that either type of phase transition would be strong enough to restore the symmetry, at least for large portions of parameter space [19,48]. The second potential problem with the scenario is that gravitinos are overproduced and spoil nucleosynthesis. This also does not look like a major obstacle because the late decay of the inflaton has the ability to sufficiently dilute the gravitino abundance produced early on [48,49].

The toy baryogenesis model we will analyze is as follows. When the production of massive particles shuts off ($\Phi = M_\chi/\sqrt{|g|}$) [50], there is a fraction of energy $\delta_0 \equiv \rho_\chi^0/\rho_\phi^0$ in the GUT

boson field χ . As indicated by our results in section III, we will take $\delta_0 \ll 1$. Since the χ bosons are only moderately relativistic at creation ($k \sim M_\chi$) they quickly become “cold” as the Universe expands and can be approximated as having zero kinetic energy. We assume that they decay into light particles with a constant decay rate Γ_χ . The decay of each $\chi - \bar{\chi}$ pair produces ϵ baryons, where ϵ should be thought of as an effective CP violating parameter [44]. In a realistic model ϵ is expected to be small. We also assume that the decay products thermalize instantly, which is a good approximation if they are strongly coupled. The decay of what remains of the inflaton field is modeled by a constant rate Γ_ϕ , and we will assume a hierarchy of time scales

$$H_0^{-1} \ll \Gamma_\chi^{-1} \ll \Gamma_\phi^{-1}, \quad (51)$$

where H_0 is the initial Hubble parameter. Finally, we make one important simplification over the model presented in [48]: it is assumed that at all times the temperature of the decay products is much smaller than the mass M_χ . This allows us to compute the baryon to entropy ratio n_B/s analytically. The precise criterion for the validity of the inequality $M_\chi \gg T_{\max}$ will be given below.

With these assumptions, the χ and baryon number densities *per comoving volume*, $N_\chi = n_\chi(a/a_0)^3$ and $N_B = n_B(a/a_0)^3$, evolve according to

$$\dot{N}_\chi = -\Gamma_\chi N_\chi, \quad \dot{N}_B = -\epsilon \dot{N}_\chi, \quad (52)$$

with initial conditions $N_B(t=0) = 0$ and $N_\chi(t=0) \equiv N_\chi^0 = n_\chi^0$. Note that we have neglected the production of χ particles via inverse decays, which is justified because of our assumption that the temperature $T \ll M_\chi$ at all times. This condition will be made quantitative below. The solutions for N_B and N_χ are

$$N_\chi = N_\chi^0 e^{-\Gamma_\chi t}, \quad N_B = \epsilon N_\chi^0 (1 - e^{-\Gamma_\chi t}) \quad (53)$$

The first step in computing the baryon to entropy ratio is to solve for the energy density of the baryon fluid, ρ_{rad} , which is related to the entropy density s by $s = (2\pi^2/45)(30/\pi^2)^{3/4} g_*^{1/4} \rho_{\text{rad}}^{3/4}$, since the baryon fluid is relativistic and thermal. Here g_* is the number of relativistic degrees of freedom, and we are assuming that the entropy is dominated by the relativistic particles. We will consider separately the *massless inflaton*, whose energy density scales as $\rho_\phi \propto a^{-4}$, and the *massive inflaton*, with $\rho_\phi \propto a^{-3}$.

For the *massless inflaton* we will assume that the universe is radiation dominated at all times, which requires $\rho_\phi^0 \gg \rho_\chi^0 (H_0/\Gamma_\chi)^{1/2}$. Then

$$\frac{d}{dt} \left(\rho_{\text{rad}} \left[\frac{a}{a_0} \right]^4 \right) = -\frac{a}{a_0} M_\chi \dot{N}_\chi - \frac{d}{dt} \left(\rho_\phi \left[\frac{a}{a_0} \right]^4 \right) \quad (54)$$

$$\frac{a}{a_0} = (2H_0 t + 1)^{1/2}, \quad H_0^2 = \frac{1}{3M_{\text{P}}^2} \rho_\phi^0. \quad (55)$$

Note that in order to compute the late time contribution of the last term on the right hand side of (54) to ρ_{rad} , we need not know the details of how the inflaton decays, *i.e.* the exact time dependence of $\rho_\phi(a/a_0)^4$. The relevant information is the time scale Γ_ϕ^{-1} at

which the decay takes place. We will first study the solution to Eq. (54) at early times ($t \ll \Gamma_\chi^{-1} \ll \Gamma_\phi^{-1}$) to obtain an expression for the maximum temperature. This will allow us to derive the inequality that needs to be satisfied in order that $T_{\max} \ll M_\chi$. Subsequently we will obtain the solution at intermediate ($\Gamma_\chi^{-1} < t < \Gamma_\phi^{-1}$) and late times ($t > \Gamma_\phi^{-1}$), which will be used to compute n_B/s .

Early times ($t \ll \Gamma_\chi^{-1}$) are relevant since, as we will see in a moment, the temperature reaches its maximum value at $t \sim H_0^{-1} \ll \Gamma_\chi^{-1}$. Using the fact that in our simple model $\rho_\phi = (a_0/a)^4 \rho_\phi^0 \exp(-\Gamma_\phi t)$ and early on $\dot{N}_\chi \approx -\Gamma_\chi N_\chi^0$, we find

$$\rho_{\text{rad}} \simeq \rho_\chi^0 \frac{\Gamma_\chi}{H_0} \frac{1}{3} \frac{(a/a_0)^3 - 1}{(a/a_0)^4} + \rho_\phi^0 \frac{\Gamma_\phi}{H_0} \frac{1}{2} \frac{(a/a_0)^2 - 1}{(a/a_0)^4} \quad (56)$$

Note that for $a/a_0 \gg 1$ the two terms on the right hand side scale as a^{-1} and a^{-2} , respectively. Hence ρ_{\max} is reached when a/a_0 is of order *one*, i.e. $t \sim H_0^{-1}$, and we obtain

$$\rho_{\max} \equiv \frac{\pi^2}{30} g_* T_{\max}^4 \simeq \begin{cases} 4^{-4/3} \rho_\chi^0 \frac{\Gamma_\chi}{H_0}, & \text{at } a = 4^{1/3}, & \text{when } \rho_\chi \Gamma_\chi > \rho_\phi \Gamma_\phi \\ \frac{1}{8} \rho_\phi^0 \frac{\Gamma_\phi}{H_0}, & \text{at } a = 2^{1/2}, & \text{when } \rho_\chi \Gamma_\chi < \rho_\phi \Gamma_\phi \end{cases} \quad (57)$$

so that $T_{\max} \ll M_\chi$ if

$$\rho_\chi^0 \Gamma_\chi, \rho_\phi^0 \Gamma_\phi \ll g_* M_\chi^4 H_0. \quad (58)$$

In this paper we assume that Eq. (58) is satisfied. In addition to Eq. (58) there is an upper bound on the baryon to entropy ratio n_B/s which can be used as a consistency check. Since we assume instant thermalization of the baryon fluid and $T_{\max} < M_\chi$, the number density of relativistic particles $g_* n_{\text{rad}}$ is always *larger* than the number density of decayed χ - $\bar{\chi}$ pairs, n_B/ϵ . Since the number density of relativistic particles is related to their entropy *via* $n_{\text{rad}} = [\zeta(2)/4\zeta(4)]s \simeq 0.28s$ (where $\zeta(z)$ is the Riemann zeta function) we hence have

$$\left(\frac{n_B}{s}\right) \leq \epsilon \frac{\zeta(3)}{4\zeta(4)}. \quad (59)$$

We will now derive an expression for the baryon to entropy ratio in our model. At intermediate ($\Gamma_\phi^{-1} > t > \Gamma_\chi^{-1}$) and late times ($t > \Gamma_\phi^{-1}$) the scale factor is to a good approximation $a \simeq (2H_0 t)^{1/2}$. Hence from Eq. (54)

$$\rho_{\text{rad}} \left(\frac{a}{a_0}\right)^4 = \left(\frac{\pi}{2}\right)^{\frac{1}{2}} \left(\frac{H_0}{\Gamma_\chi}\right)^{\frac{1}{2}} \rho_\chi^0 + \left\{1 - \exp\left[-\frac{\Gamma_\phi}{2H_0} \left(\frac{a}{a_0}\right)^2\right]\right\} \rho_\phi^0, \quad (60)$$

where we used $\int_0^\infty dt t^{1/2} \exp(-t) = \pi^{1/2}/2$. The second term on the right hand side of Eq. (60) first grows $\propto a^2$ and then, when the inflaton decays at $t \sim \Gamma_\phi^{-1}$, it attains a constant value ρ_ϕ^0 . Since we are assuming that $\rho_\phi^0 \gg \rho_\chi^0 (H_0/\Gamma_\chi)^{1/2}$ we find the “final” baryon to entropy ratio

$$\frac{n_B}{s} \simeq \epsilon \left(\frac{\rho_\chi^0}{g_* M_\chi^4}\right)^{\frac{1}{4}} \left(\frac{\rho_\chi^0}{\rho_\phi^0}\right)^{\frac{3}{4}} \quad (\text{massless inflaton}), \quad (61)$$

where we used $N_B = \epsilon N_\chi^0$ for $t \gg \Gamma_\chi^{-1}$. For simplicity in this, and in the results below, we ignore multiplicative numerical constants that change the final result by less than about 20%. The remarkable feature of Eq. (61) is that the final baryon to entropy ratio does not depend on the decay constants Γ_χ and Γ_ϕ . Why this is so can be understood as follows. As long as the temperature never rises close to M_χ , so that the massive χ particles are never re-populated by inverse decays, they simply decay out of equilibrium and create $N_B \simeq \epsilon N_\chi^0$ baryons, which is independent of the decay rate Γ_χ . The entropy produced per comoving volume, if dominated by the inflaton decay, is $s(a/a_0)^3 \simeq [\rho_\phi(a/a_0)^4]^{3/4} \simeq (\rho_\phi^0)^{3/4}$, again independent of the decay rate Γ_ϕ . Hence the final baryon to entropy ratio is also independent of the decay rates. In particular, even if the decay is not as simple as the one-particle out-of-equilibrium decay, but a more complex process like parametric resonance, we expect Eq. (61) to be valid as long as the inflaton decay time is much greater than the massive particles decay time, $\Gamma_\phi \ll \Gamma_\chi$, and the entropy production is dominated by the late time inflaton decay. This concludes our discussion of the massless inflaton, and we now turn to the massive case.

When the inflaton is *massive*, its number density per comoving volume decays as $N_\phi \equiv n_\phi(a/a_0)^3 = N_\phi^0 \exp(-\Gamma_\phi t)$. The evolution equation for the radiation density is then

$$\frac{d}{dt} \left(\rho_{\text{rad}} \left[\frac{a}{a_0} \right]^4 \right) = -\frac{a}{a_0} (M_\chi \dot{N}_\chi + M_\phi \dot{N}_\phi) \quad (62)$$

$$\frac{a}{a_0} = \left(\frac{3}{2} H_0 t + 1 \right)^{\frac{2}{3}}, \quad H_0^2 = \frac{1}{3M_{\text{P}}^2} \rho_\phi^0. \quad (63)$$

Note that because of our assumption that $\rho_\phi^0 \gg \rho_\chi^0$ the universe will remain matter dominated until the inflaton decays at $t \sim \Gamma_\phi^{-1}$. At early times ($t \ll \Gamma_\chi^{-1} \ll \Gamma_\phi^{-1}$) $\dot{N}_\chi \approx -\Gamma_\chi N_\chi^0$, and hence

$$\rho_{\text{rad}} \simeq \left[\rho_\chi^0 \frac{\Gamma_\chi}{H_0} + \rho_\phi^0 \frac{\Gamma_\phi}{H_0} \right] \frac{2(a/a_0)^{5/2} - 1}{5(a/a_0)^4}. \quad (64)$$

This peaks at $a/a_0 = (8/3)^{2/5} \simeq 1.48$ ($t \simeq 0.52 H_0^{-1}$), leading to a maximum temperature

$$\frac{T_{\text{max}}}{M_\chi} \simeq \left(\frac{\rho_\chi^0}{g_* M_\chi^4} \frac{\Gamma_\chi}{H_0} + \frac{\rho_\phi^0}{g_* M_\chi^4} \frac{\Gamma_\phi}{H_0} \right)^{\frac{1}{4}}, \quad (65)$$

Thus $T_{\text{max}} \ll M_\chi$ requires

$$\rho_\chi^0 \Gamma_\chi + \rho_\phi^0 \Gamma_\phi \ll g_* M_\chi^4 H_0, \quad (66)$$

which is the same constraint as in the massless inflaton case, Eq. (58).

At intermediate times ($\Gamma_\phi^{-1} > t > \Gamma_\chi^{-1}$) the scale factor is approximately $a/a_0 \simeq (3H_0 t/2)^{2/3}$ and hence

$$\rho_{\text{rad}} \left(\frac{a}{a_0} \right)^4 = \left(\frac{2}{3} \right)^{\frac{1}{3}} \Gamma \left(\frac{2}{3} \right) \left(\frac{H_0}{\Gamma_\chi} \right)^{\frac{2}{3}} \rho_\chi^0 + \frac{2}{5} \frac{\Gamma_\phi}{H_0} \rho_\phi^0 \left(\frac{a}{a_0} \right)^{\frac{5}{2}}, \quad (67)$$

where we used $\int_0^\infty dt t^{2/3} \exp(-t) = (2/3)\Gamma(2/3) \simeq 0.90$. This leads to a baryon to entropy ratio

$$\frac{n_B}{s} \simeq \epsilon \left(\frac{\rho_\chi^0}{g_* M_\chi^4} \right)^{\frac{1}{4}} \left(\frac{\Gamma_\chi}{H_0} \right)^{\frac{1}{2}} \left[1 + \frac{2}{5\Gamma(2/3)} \left(\frac{3}{2} \right)^{\frac{1}{3}} \frac{\rho_\phi^0}{\rho_\chi^0} \left(\frac{\Gamma_\chi}{H_0} \right)^{\frac{2}{3}} \left(\frac{\Gamma_\phi}{H_0} \right) \left(\frac{a}{a_0} \right)^{\frac{5}{2}} \right]^{-\frac{3}{4}}. \quad (68)$$

While the second term in square brackets is subdominant, n_B/s is to a good approximation constant and determined by the entropy release from the massive particle decay. Eventually the second term takes over and $n_B/s \propto a^{-15/8}$ until the inflaton decays at $t \sim \Gamma_\phi^{-1}$.

At late times ($t > \Gamma_\phi^{-1}$) the radiation energy density is

$$\rho_{\text{rad}} \left(\frac{a}{a_0} \right)^4 = \left(\frac{2}{3} \right)^{\frac{1}{3}} \Gamma \left(\frac{2}{3} \right) \left(\frac{H_0}{\Gamma_\phi} \right)^{\frac{2}{3}} \rho_\phi^0, \quad (69)$$

leading to a “final” baryon to entropy ratio

$$\frac{n_B}{s} \simeq \epsilon \left(\frac{\rho_\chi^0}{g_* M_\chi^4} \right)^{\frac{1}{4}} \left(\frac{\Gamma_\phi}{H_0} \right)^{\frac{1}{2}} \left(\frac{\rho_\chi^0}{\rho_\phi^0} \right)^{\frac{3}{4}} \quad (\text{massive inflaton}). \quad (70)$$

This means that for a massive inflaton the final value of the baryon to entropy ratio is suppressed by a factor $(\Gamma_\phi/H_0)^{1/2}$ in comparison to the massless case, Eq. (61). Note also that n_B/s is dependent on the decay rate Γ_ϕ , unlike in the massless case, but still independent of Γ_χ . Intuitively, this dependence can be understood as follows. For a massive inflaton the energy density scales as a^{-3} , which is slower than for the massless baryonic fluid ($\propto a^{-4}$). Hence, later inflaton decay leads to more abundant entropy production relative to the entropy of the baryonic fluid.

Before giving an estimate of n_B/s based on the equations derived above we would like to emphasize that the assumptions $T_{\text{max}} \ll M_\chi$ and $\rho_\phi^0 \gg \rho_\chi^0$ are in no way necessary for successful GUT baryogenesis after preheating. These conditions were imposed only to enable us to obtain simple analytical expressions for the baryon to entropy ratio. For a more sophisticated numerical treatment in which both these assumptions are relaxed see [48].

In order to obtain estimates for the baryon to entropy ratios that could be produced at preheating in a theory with negative coupling we need to know ρ_χ/ρ_ϕ at the time when the massive particle production shuts off. To this end we ran our code for a range of “natural” g values with $m_\chi = 10^{14}\text{GeV}$. The results are shown in figures 12(a) for a massless inflaton and 12(b) for a massive inflaton. We used the COBE values $\lambda_\phi = 3 \times 10^{-13}$ in the former case and $\lambda_\phi = 3 \times 10^{-13}$, $m_\phi = 10^{13}\text{GeV}$ in the latter case. We point out that for natural values of g there is no production with these parameters if $g > 0$. The coupling λ_χ was chosen so that $r = 10$ in all of the runs.

The ratio of energy densities ρ_χ^0/ρ_ϕ^0 can be easily obtained from figure 12. To see this recall that for the massive nonrelativistic χ particles the variance is simply related to the energy density by $\rho_\chi = M_\chi^2 \langle (\delta\chi)^2 \rangle$. Now if there is any growth at all we find that $\langle (\delta\chi)^2 \rangle$ does not *decrease* until the time at which the massive particle production is shut off. Hence the values in figure 12 are proportional to ρ_χ^0 , the energy density at the instant when production ceases. The corresponding value ρ_ϕ^0 can be obtained by estimating Φ at this time from Eq. (40). Note that this last step is a good approximation only for very heavy particles such as the ones we are considering here. For lighter χ particles the $3\lambda_\chi \langle (\delta\chi)^2 \rangle$ contribution to $m_\chi^2_{\text{eff}}$ dominates over m_χ^2 when the production shuts off.

Here we will concentrate on the massless inflaton case and obtain an estimate for n_B/s based on Eq. (61) [51]. Using $\rho_\chi^0 = M_\chi^2 \langle (\delta\chi)^2 \rangle_0$ and $\rho_\phi^0 = \lambda_\phi (\Phi^0)^4/4 \approx \lambda_\phi M_\chi^4/4|g|^2$ we obtain

$$\frac{1}{\epsilon} \frac{n_B}{s} \simeq g_*^{-\frac{1}{4}} \left(\frac{4g^2}{\lambda_\phi} \right)^{3/4} \frac{\langle (\delta\chi)^2 \rangle_0}{M_\chi^2}. \quad (71)$$

From figure 12(a) we see that the largest valley values are about $\langle (\delta\chi)^2 \rangle_0/M_\chi^2 \approx 5 \times 10^{-10}$. It is easy to check that for these values the constraint Eq. (58) is indeed satisfied provided $\Gamma_\phi, \Gamma_\chi \ll H_0$. Using this value for $\langle (\delta\chi)^2 \rangle_0$ in Eq. (71) we find

$$\frac{1}{\epsilon} \frac{n_B}{s} \sim 10^{-3}, \quad (72)$$

where we have set $g_* = 100$. This leaves plenty of parameter space for baryogenesis consistent with the observed value $(n_B/s)_{\text{observed}} \sim 4 - 7 \times 10^{-11}$.

V. SUMMARY AND CONCLUDING REMARKS

In this work we investigate the preheating dynamics in chaotic inflationary models with a negative cross-coupling between the inflaton and a second scalar field. Such couplings are completely natural in theories with more than one scalar multiplet. The details of the inflaton decay are extremely complicated, and an accurate treatment requires that one solve the full nonlinear problem. Fortunately the dynamics is dominated by states with large occupation numbers which admit a semiclassical description, so the problem can be treated by solving the classical equations of motion numerically on the lattice. We use a general renormalizable two field scalar theory that respects a $\mathbb{Z}2 \times \mathbb{Z}2$ discrete symmetry, *i.e.* the potential contains quadratic and quartic terms as in Eq. (1). Perhaps our most important finding is that the negative coupling can catalyze the inflaton decay into a heavy scalar field, opening a new window for baryogenesis at the grand unified scale with a natural choice of parameters.

In order to make our presentation self-contained, we review some of the important properties of inflaton decay for massless fields with positive coupling in section II. In the old theory of reheating with perturbative inflaton decay [45] the relevant quantity was assumed to be the reheat temperature. Based on the reheat temperature one can infer whether the grand unified symmetry is restored, whether there is a monopole problem, whether GUT baryogenesis is feasible, etc. In the new theory of reheating the inflaton decay products are typically low energy, far from equilibrium excitations, so that one cannot meaningfully assign a temperature to this infrared condensate. Instead, the relevant measure of the inflaton decay efficiency is the maximum variance the decay products reach since, with the variance known, all of the problems mentioned above can be addressed. Hence we focus on obtaining estimates of the maximum variances reached during preheating. The numerical results for cross-coupling $g > 0$ are presented in figures 3 and 5, and estimates for the maximum variances are given in Eqs. (12) - (16). (Recall that ϕ is the inflaton and χ is a scalar field coupled to it). The estimates are based on the observation that for much of the relevant parameter space the backreaction of the produced particles terminates the exponential growth when the variances reach a certain magnitude, which can be understood intuitively in terms

of the stability chart of the Mathieu equation, shown in figures 1(a) and (b). Once the critical variance is reached, a slowly varying state, which we call the scattering regime, sets in. At this stage of the evolution the slow particle production cannot keep up with the expansion of the universe and the variances start decreasing. As explained in section II B and [12], the fact that our nonlinear lattice calculations take scatterings into account is crucial for the determination of the correct maximum variances. An important consequence of the existence of the scattering regime for large values of g and λ_χ is the fact that the inflaton decays more efficiently for smaller couplings. For example, a massless inflaton decays fastest and produces the largest variances if the cross-coupling satisfies $\lambda_\phi \leq g \leq 10^2 \lambda_\phi$ (provided the self coupling of the decay product χ is not too large, $\lambda_\chi \leq g^{3/2}/\lambda_\phi^{1/2}$). The explanation of this rather counter intuitive result – that larger couplings lead to less efficient decay – is simply that larger couplings lead to more efficient scatterings and stronger backreaction, and consequently lower maximum variances. (For completeness we note that for a massive inflaton the most efficient decay into massless χ particles occurs when $q_0 \sim q_0^{\min}$ as given in Eq. (38), which translates into $10^{-7} \lesssim g \lesssim 10^{-6}$ in the case when λ_χ is small. Here we took for the inflaton mass $m_\phi \approx 2 \times 10^{13} \text{GeV}$.)

We begin our investigation of the negative cross-coupling case by considering the instability chart of the Mathieu equation (see Eqs. (2) and (3), and figure 1), which is essentially an oscillator equation with a time dependent frequency. The Mathieu equation is a good starting point since it describes the simplest possible case, namely the linearized mode equations of the second field in a static space-time when the inflaton is massive. Its usefulness goes far beyond that simple case, however. The reason is that the main features of the stability chart are extremely robust and carry over to both other models (such as a massless inflaton) as well as the expanding universe. The Mathieu equation contains the two parameters A and q which parametrize the frequency squared of the oscillator. The third important parameter is the instability index μ . The meaning of μ is simply that in one oscillation of the inflaton, the amplitude of an unstable χ mode increases by a factor $e^{2\pi\mu}$. In figures 1(a) and (b) we show the regions of stable and unstable solutions as a function of A and q , as well as some curves of constant μ . The only features of these charts which we need in order to obtain analytical estimates for the maximum variances are (i) that the maximal distance to the first instability band above the line $A = 2|q|$ is approximately $\sqrt{|q|}$, and (ii) that μ is a rapidly decreasing function of A above the line $A = 2|q|$. As stated above, these features are extremely robust, and from them one can derive the resonance shut-off condition Eq. (10) on which all of our estimates, for both positive and negative coupling, are based.

For a quartic interaction term $g\phi^2\chi^2/2$ with a positive cross-coupling g , the phase space is limited to $A \geq 2|q|$. As a consequence the instability exponent $\mu \lesssim 0.3$ for any q , which can be seen nicely in figures 1(a) and (b). Notice also that in the first unstable band above $A = 2|q|$ μ may peak at a value between $\mu \approx 0.1$ and $\mu \approx 0.3$, depending on the exact value of $|q|$. On the other hand, for a negative cross-coupling, all of the parameter space above $A = -2|q|$ is accessible. This means that $\mu \leq (4/\pi)|q|^{1/2} \gg 1$ (*cf.* Eq. (7)), and that there is a wide range of unstable modes: $\Delta k_{\text{physical}} \sim 2|q|^{1/2}\omega_\phi$. The possibility of an extremely rapid decay into a broad range of momenta motivated us to study the negative cross-coupling case in detail.

The following are our main observations and findings. As explained above, naively the maximum value of the instability coefficient is $\mu_{\text{max}} \simeq (4/\pi)|q|^{1/2}$. However, such an

instability occurs only if the expectation value of the second field is zero at the end of inflation, *i.e.* $\chi_0 = 0$. In a realistic situation this is not the case since for g negative the true minimum of the χ potential energy is displaced from the origin (note that in order to have a potential which is bounded from below the stability condition Eq. (6) must be satisfied). Our analytical analysis and numerical simulations show that quite generically the dynamics of the fields during inflation will drive χ_0 towards its true minimum. This implies that the natural initial condition at the end of inflation is $\chi_0 = \tilde{\chi}_0$, where $\tilde{\chi}_0$ is the (ϕ_0 dependent) location of the minimum of the χ potential, given by Eq. (8). Using this initial condition we studied the case of massless fields with negative coupling in section II. We found that during the early stages of the post inflationary evolution the unstable modes grow just as in the positive coupling case, with instability coefficient $\mu \sim 0.2$. This can be observed in figures 2 and 4. The reason for this behavior is as follows. As long as the χ zeromode follows its true minimum $\chi_0 = \tilde{\chi}_0$, no χ modes encounter genuine *negative coupling instability* (negative frequency squared), and hence they grow only via the standard positive g resonance mechanism, with $q_{\text{eff}} \simeq 2|g|$. This picture breaks down once the backreaction of the created χ particles becomes large enough to disrupt the evolution of χ_0 so that it stops following $\tilde{\chi}_0$. When this happens the mode amplitudes become unstable and grow very fast, quickly reaching values large enough to terminate the instability, and the slowly varying scattering regime sets in. During this stage we find that the dynamics of the negative cross-coupling model differs profoundly from that with a positive cross-coupling. Perhaps the most striking difference is that the χ variance peaks at a significantly larger value – by a factor $4|g|^{1/2}$ larger than in the positive g case – leading to a much more complete inflaton decay into χ particles. This difference can be understood from the instability chart in figure 1. To shut off the resonance in the positive g case, one needs a backreaction of order $\delta A \sim q^{1/2}$, while in the negative g case a much larger shift $\delta A \sim 4|g|$ is required. Estimates for the maximum variances with a negative cross-coupling are given in Eqs. (20) and (21). Another notable difference between $g > 0$ and $g < 0$ is the way the variances fluctuate between “peak” and “valley” values as the inflaton oscillates in the scattering regime. We present a simple explanation of this phenomenon using the matching of two oscillator solutions with different frequencies (see Eqs. (24) – (28)). The peak to valley ratio in the case of massive fields is discussed at the end of section III B 3.

In section III we study in detail the decay of the inflaton into massive particles ($m_\chi \neq 0$). Sections III B 1 and III B 2 discuss the positive coupling case for a massless and massive inflaton, respectively. The main conclusion is that the estimates for the maximum variances obtained in section II B (Eqs. (12), (13), and (15)) hold also for a massive χ field *provided* that q_0 is larger than a critical value q_0^{min} given by Eqs. (35) and (39). (see also [39].)

For $g < 0$ the situation is very different. The criterion for the *complete* particle production shut-down is $m_\chi^2 > |g|\Phi^2$ (*cf.* Eq. (40)), where $\Phi = \Phi(t)$ is the inflaton amplitude, which decreases due to the expansion of the Universe. As explained in section III B 3, particles can be produced only at the moment when $m_\chi = |g|\phi_0^2(t)$, and while $\phi_0(t)$ is growing. The minimum condition to encounter *any* massive particle production is hence $|g| \geq m_\chi^2/\Phi_1^2$, where $\Phi_1 \approx 10^{18}\text{GeV}$ is the inflaton amplitude at the first extremum in the oscillatory regime. For $m_\chi = 10^{14}\text{GeV}$, this gives $|g| \gtrsim 10^{-8}$, which agrees well with our numerical results in figures 12(a) and (b). To encounter n chances to grow, the required value of $|g|$ increases as given in Eq. (46). Note that this value is many orders of magnitude *smaller* than the value

$g \gtrsim 10^{-3}$ required for the production of equally massive particles in the positive g case. The particle production mechanism is very different from the usual positive g resonance, and we call it *negative coupling instability*. The details are complicated, but the main mechanism can be readily understood and is explained in sections III B 3 - III B 5. Characteristic features of this new process are that massive particles are produced in extremely rapid bursts over a broad range of momenta (much faster and broader than in the positive g case). This is illustrated in figures 9 and 11(a). Another important feature are the sharp spikes in the production of massive χ particles as a function of the parameters, seen in figures 7, 10, and 12. This behavior is explained with the aid of a simple analytical model in section III B 3 (see Eqs. (41) – (46)). The system may be considered “chaotic” in the sense that it is quite impossible to predict the exact position and amplitude of the spikes as a function of the parameters.

The main result of section III can be re-stated as follows. For a realistic choice of couplings, which in chaotic inflationary models is constrained by the COBE satellite measurements to be $\lambda_\phi \approx 3 \times 10^{-13}$ or $m_\phi \lesssim 2 \times 10^{13} \text{GeV}$, one can produce massive particles with $m_\chi \sim 10^{14} \text{GeV}$ (as required by GUT baryogenesis models), provided $|g| \gtrsim 10^{-8}$ and $\lambda_\chi > 3 \times 10^{-4}$ (for stability) (see figures 12(a) and (b)). This means that the parameter space available for production of massive particles with “natural” coupling constants is appreciable: $10^{-6} \gtrsim |g| \gtrsim 10^{-8}$, $1 > \lambda_\chi > 3 \times 10^{-4}$, leaving plenty of opportunity for baryogenesis model building. This is to be contrasted with the positive g case for which $g \gtrsim 10^{-3}$ is required. Such a large value leads to an unpleasant fine tuning problem since the small value of λ_ϕ needs to be protected against radiative corrections.

To obtain an estimate of the baryon asymmetry that could be produced during preheating we study a simple toy model in section IV. In short, the model can be described as follows. Initially a certain amount of energy is transferred from the inflaton to a heavy GUT scalar field *via* the nonperturbative mechanisms described in this paper. The result is a cold (far from equilibrium) fluid of massive particles (with a mass M_χ), which we assume decays in a B and CP violating manner into light degrees of freedom that instantly thermalize. In order to treat the problem analytically we further assume that at all times the temperature T of the light relativistic particles is $\ll M_\chi$, which requires that Eq. (58) is satisfied. The main results of this investigation are the final baryon to entropy ratios given in Eqs. (61) and (70) for a massless and massive inflaton, respectively. These equations are obtained assuming a “natural” hierarchy of time scales, $H_0 \gg \Gamma_\chi \gg \Gamma_\phi$. As can be seen from Eq. (61), under these conditions the baryon to entropy ratio for a massless inflaton has the pleasant property that it is independent of the decay rates Γ_χ and Γ_ϕ . We believe that this feature, which can be understood intuitively and is explained in section IV, lends more credibility to our result since the final estimate is somewhat independent of the details of the model. Eqs. (61) and (70) say that the final baryon to entropy ratio is proportional to the initial energy density in χ particles. Since the energy density of the (nonrelativistic) χ particles is proportional to their variance ($\rho_\chi \approx M_\chi^2 \langle (\delta\chi)^2 \rangle$), the spikes in figure 12 are directly imaged to spikes in baryon production. For a massless inflaton the final baryon to entropy ratio is expressed in terms of the maximum variance in Eq. (71) [51]. Our numerical results indicate that it is not hard to obtain values in the range $n_B/s \sim \epsilon \times 10^{-3}$, where ϵ is the effective CP violating parameter in our model. Clearly more realistic models for GUT baryogenesis at preheating will have to be constructed to verify the viability of this scenario, but the

preliminary results look promising.

Another interesting question that deserves further study is whether it is possible to construct a model such that the *negative coupling instability* discussed in this paper does not require any “phase mismatch” to become operational. In other words, the aim is to obtain natural initial conditions at the end of inflation that immediately allow the inflaton to decay rapidly into a heavy scalar field. The preliminary investigation of one realization of such a scenario is underway.

Close to completion of this work we received a preprint [hep-ph/9704452] [52] in which the preheating dynamics in an expanding universe is also studied in detail. In this very interesting paper the authors focus exclusively on the *massive inflaton, positive g , small λ_χ* case, for which their conclusions partially overlap with ours. A detailed comparison will be deferred to future publications.

ACKNOWLEDGMENTS

This research was conducted using the resources of the Cornell Theory Center, which receives major funding from the National Science Foundation (NSF) and New York State, with additional support from the Advanced Research Projects Agency (ARPA), the National Center for Research Resources at the National Institutes of Health (NIH), IBM Corporation, and other members of the center’s Corporate Partnership Program. We would like to thank Andrei Linde for useful comments. BRG acknowledges partial funding from the NSF and Alfred P. Sloan Foundation. TP acknowledges funding from the NSF, and hospitality of Columbia University, where part of this work was done.

REFERENCES

- [1] J. H. Traschen and R. H. Brandenberger, Phys. Rev. D **42**, 2491 (1990).
- [2] L. Kofman, A. D. Linde and A. A. Starobinskii, Phys. Rev. Lett. **73**, 3195 (1994).
- [3] Parametric resonance is not effective for fermions due to the Pauli principle, as first demonstrated in A. D. Dolgov and D. P. Kirilova, Sov. Nucl. Phys. **51**, 172 (1990).
- [4] For a recent review see A. Linde, *Lectures on Inflationary Cosmology*, report No. SU-ITP-94-36, hep-th/9410082 (1994).
- [5] This is the case when $m_\phi^2 \gg \lambda_\phi \Phi_0^2$, where Φ_0 is the oscillation amplitude. In the opposite limit the oscillations are given by elliptic functions, but for the purposes of this illustration the difference is immaterial.
- [6] Y. Shtanov, J. Traschen and R. Brandenberger, Phys. Rev. D **51**, 5438 (1995).
- [7] S. Yu. Khlebnikov and I. I. Tkachev, report No. PURD-TH-96-06, hep-ph/9608458 (1996).
- [8] David I. Kaiser, report No. HUTP-97-A005, hep-ph/9702244 (1997); R. Allahverdi and B. A. Campbell, report No. A LBERTA-THY-18-96, hep-ph/9606463 (1996); D. T. Son, Phys. Rev. D **54**, 3745 (1996). D. Kaiser, Phys. Rev. D **53**, 1776 (1996).
- [9] H. Fujisaki, K. Kumekawa, M. Yamaguchi, and M. Yoshimura, Phys. Rev. D **53**, 6805 (1996); H. Fujisaki, K. Kumekawa, M. Yamaguchi, and M. Yoshimura, Phys. Rev. D **54**, 2494 (1996); M. Yoshimura, Prog. Theor. Phys. **94**, 873 (1995).
- [10] For a fully quantum mechanical treatment, but neglecting scattering, see D. Boyanovsky, D. Cormier, H.J. de Vega, R. Holman, A. Singh, and M. Srednicki, report No. CMU-HEP-97-05, hep-ph/9703327 (1997); D. Boyanovsky, D. Cormier, H. J. de Vega, R. Holman, A. Singh, M. Srednicki, report No. UCSBTH-96-23, hep-ph/9609527 (1996); D. Boyanovsky, H. J. de Vega, R. Holman, and J. F. J. Salgado, Phys. Rev. D **54**, 7570 (1996); D. Boyanovsky, M. D'Attanasio, H. J. de Vega, R. Holman, and D.-S. Lee, Phys. Rev. D **52**, 6805 (1995); and references therein.
- [11] S. Yu. Khlebnikov, I. I. Tkachev, Phys. Rev. Lett. **77**, 219 (1996).
- [12] Tomislav Prokopec and Thomas G. Roos, Phys. Rev. D **55**, 3768 (1997);
- [13] S. Yu. Khlebnikov and I. I. Tkachev, report No. PURD-TH-96-08, hep-ph/9610477 (1996).
- [14] M. J. O. Strutt, *Ergebnisse der Mathematik und ihrer Grenzgebiete*, Vol. I, no. 3, Springer, Berlin (1932); A. Erdélyi, W. Magnus, F. Oberhettinger, and F. G. Tricomi, *Higher transcendental functions*, Vol. 3, McGraw-Hill, New York (1955).
- [15] A simple estimate can be obtained as follows. Note that $\Omega_\chi^2 \equiv A_0 - 2q_0 \cos(2z)$ oscillates in the range $[-4|q_0|, 0]$ along the line $A_0 = -2|q_0|$. Eq. (2) then reduces to an inverted harmonic oscillator with a time dependent frequency. Naively one can write $\Omega_\chi^2 = -2|q_0|$, its average value over one oscillation, to obtain $\mu \sim (2|q_0|)^{1/2}$ which is close to $\mu = (4/\pi)|q_0|^{1/2}$, the value obtained from the exact expression Eq. (7).
- [16] The initial conditions for the inhomogeneous modes are chosen as follows. Each mode with momentum k is treated like a quantum harmonic oscillator in its ground state. The initial amplitudes of the mode and its velocity are then picked randomly from gaussian distributions with variances proportional to $1/(4\omega_k)$ and $\omega_k/4$, respectively. Here $\omega_k^2 = k^2 + m^2$, $m^2 = V''(\phi_0, \chi_0)$ (the derivatives are with respect to the appropriate field), and ϕ_0 and χ_0 are the initial values of the field zero modes. See [12] for details.

- [17] This can be seen as follows. Since any inhomogeneities are quickly redshifted, one can neglect the gradient terms in the EOM for the fields during inflation. In addition the second order time derivatives can be neglected during the slow roll. In order to investigate what is the deviation of χ_0 from $\tilde{\chi}_0$, we write $\chi_0 = \tilde{\chi}_0 + \delta\chi$, and hence $3H\dot{\tilde{\chi}}_0 + (m_\chi^2 + g\Phi_0^2 + 3\lambda_\chi\tilde{\chi}_0^2)\delta\chi = 0$. This leads to $\delta\chi/\tilde{\chi}_0 \simeq 0.1|q|^{-1}$ for $r \gg 1$ and $m_\chi \ll (|g|/\lambda_\phi)^{1/2}\omega_\phi$. Note that this last condition reduces to $m_\chi \ll |g|^{1/2}\Phi$ for a massless inflaton. In section III B we show that particles with mass $m_\chi > |g|^{1/2}\Phi$ cannot be produced, and so are not interesting for the purpose at hand.
- [18] L. Kofman, A. Linde, A. A. Starobinskii, Phys. Rev. Lett. **76**, 1011 (1996); I. I. Tkachev, Phys. Lett. **B 376**, 35 (1996); A. Riotto and I. I. Tkachev, Phys. Lett. **B 385**, 57 (1996); G. W. Anderson, A. Linde and A. Riotto, Phys. Rev. Lett. **77**, 3716 (1996).
- [19] S. Kasuya and M. Kawasaki, report No. KUNS-9999, hep-ph/9703354 (1997).
- [20] We define the end of slow roll by the time at which $\dot{\phi}_0 = H\phi_0$, where ϕ_0 is determined by its slow roll value $-(3H)^{-1}dV(\phi_0, \tilde{\chi}_0)/d\phi$. The ratio ϕ_0/M_{P} is actually dependent on $|g|/\lambda_\chi$, but for our runs $|g|/\lambda_\chi < 1/2$ and the effect on the value of ϕ_0/M_{P} is negligible.
- [21] We speak of a scattering regime when the resonance is shut off while most of the energy is still in the inflaton zeromode. The result is a state with slowly evolving variances and smooth power spectra characteristic of efficient scattering [11–13]. For massless fields, positive g and $q_0^{1/2}r < 1$ the scattering regime is reached when $q_0 \gtrsim 25$. For $q_0^{1/2}r \gtrsim 1$ the condition becomes $q_0r \gtrsim 2$. For negative g the scattering regime is reached when $|q_0|^{2/3}r > 1$. All of these conditions are derived by comparing the energy in fluctuations at the time the maximum variances are reached to the energy remaining in the zeromode of the inflaton. The maximum variances reached are derived in section II B.
- [22] We found in [12] that for the first few resonances above $A = 2|q|$ the maximum μ_k decays approximately as $\mu_k \propto \exp[-\alpha(k^2 + m_{\chi,\text{eff}}^2)/\Delta k_{\text{res}}^2]$, where $\Delta k_{\text{res}}^2 \simeq \sqrt{g}\omega_\phi\Phi_0/2 = q^{1/2}\omega_\phi$ is the distance between the resonances, and $\alpha \simeq 1.1$. The width of the resonances is also decreasing exponentially. See [9] for analytical estimates.
- [23] At first sight one may think that the shift required to kill the first resonance above $A = 2|q|$ is given by the width of this first band and not by its distance to the one above it. It must be remembered, however, that the parameters that enter q are changing due to the decay (as well as due to the expansion in the massive case, see section III), shifting q to smaller values. This means that the position of the first band constantly sweeps through a range of order \sqrt{q} above $A = 2q$. The shift required to shut off this band is hence \sqrt{q} .
- [24] Φ_s is always the amplitude of the inflaton zeromode oscillations at the time when $\langle(\delta\chi)^2\rangle$ reaches its maximum in an expanding universe. As discussed in the text, depending on the parameters ϕ can decay into its own fluctuations, so $\langle(\delta\phi)^2\rangle$ may still grow after $\langle(\delta\chi)^2\rangle$ reaches its maximum.
- [25] A simple estimate based on a WKB approximation can be obtained as follows: $\langle(\delta\phi)^2\rangle_{\text{scatt}} = \int[d^3k/((2\pi)^3\omega_k)]n_k \sim (2\pi^2)^{-1}\omega_\phi^2/\lambda_\phi \simeq 0.05\Phi^2(\tau_s^\phi)$, where we assumed that the scattering regime is reached when the occupation numbers $n_k \sim \lambda_\phi^{-1}$, and that the variance is dominated by momenta of order $\omega_\phi = c\sqrt{\lambda_\phi}\Phi$. This estimate is in reasonable agreement with the maximum variances reached in our runs. The amplitude $\Phi(\tau)$ at the time τ_s^ϕ at which the maximum variance is reached can be estimated from $\Phi \propto a^{-1}$, $a = (1 + H_0\tau)$, and $n_{\text{res}}^\phi \approx \exp 2\mu_\phi\omega_\phi^0\tau$. With $n(\tau_s^\phi) \sim \lambda_\phi^{-1}$ and $H_0 \sim \sqrt{\lambda_\phi}M_{\text{P}}$

- one obtains $\Phi(\tau_s^\phi) \sim 2c\mu_\phi\Phi_0/\ln(\lambda_\phi^{-1})$. For $\lambda_\phi = 10^{-12}$, $\Phi_0 = 1.8M_P$, and $\mu_\phi \sim 0.04$ one finds $\langle(\delta\phi)^2\rangle_{\text{scatt}} \sim 10^{-6}M_P^2$.
- [26] The fraction of the total energy in χ fluctuations at the beginning of the scattering regime is of order $0.2 \times q^{-1/2}$ for small λ_χ , and of order $0.2 \times g/\lambda_\chi$ for large λ_χ . These estimates apply to both massive and massless particles. For a massless inflaton the last expression can be rewritten as $\sim 0.1 \times (rq)^{-1}$. In deriving these expressions, we used the fact that the energy density in fluctuations and the variance are at the beginning of the scattering regime dominated by the same momenta, and hence $\rho_\chi \sim (k_{\text{res}}^\chi)^2 \langle(\delta\chi)^2\rangle_{\text{peak}}$.
- [27] In our runs we observe that even after χ_0 stops following $\tilde{\chi}_0$ its dynamics is still strongly influenced by ϕ_0 and it often oscillates with frequency $n\omega_\phi/2$, where typically $n = 3, 4$ or 5 . For n odd, χ_0 develops an expectation value, indicating symmetry breaking. Here we will not investigate further the physical implications of this observation.
- [28] For negative g , $3\lambda_\chi \langle(\delta\chi)^2\rangle$ always dominates over $|g| \langle(\delta\phi)^2\rangle$ for $q \gtrsim 1$ due to the stability bound $r > 1$ (*cf.* Eq. (6)). Here we are concerned with the early evolution before the χ production shuts off. At late times ϕ can decay into its own fluctuations and hence $\langle(\delta\phi)^2\rangle$ can grow significantly larger than $\langle(\delta\chi)^2\rangle$, but this is obviously irrelevant for obtaining an estimate of $\langle(\delta\chi)^2\rangle_{\text{peak}}$.
- [29] Equipartition of energy implies that $\rho_{\delta\phi} \sim \rho_{\delta\chi}$. The energies can be related to the variances as follows. In terms of the occupation numbers, the variances can be written as: $\langle(\delta\chi)^2\rangle_{\text{scatt}} \sim (2\pi^2)^{-1}n_k^\chi(k\Delta k)_\chi \sim (2\pi^2)^{-1}n_k^\chi(2|q|^{1/2})\omega_\phi^2$ and $\langle(\delta\phi)^2\rangle_{\text{scatt}} \sim (2\pi^2)^{-1}n_k^\phi(k\Delta k)_\phi \sim (2\pi^2)^{-1}n_k^\phi\omega_\phi^2$, where we have assumed that the variances are dominated by the momenta of order $k_\chi \sim \Delta k_\chi \sim k_{\text{res}} \simeq (4|q|)^{1/4}\omega_\phi$ and $k_\phi \sim \Delta k_\phi \sim \omega_\phi$, respectively. At early stages of the scattering regime the same momenta dominate the energy densities, so we can write $\rho_\chi \sim (2\pi^2)^{-1}n_k^\chi(k^3\Delta k)_\chi \sim (2\pi^2)^{-1}n_k^\chi(4|q|)\omega_\phi^4 \sim 2|q|^{1/2}\omega_\phi^2 \langle(\delta\chi)^2\rangle$ and $\rho_\phi \sim (2\pi^2)^{-1}n_k^\phi(k^3\Delta k)_\phi \sim (2\pi^2)^{-1}n_k^\phi\omega_\phi^4 \sim \omega_\phi^2 \langle(\delta\phi)^2\rangle$. This then leads immediately to $\langle(\delta\phi)^2\rangle \sim 2|q|^{1/2} \langle(\delta\chi)^2\rangle$, implying Eq. (21).
- [30] The maximum unstable momentum of the χ field is approximately $k_{\text{res}}^\chi \sim \omega_\phi q^{1/2}$ in the negative g case, while $k_{\text{res}}^\phi \sim \omega_\phi$. The ratio hence goes like $q^{1/2}$, which requires excellent IR resolution in order to capture both accurately. This must be combined with sufficient ultraviolet (UV) range to accommodate the created particles and model their scattering towards higher momenta. Since the χ particles scatter more efficiently for larger r the UV cutoff must be increased as r is increased.
- [31] Our numerical results indicate that the dependence of n_{scatt} on the parameters is actually more complicated, but the expressions given in the text are roughly correct. Since the dependence of τ_s on n_{scatt} is anyway only logarithmic and since as discussed in the text there is significant variation in the relevant value of μ for small changes in the parameters the uncertainty in the value of n_{scatt} need not concern us here.
- [32] When $g\phi_0^2$ is large, χ_0 is trapped in the deep minimum at $\tilde{\chi}_0$. However, as ϕ_0 approaches zero it loses its grip on χ_0 and χ_0 wants to oscillate about the origin with frequency $\omega_\chi \approx (3\lambda_\chi \langle(\delta\chi)^2\rangle)^{1/2}$. In the beginning ω_χ is very small and χ_0 does not have time to complete a significant portion of an oscillation in the interval when ϕ_0 is small (more precisely, when $g\phi_0^2 < 3\lambda_\chi \langle(\delta\chi)^2\rangle$). It is easy to show that when $3\lambda_\chi \langle(\delta\chi)^2\rangle \approx 2g^{1/2}\omega_\phi\Phi$ the χ zeromode has enough time to complete half an oscillation. It is then completely out of phase with $\tilde{\chi}_0$ when ϕ_0 becomes large again, and consequently stops following its minimum. Note that even before this complete phase mismatch occurs there are small

- mismatches each time ϕ_0 grows after crossing zero, once $\langle(\delta\chi)^2\rangle$ becomes appreciable. This is the reason why the χ variance can grow larger than its positive g value given in Eq. (16) before χ_0 stops following $\tilde{\chi}_0$. We point out that the mechanism of χ_0 falling out of phase with $\tilde{\chi}_0$ will play an important role when we discuss the massive χ case in section III. As we will see, in that case the effects can be even more dramatic.
- [33] As we will see in section III, this is no longer correct when the χ field is massive.
- [34] This “random phase” approximation is clearly only sensible if there is enough time between matchings for the solution to “oscillate”. This requires that the n^{th} time interval Δt_n between matchings satisfies $\Delta t_n \gtrsim 1/\omega_n = e^{n\epsilon}/\omega_{\text{max}}$. The minimum total time required is then $T = \sum_{n=0}^{N-1} \Delta t_n = \omega_{\text{max}}^{-1} [(\omega_{\text{max}}/\omega_{\text{min}} - 1)/(e^\epsilon - 1)]$. In the text we are interested in the limit when ϵ is small and the ratio of frequencies is large, so $T \simeq (\epsilon\omega_{\text{min}})^{-1}$. Now from Eq. (25) we found $\omega_{\text{min}}^2 \sim q^{1/2}\omega_\phi^2$, and the total time for the frequency to change between ω_{max} and ω_{min} is a quarter period of ϕ_0 , $T = \pi/(2\omega_\phi)$. This yields $\epsilon \sim q^{-1/4}$, and so the approximation in the text is reasonable for large q .
- [35] Note that we are applying the COBE constraints to the couplings of the ϕ field even though the slow roll during inflation takes place in the direction $(\phi_0, \tilde{\chi}_0)$. This is justified because the ϕ field dominates the dynamics during inflation, in the sense that the energy density and the slope of the potential at the point $(\phi_0, \tilde{\chi}_0)$ are given by $\lambda_\phi\phi_0^4/4$ and $\lambda_\phi\phi_0^3$, respectively, up to corrections of order $1/r$. Since r is larger than one (*cf.* Eq. (6)), and there is no reason for r to be close to this bound, these corrections are generally small. We have chosen $r = 10$ for all of the runs presented in this paper, except for a few of the points in figure 6. For a derivation of the COBE bounds, see, for example, M.S. Turner, in *Particle Physics, Astrophysics, and Cosmology* (XXIIth SLAC Summer Institute), edited by J. Chan and L. DePorcel; astro-ph/9703196.
- [36] The “occupation numbers” plotted in figures 8(b) and 9(b) are defined in terms of the fourier modes of the field *via* $n_k^\chi = \frac{\omega_k^\chi}{2} \langle \chi_{\vec{k}} \chi_{-\vec{k}} \rangle + \frac{1}{2\omega_k^\chi} \langle \dot{\chi}_{\vec{k}} \dot{\chi}_{-\vec{k}} \rangle$, where $\omega_k^\chi = (k^2 + m_\chi^2 + g\langle(\delta\phi)^2\rangle + 3\lambda_\chi\langle(\delta\chi)^2\rangle)^{1/2}$, and the brackets denote averaging over directions.
- [37] We point out that for the run in figure 8 the production is so low that the χ variance barely rises above the level of background fluctuations as set by the initial conditions. This contribution is proportional to the ultraviolet cutoff and therefore has no physical relevance. It scales with the expansion of the Universe as a^{-2} since it is dominated by the relativistic UV modes. For typical runs we present, the background variance is negligible in comparison to the variance from resonant production. There are, however, a few runs with very little production, and for these the variance we record on the figures is dominated by the background fluctuations. Examples are a few of the lowest points on figures 7, 10, and 12 with typical values of order $10^{-13} - 10^{-12} M_{\text{P}}^2$.
- [38] Note that for $\lambda_\phi \lesssim 10^{-12}$, as required by COBE [35], and $\Phi_0 = 1.8M_{\text{P}}$, $\omega_\phi^0 = c\lambda_\phi^{1/2}\Phi_0 \simeq 4 \times 10^{12}\text{GeV}$, which is a few times smaller than the value of the inflaton mass (in the massive case) given by COBE. This means that, in order to reach the scattering regime for $m_\chi \simeq 10^{14}\text{GeV}$ in the massless inflaton case, one needs values of q_0 about two orders of magnitude larger than for $m_\chi/\omega_\phi^0 = 10$, *i.e.* $q_0 \gtrsim 10^{11}$.
- [39] Note that the expression for $\langle(\delta\chi)^2\rangle_{\text{peak}}$ given in Eq. (16) is *not* valid for a massive inflaton. Also, the criterion determining “large λ_χ ” becomes $\lambda_\chi > (2/3)g^{3/2}\Phi_s/m_\phi$, with Φ_s given by Eq. (36).
- [40] Note that reference [13] uses $M_{\text{Pl}} \equiv G^{-1/2}$ while in this paper $M_{\text{P}} \equiv (8\pi G)^{-1/2} \simeq$

- $2.4 \times 10^{18} \text{GeV}$.
- [41] The reader may have noticed that initially the variances of the $m_\chi^2 = 5.4 \times 10^{-11} M_{\text{P}}^2$ and $5.5 \times 10^{-11} M_{\text{P}}^2$ runs overlap almost perfectly while the variance of the $5.3 \times 10^{-11} M_{\text{P}}^2$ run is slightly larger. This is simply due to the fact that the lattice spacing, and hence the ultraviolet cutoff of the theory, is slightly different for the latter run.
 - [42] Since we are interested in large growth factors for which the probability is small we can replace $1 - (1 - \mathcal{P}_\epsilon)^n$ with $n\mathcal{P}_\epsilon$. We will also not distinguish between growing “at least once” *vs.* growing “exactly once”, *etc.*
 - [43] This is easily established by comparing the maximum positive g resonant momentum $k_{\text{res}}^{\text{phys}}(g > 0) \approx q^{1/4} m_\phi$ to m_χ at the time of the first zero crossing of the inflaton zero mode $\phi_0(t)$ (which is the first time that particles could be produced in the positive g case).
 - [44] For an introduction, see *The Early Universe*, Edward W. Kolb and Michael S. Turner, Addison-Wesley (1990).
 - [45] A. A. Starobinskii, in *Quantum Gravity, Proceedings of the Second Seminar “Quantum Theory of Gravity”* (Moscow, 13 - 15 Oct. 1981), eds. M. A. Markov and P. C. West (Plenum, New York, 1984), p. 103; A. Dolgov and A. Linde, *Phys. Lett.* **116B**, 329 (1982); L. F. Abbott, E. Farhi, and M. Wise, *Phys. Lett.* **117B**, 29 (1982).
 - [46] We are assuming here the same chaotic inflationary framework as in the rest of the paper.
 - [47] In the old theory the reheat temperature is of order $T_r \sim \sqrt{\Gamma M_{\text{P}}}$, where Γ is the total decay rate of the inflaton. Imposing naturalness conditions on the couplings of the inflaton to other fields in order to stabilize the small value $\lambda_\phi \approx 3 \times 10^{-13}$ against radiative corrections then implies $T_r \lesssim 10^{10} \text{GeV}$.
 - [48] Edward W. Kolb, Andrei Linde, and Antonio Riotto, *Phys. Rev. Lett.* **77**, 4290 (1996).
 - [49] M. Yoshimura, report No. TU-96-500, hep-ph/9605246 (1996); reference 2 of [9].
 - [50] We will use M_χ from now on for the mass of the GUT boson. This is to remind the reader that the field in question is not quite the real scalar field χ with mass m_χ used in our numerical simulations.
 - [51] The analysis is equally simple for the massive case, but as discussed previously we prefer the massless inflaton because a ϕ^4 term is anyway required if $g < 0$ and setting $m_\phi^2 \sim \lambda_\phi \Phi_0^2$, as we have done by choosing the COBE values for both parameters, actually corresponds to mild tuning. Additionally, unlike Eq. (70), Eq. (61) has the nice feature that n_B/s is independent of the unknown decay rates Γ_ϕ and Γ_χ .
 - [52] L. Kofman, A. Linde, and A. A. Starobinskii, report no. hep-ph/9704452.

FIGURES

FIG. 1. (a) : The stability chart of the Mathieu equation, Eq. (2). The dark regions correspond to stable solutions while the light regions correspond to exponential instabilities. We also show contours of constant μ , where μ is the instability index. The curve $\mu = 0$ divides the parameter space into stable and unstable regions. The contours shown are $\mu = \{0, 0.1, 0.2, 0.3, 0.5, 1.0, 2.0, 3.0\}$. The lines $A_0 = 2|q_0|$ and $A_0 = -2|q_0|$ are also plotted. (The plot was generated numerically, and in order to keep the file size small we used a fairly coarse grid. The instability bands really extend all the way to $q_0 = 0$ at the points $A_0 = n^2$, $n = 1, 2, 3, \dots$. Also, for negative A_0 the narrow regions of stability form continuous bands rather than the “island” structure shown.)

FIG. 1. (b) : The stability chart of the Mathieu equation for large A_0 and q_0 . As in figure 1(a) the dark regions correspond to stable solutions while the light regions correspond to exponential instabilities. The contours shown are $\mu = \{0, 0.1, 0.2, 0.3, 0.5, 1.0\}$, and the line $A_0 = 2|q_0|$ is also plotted. Notice that the distance between resonance bands above $A_0 = 2|q_0|$ for fixed q_0 is $\delta A_0 \approx |q_0|^{1/2}$. Notice also that the instability index μ decreases rapidly with increasing A_0 .

FIG. 2. The expectation values of the fields as a function of time for negative coupling, $|q_0| \approx 35$, $r = 10$ ($m_\chi = m_\phi = 0$, $\lambda_\phi = 10^{-12}$, $\lambda_\chi = 10^{-7}$, $g = -10^{-10}$).

FIG. 3. The expectation values of the fields as a function of time for positive coupling, $q_0 \approx 35$, $r = 10$ ($m_\chi = m_\phi = 0$, $\lambda_\phi = 10^{-12}$, $\lambda_\chi = 10^{-7}$, $g = 10^{-10}$).

FIG. 4. The variances of the fields as a function of time for negative coupling, $|q_0| \approx 35$, $r = 10$ ($m_\chi = m_\phi = 0$, $\lambda_\phi = 10^{-12}$, $\lambda_\chi = 10^{-7}$, $g = -10^{-10}$).

FIG. 5. The variances of the fields as a function of time for positive coupling, $q_0 \approx 35$, $r = 10$ ($m_\chi = m_\phi = 0$, $\lambda_\phi = 10^{-12}$, $\lambda_\chi = 10^{-7}$, $g = 10^{-10}$).

FIG. 6. (a): Peak and valley lattice variances at the beginning of the scattering regime as a function of $|q_0|$ for negative coupling and two values of r .

FIG. 6. (b): Maximum physical peak and valley variances reached in the expanding universe as a function of $|q_0|$ for negative coupling and two values of r .

FIG. 7. (a): Maximum variances as a function of m_χ for several values of $|q_0|$, with $r = 10$ and $g < 0$. The inflaton is massless ($m_\phi = 0$) and $\lambda_\phi = 10^{-12}$ throughout.

FIG. 7. (b): A blow-up of the $q_0 = -350$ curve shown in figure 7(a).

FIG. 8. (a): The variances for a set of parameters for which there is little particle production. $|q_0| = 350$, $r = 10$ ($m_\phi^2 = 0$, $m_\chi^2 = 2.9 \times 10^{-11} M_{\text{P}}^2$, $\lambda_\phi = 10^{-12}$, $\lambda_\chi = 10^{-5}$, $g = -10^{-9}$).

FIG. 8. (b): The χ field occupation numbers at various times for the run of figure 8(a).

FIG. 9. (a): The variances for a set of parameters for which there is significant particle production. $|q_0| = 350$, $r = 10$ ($m_\phi^2 = 0$, $m_\chi^2 = 4 \times 10^{-11} M_{\text{P}}^2$, $\lambda_\phi = 10^{-12}$, $\lambda_\chi = 10^{-5}$, $g = -10^{-9}$).

FIG. 9. (b): The χ field occupation numbers at various times for the run of figure 9(a).

FIG. 10. Maximum variances as a function of m_χ for $|q_0| \approx 350$, $r = 10$ and $g < 0$. The inflaton is massive ($m_\phi^2 = 7.2 \times 10^{-13} M_{\text{P}}^2$, $\lambda_\phi = 10^{-12}$, $\lambda_\chi = 10^{-5}$, $g = -10^{-9}$).

FIG. 11. (a): The χ field variances for three runs with slightly different χ masses ($m_\phi^2 = 7.2 \times 10^{-13} M_{\text{P}}^2$, $\lambda_\phi = 10^{-12}$, $\lambda_\chi = 10^{-5}$, $g = -10^{-9}$).

FIG. 11. (b): The evolution of the χ field zeromode χ_0 for the three runs with slightly different χ masses shown in figure 11(a) ($m_\phi^2 = 7.2 \times 10^{-13} M_{\text{P}}^2$, $\lambda_\phi = 10^{-12}$, $\lambda_\chi = 10^{-5}$, $g = -10^{-9}$).

FIG. 12. (a): Maximum peak and valley variances as a function of $|g|$ for $m_\chi = 10^{14} \text{GeV}$. The inflaton is massless ($m_\phi = 0$), $\lambda_\phi = 3 \times 10^{-13}$, $g < 0$ and λ_χ is adjusted to keep $r = 10$.

FIG. 12. (b): Maximum peak and valley variances as a function of $|g|$ for $m_\chi = 10^{14} \text{GeV}$, $m_\phi = 10^{13} \text{GeV}$, and $\lambda_\phi = 3 \times 10^{-13}$. Here λ_χ is adjusted to keep $r = 10$ and $g < 0$.

Figure 1(a)

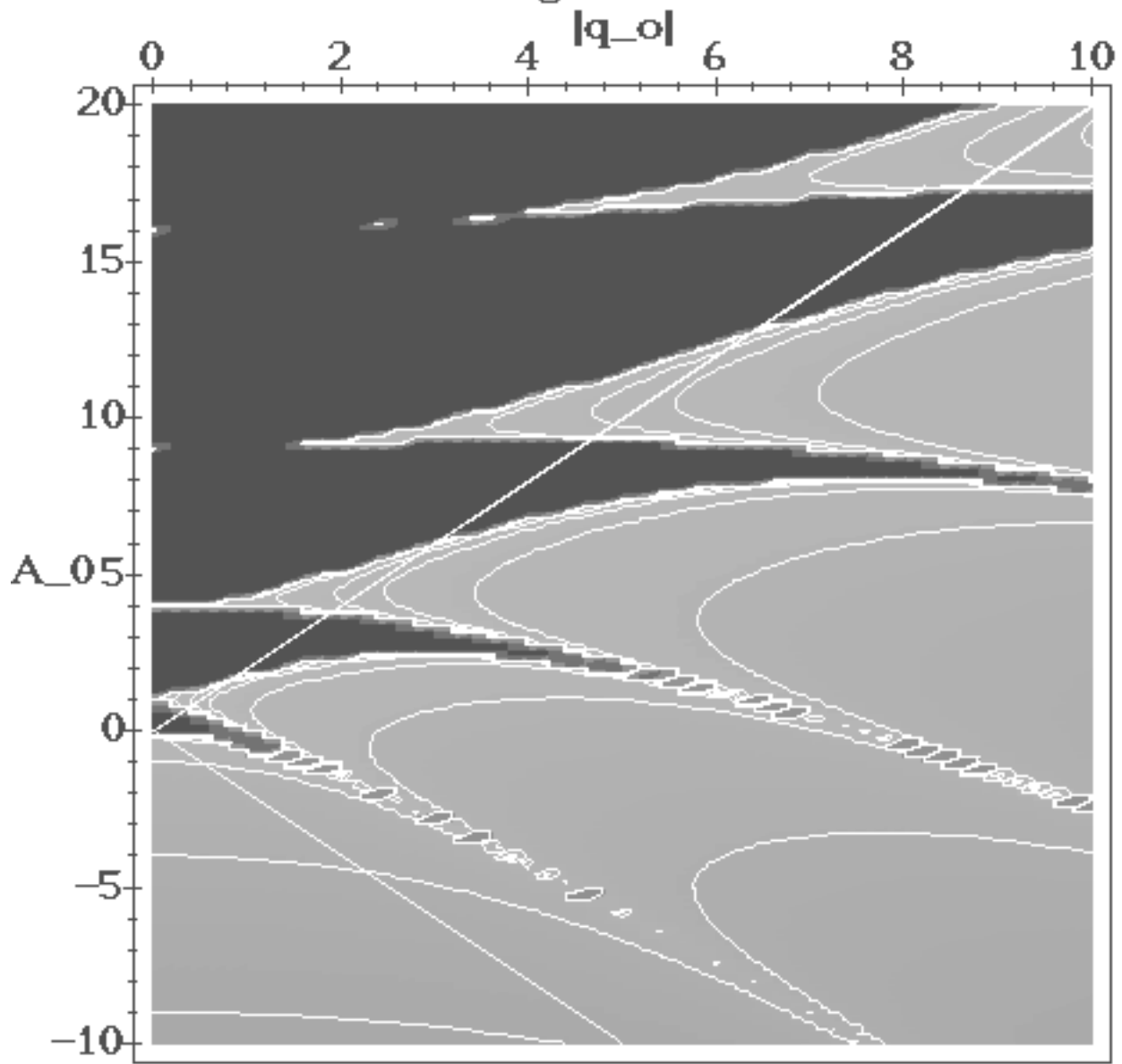


Figure 1(b)

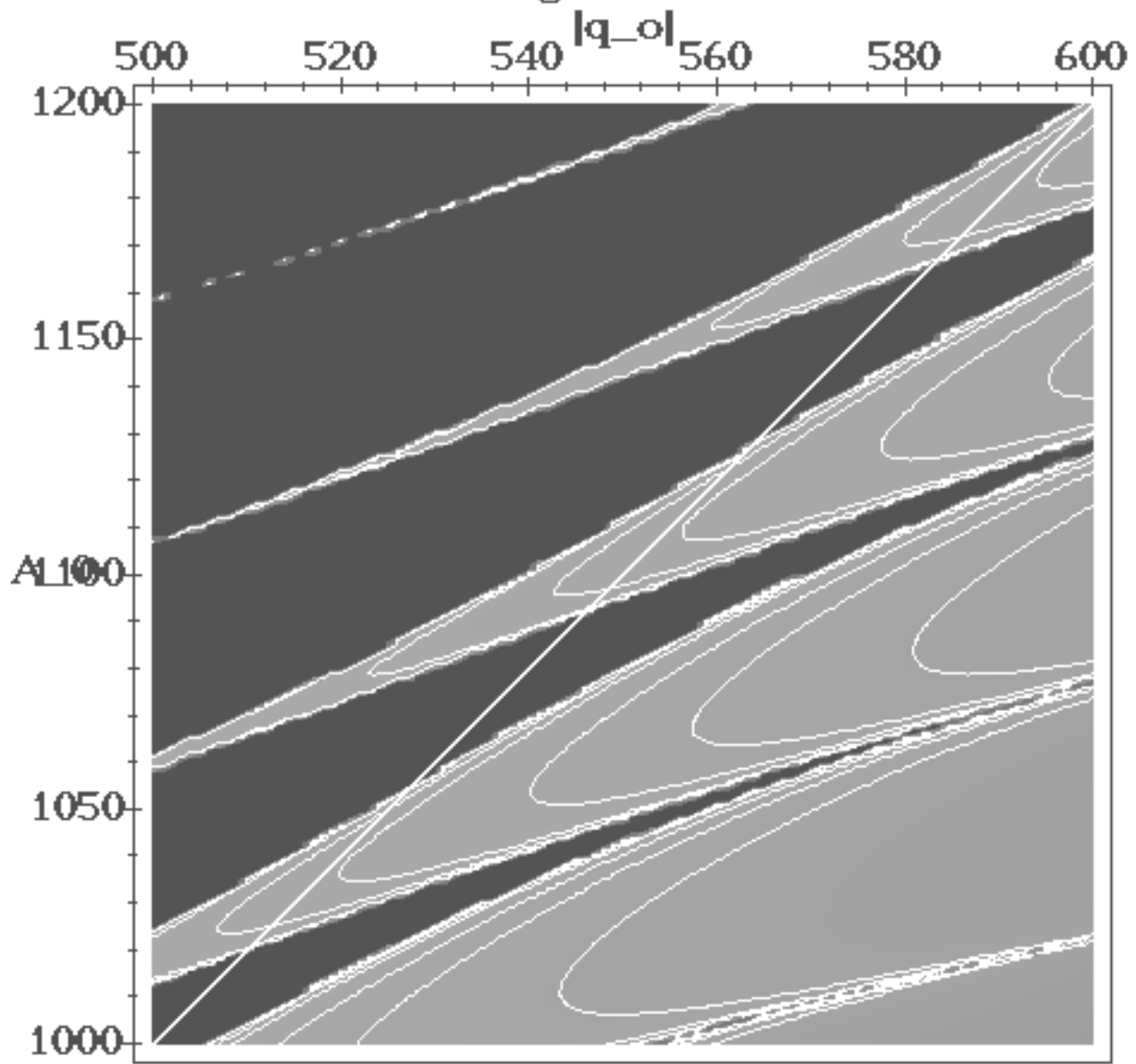


Figure 2

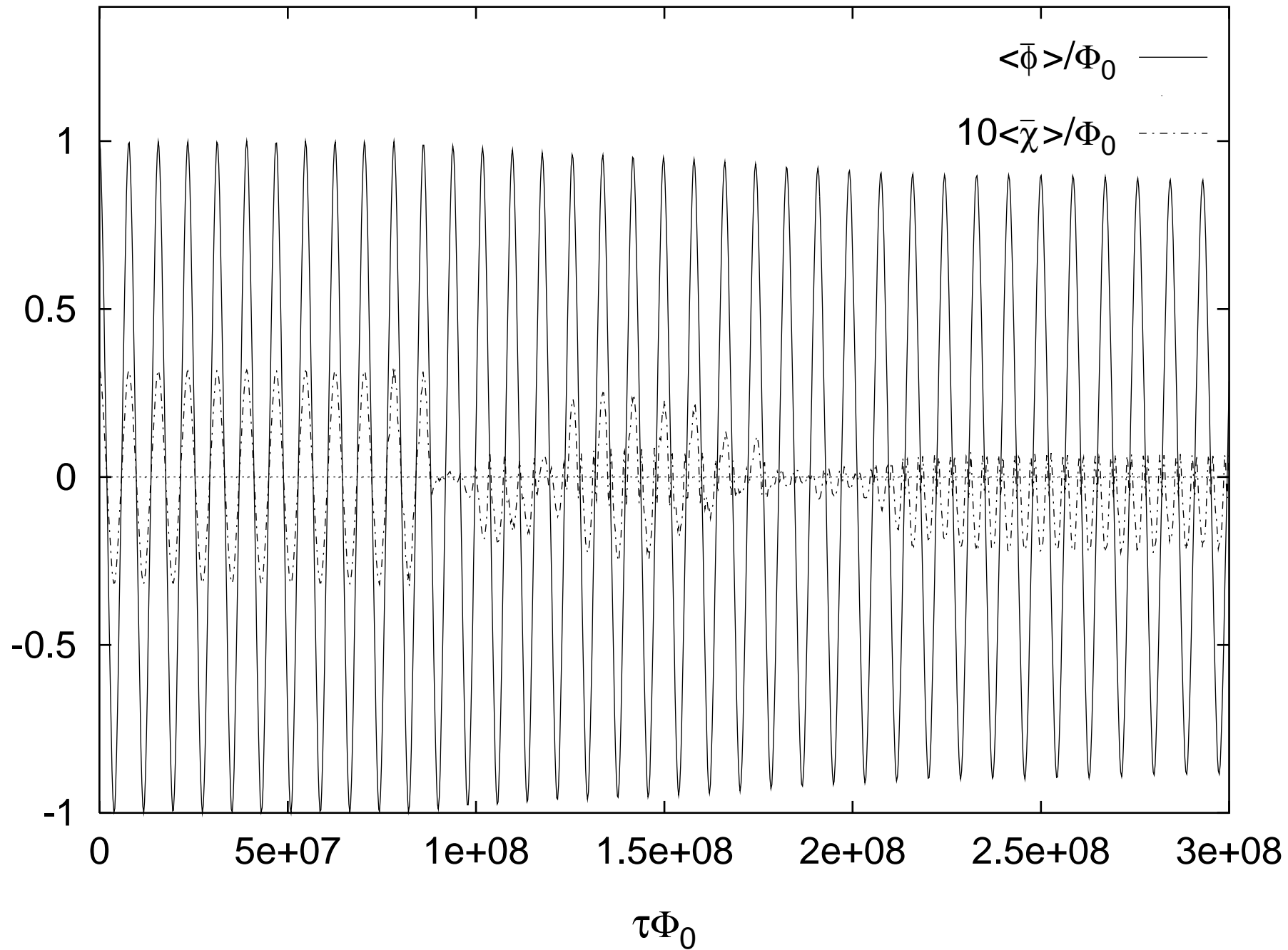


Figure 3

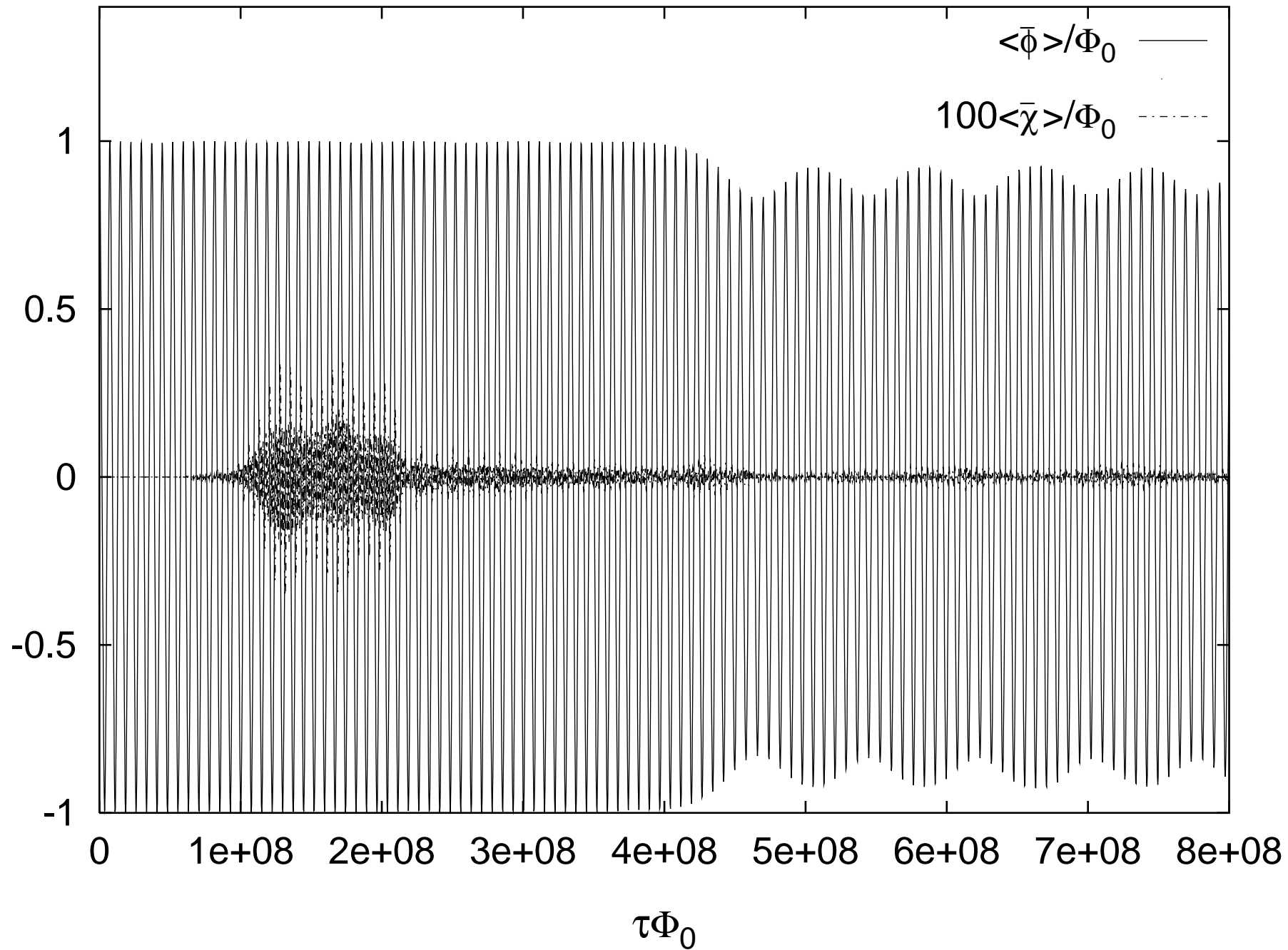


Figure 4

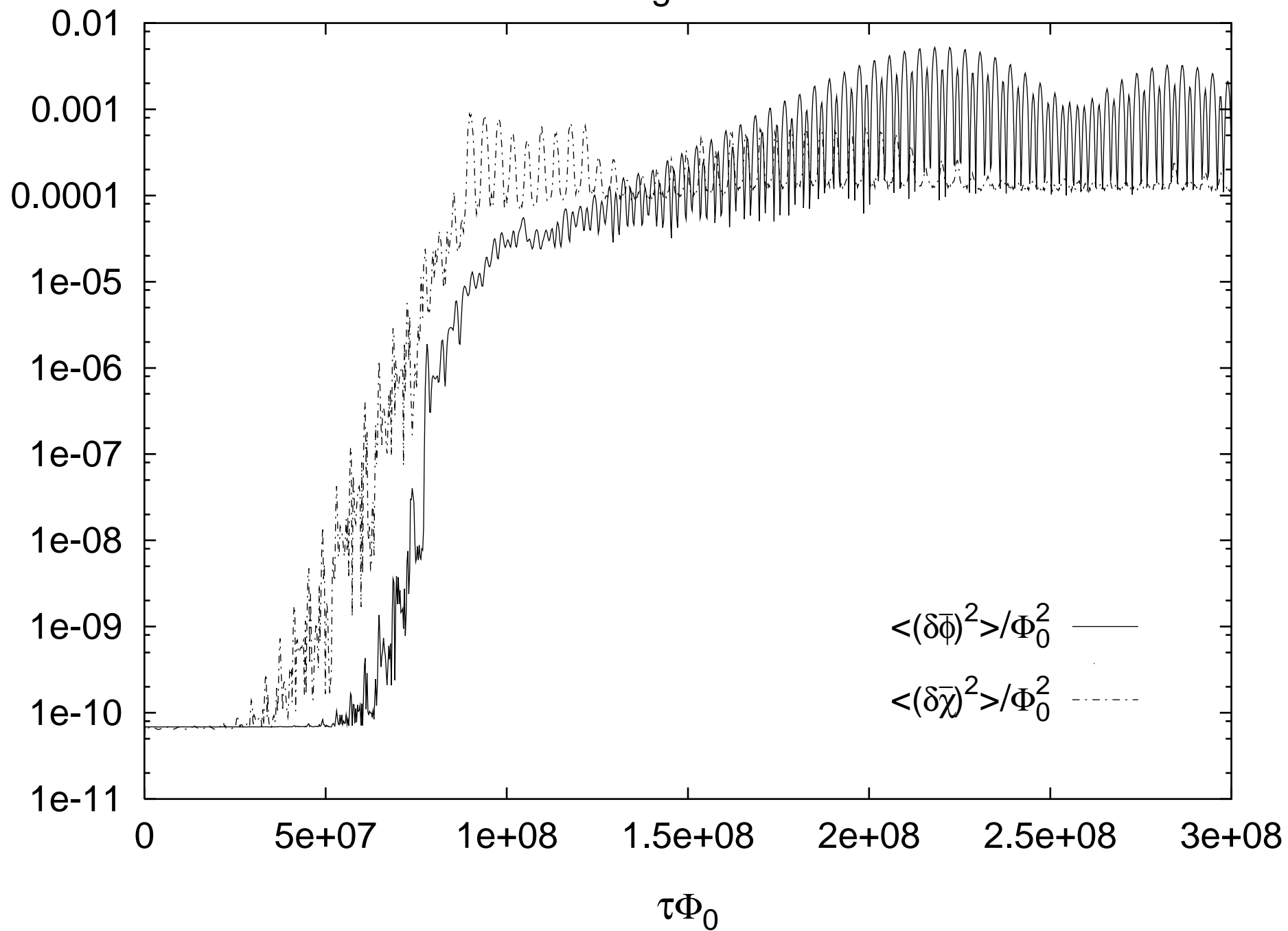


Figure 5

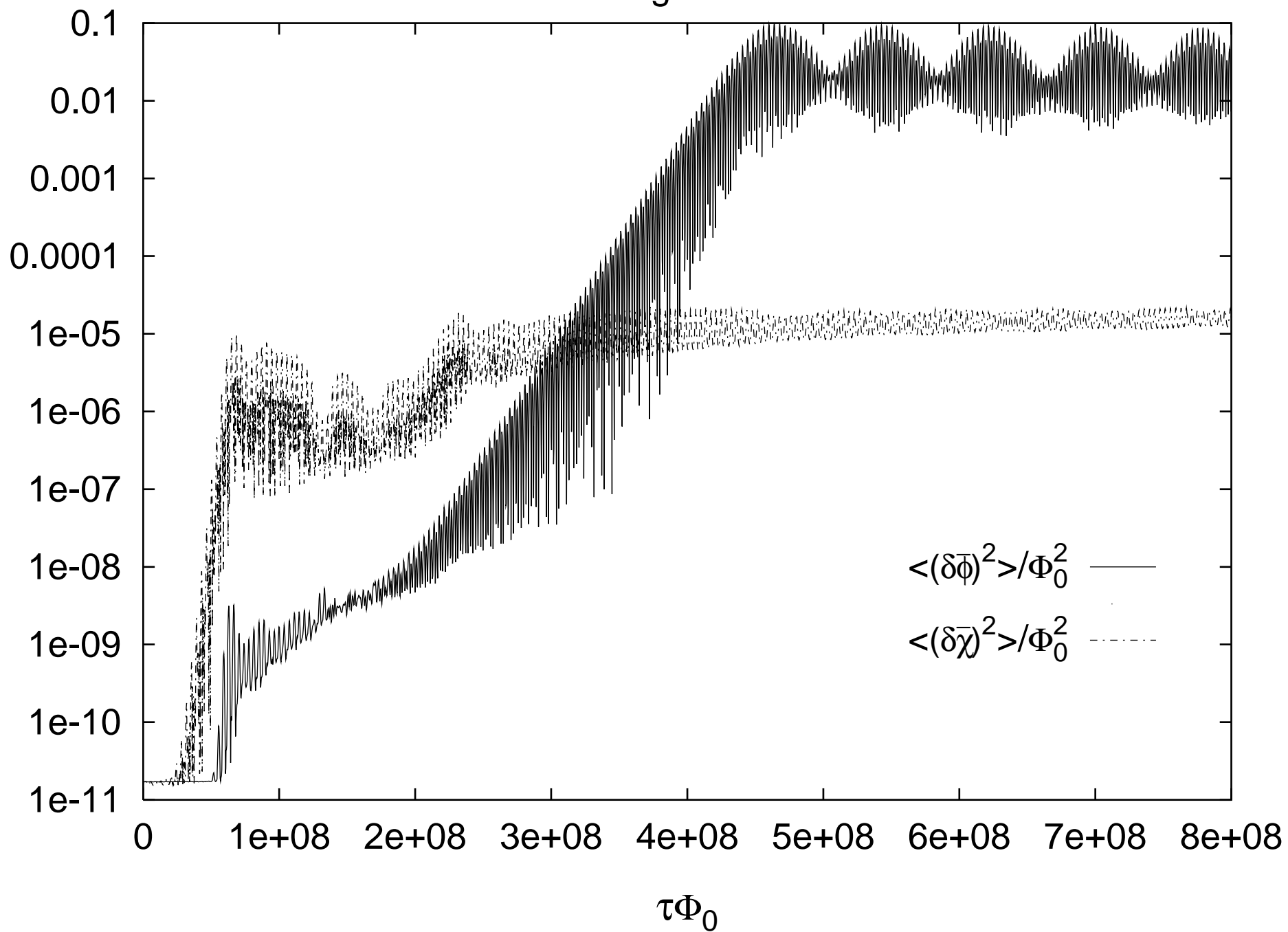


Figure 6(a)

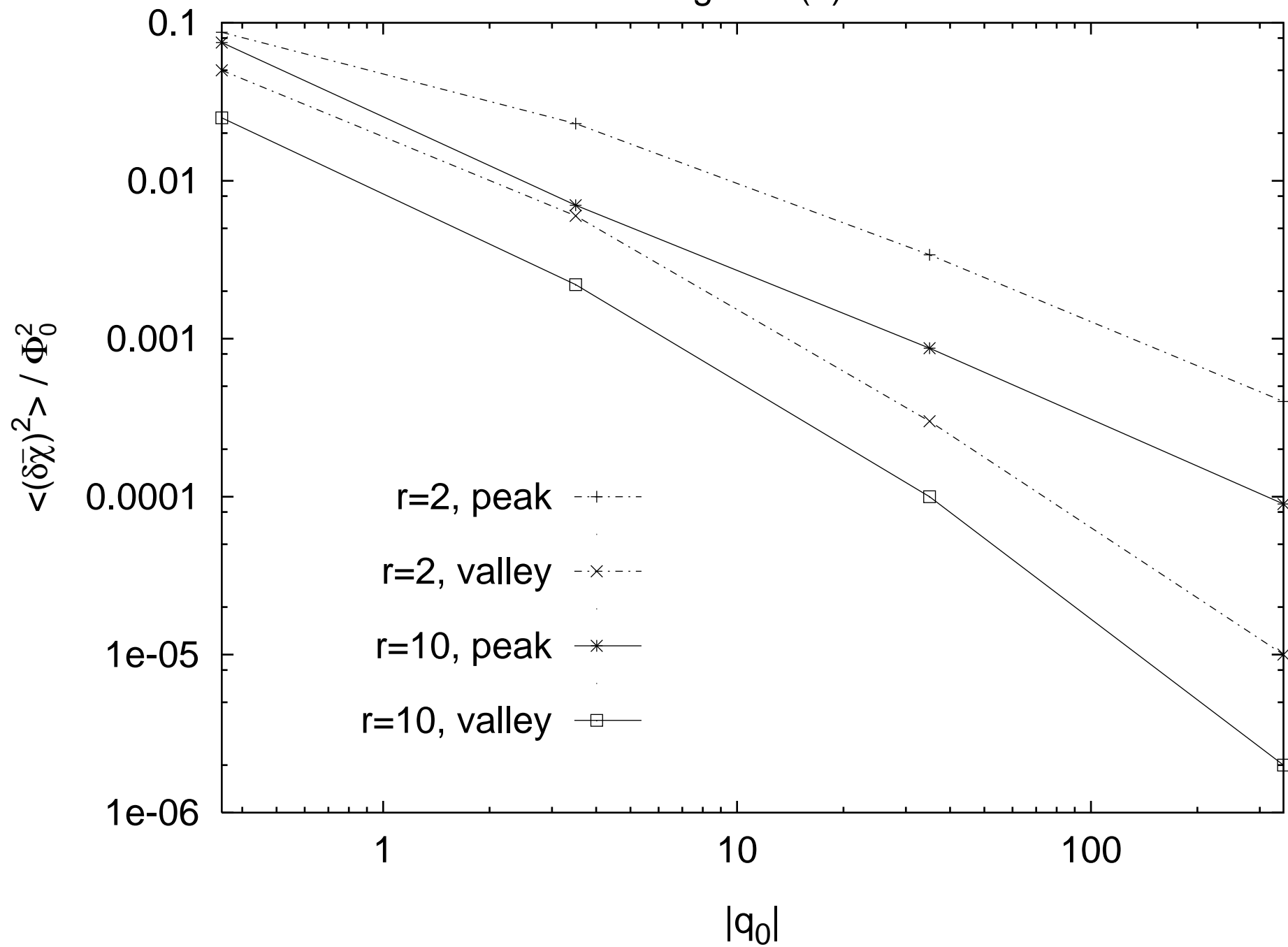


Figure 6(b)

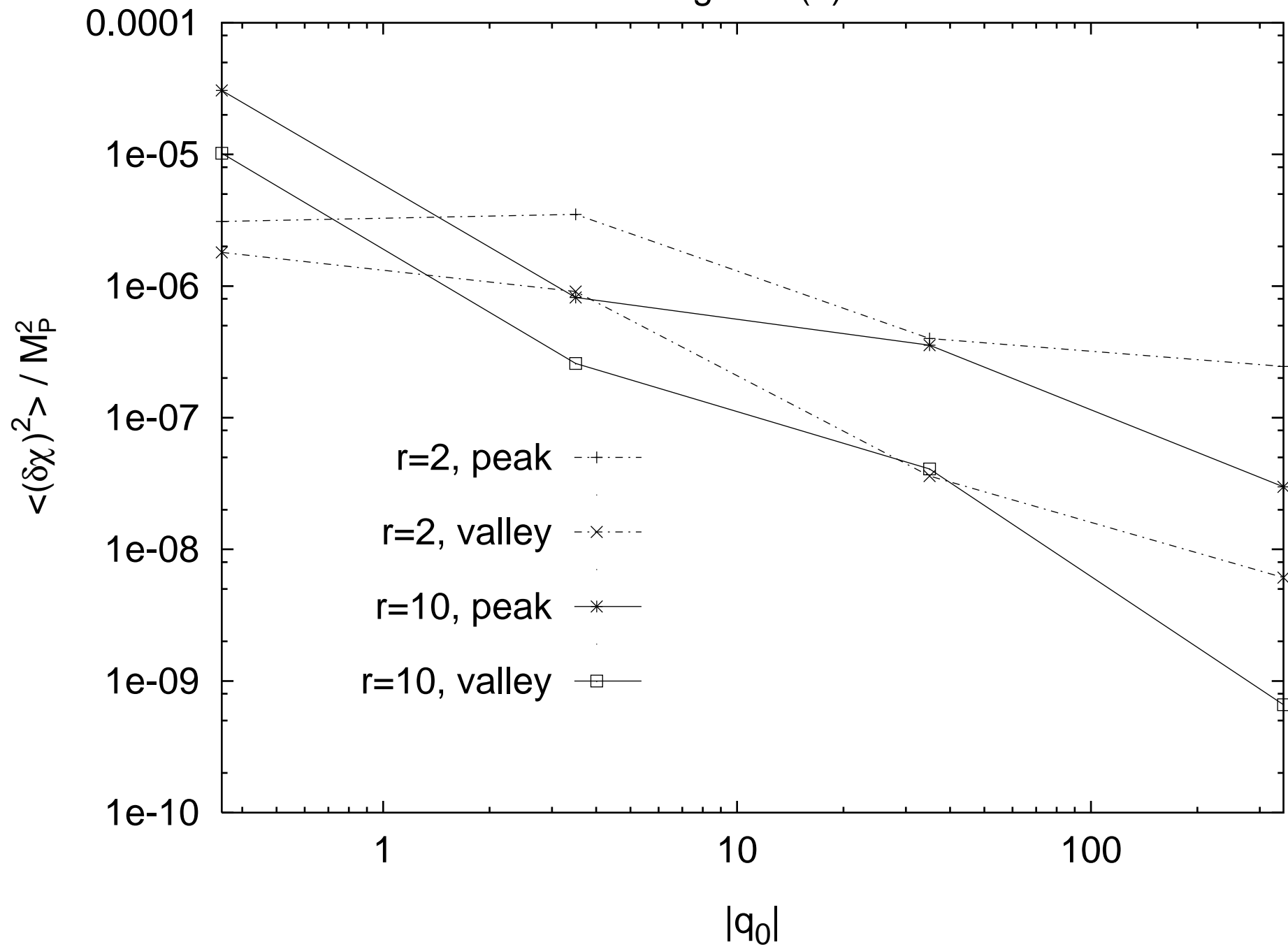


Figure 7(a)

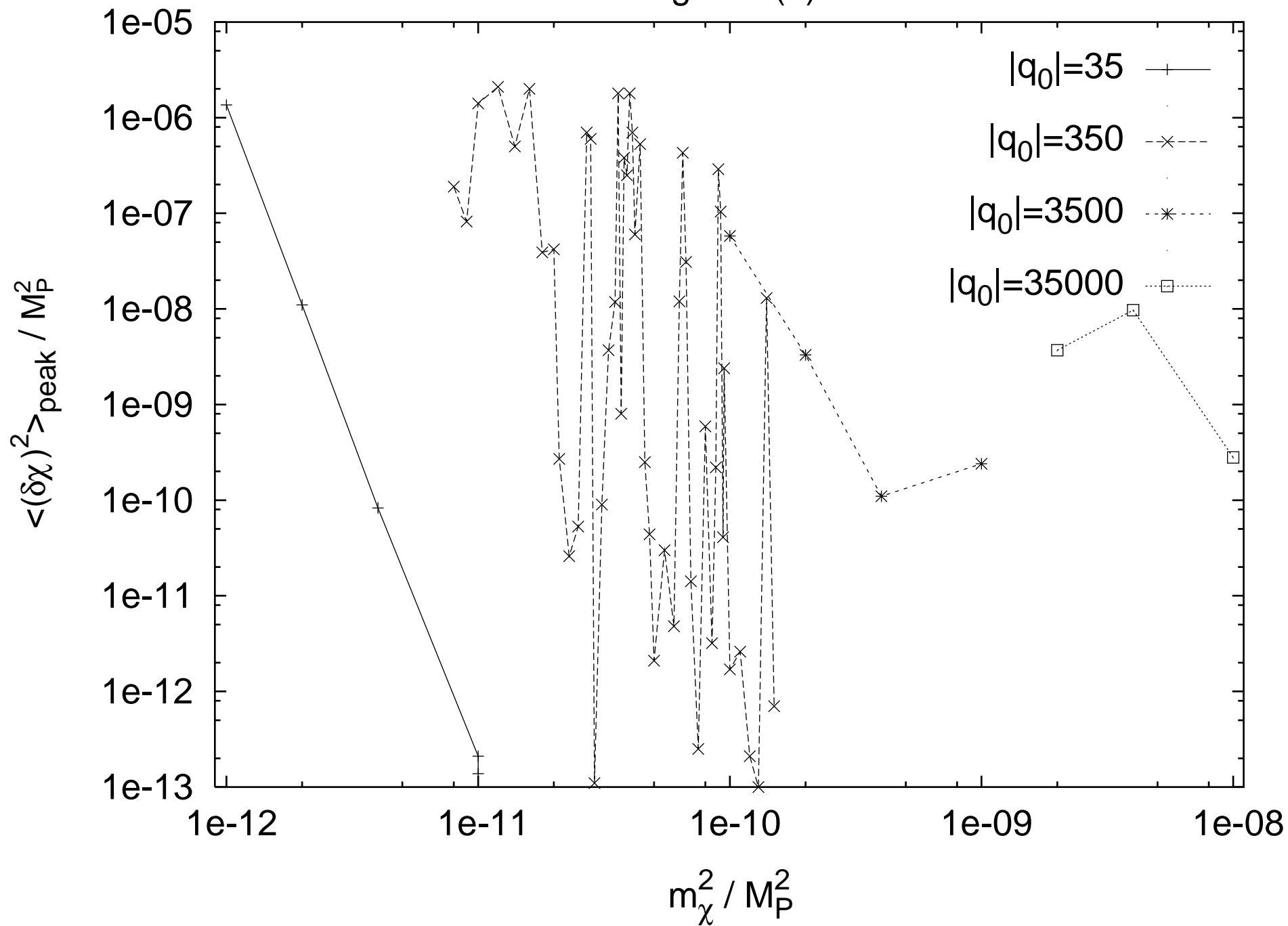


Figure 7(b)

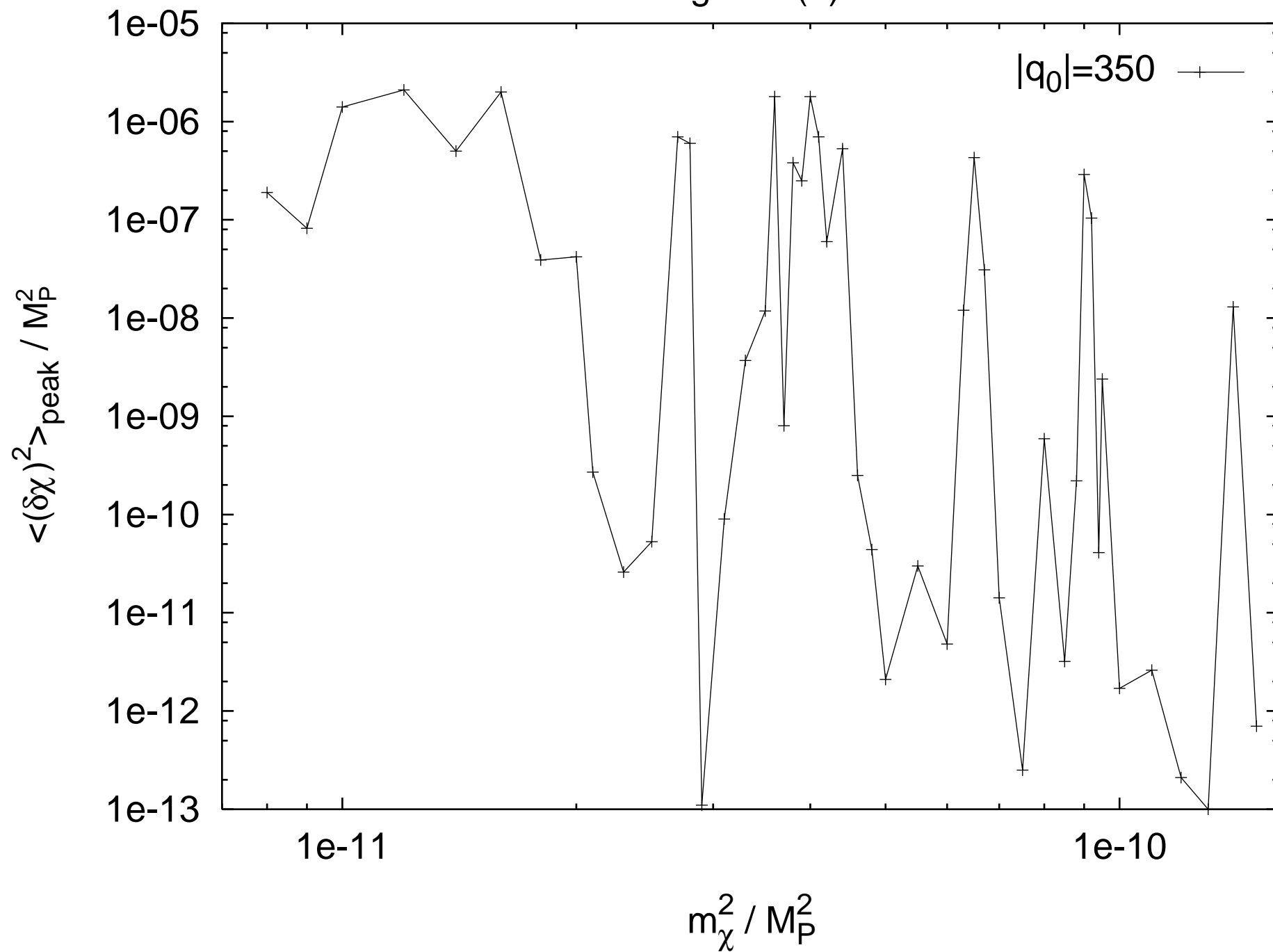


Figure 8(a)

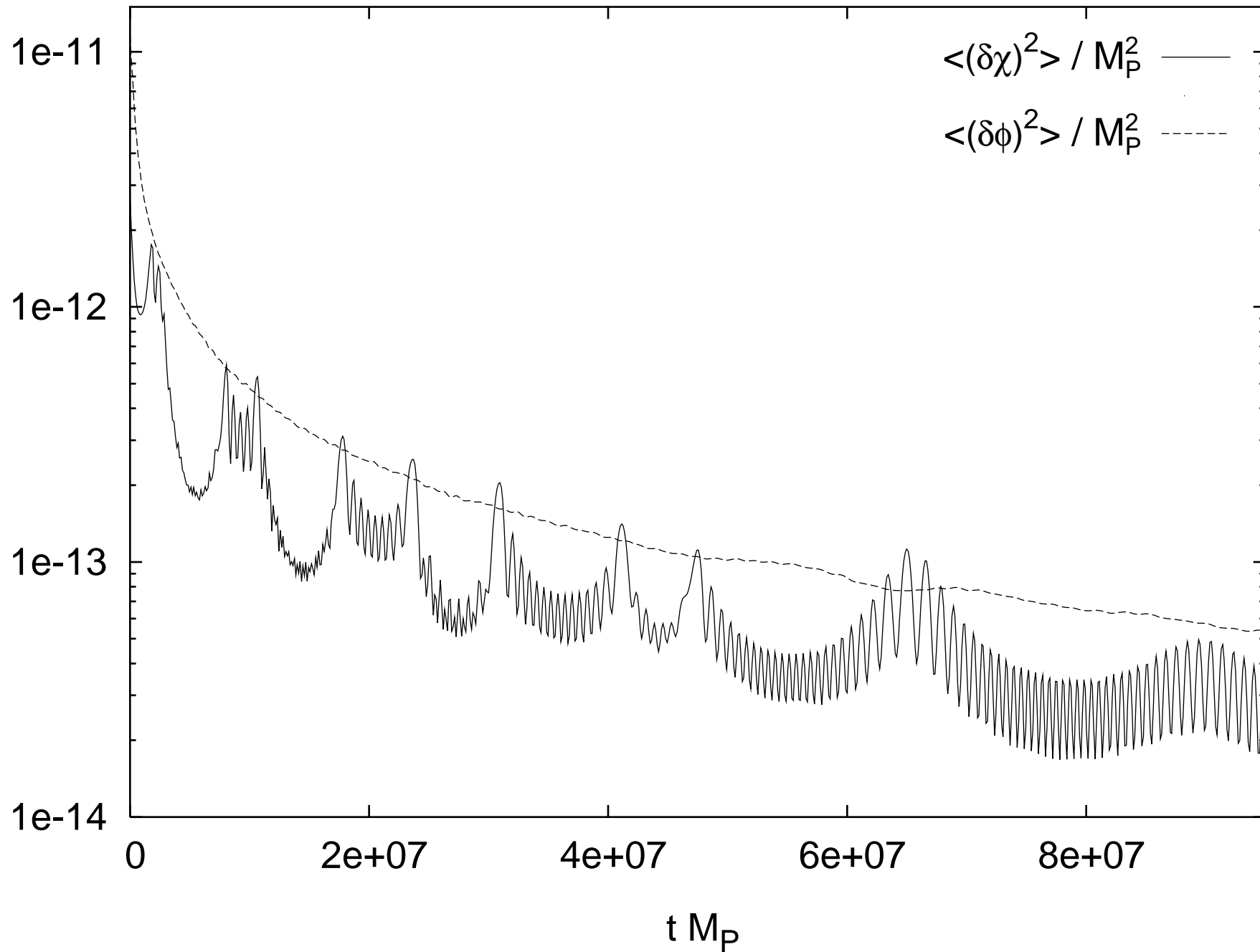


Figure 8(b)

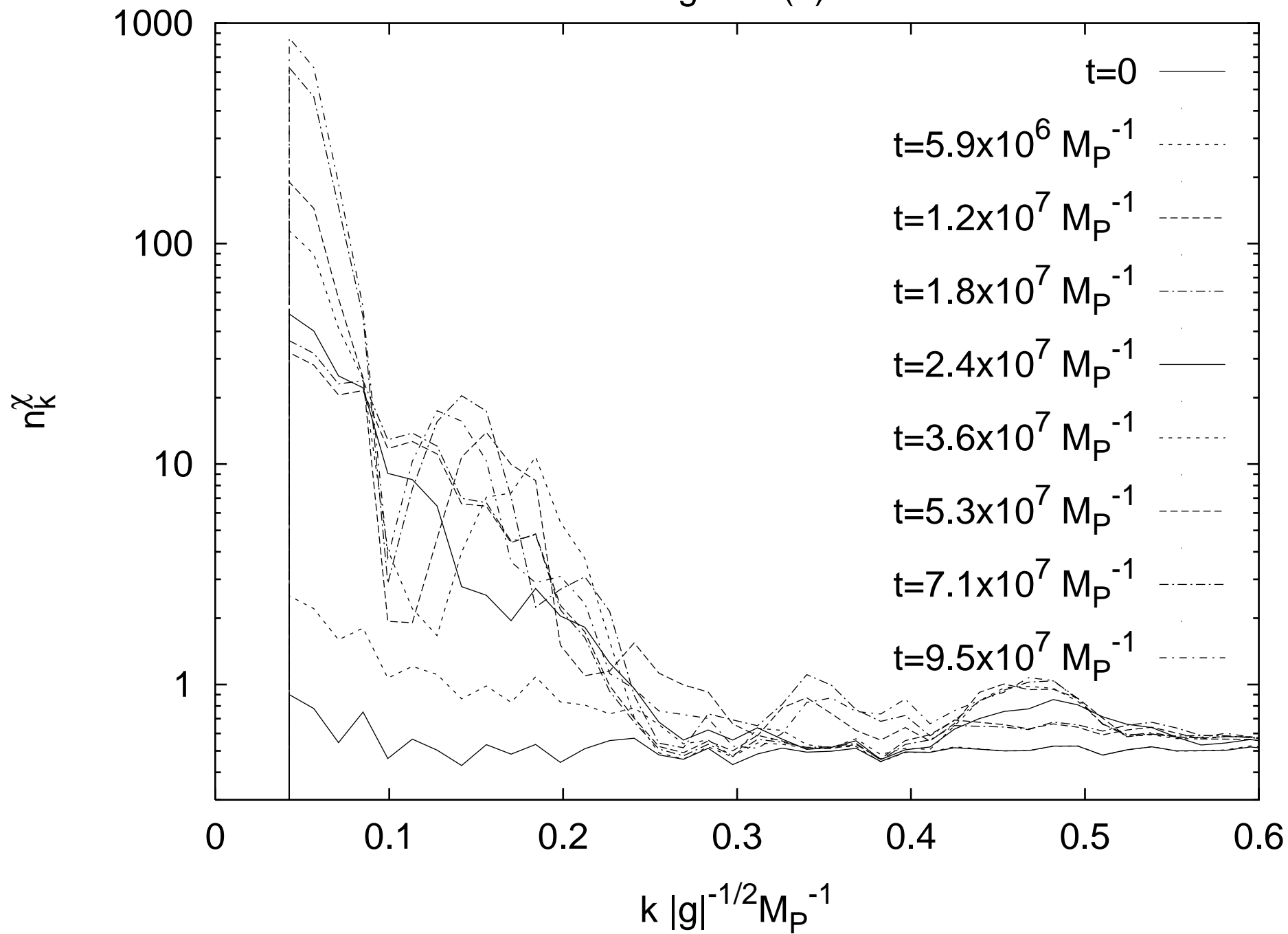


Figure 9(a)

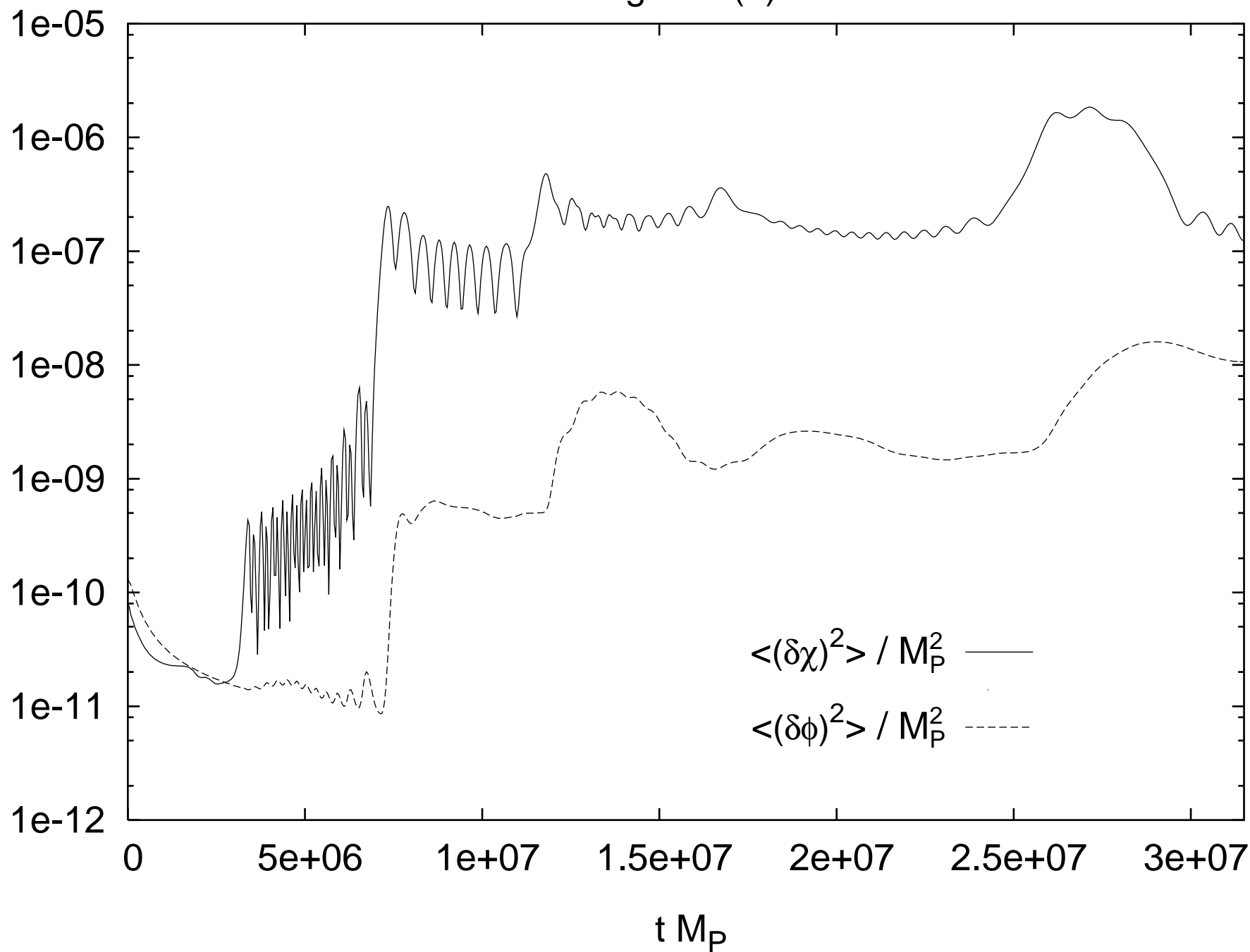


Figure 9(b)

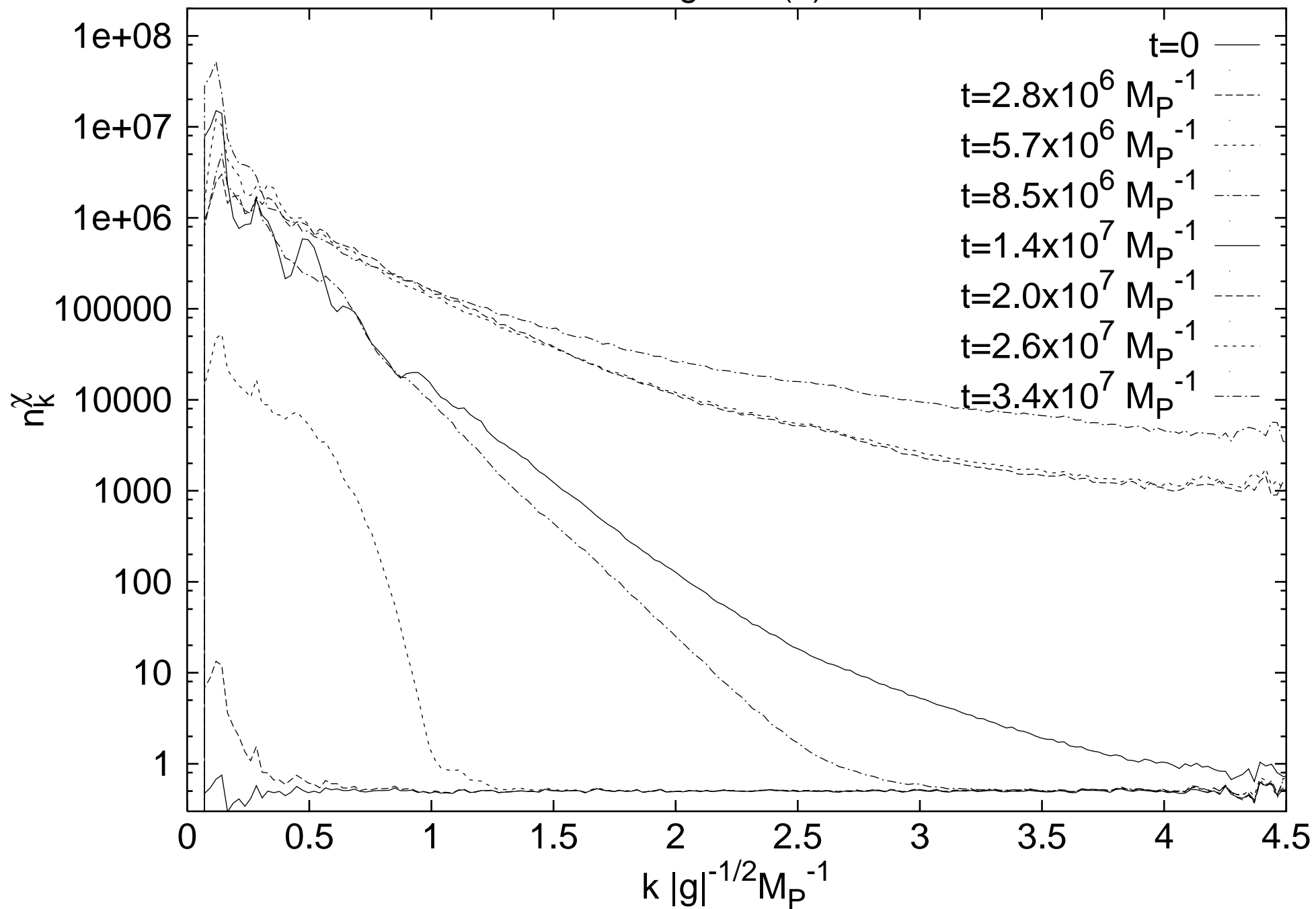


Figure 11(a)

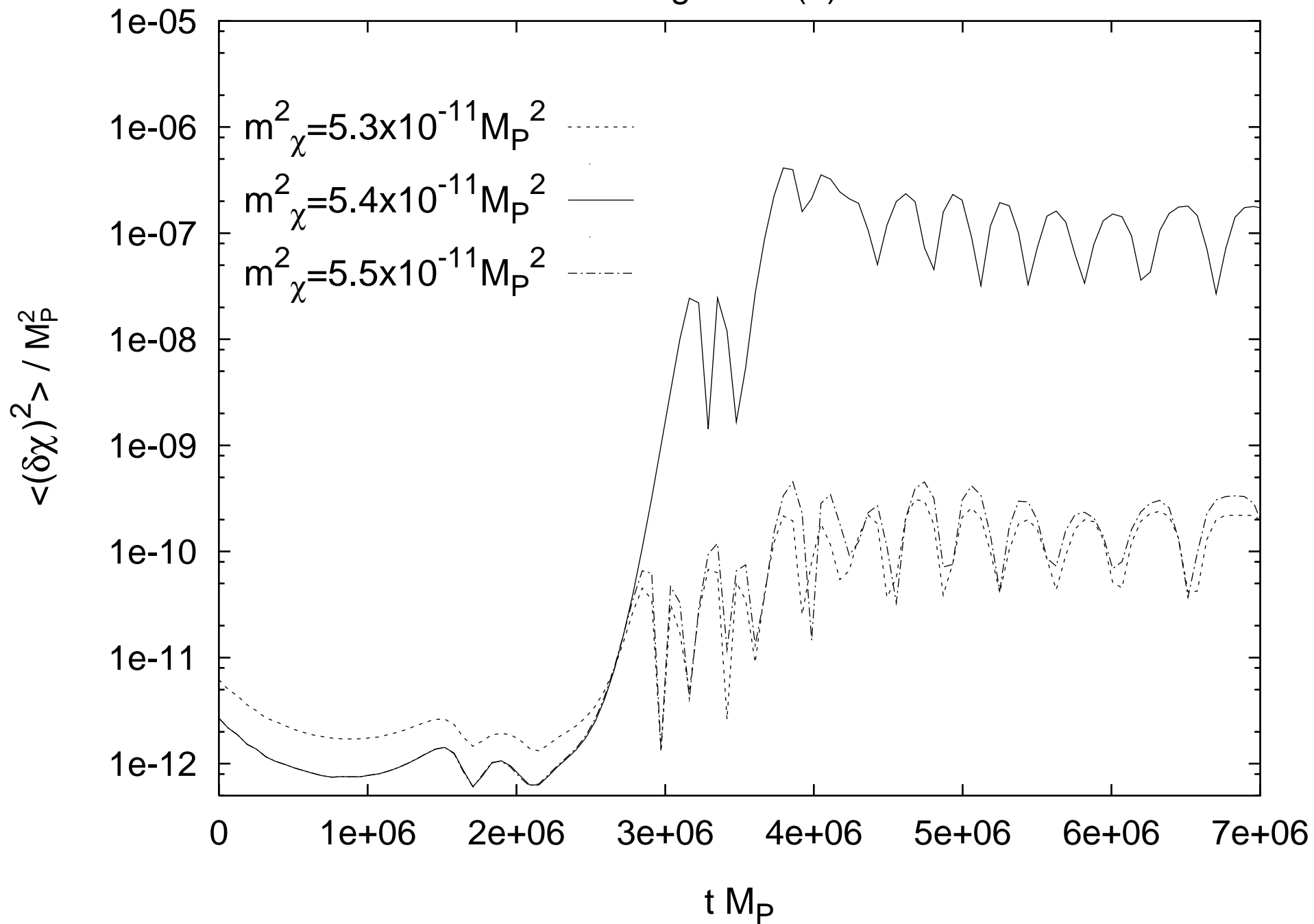


Figure 11(b)

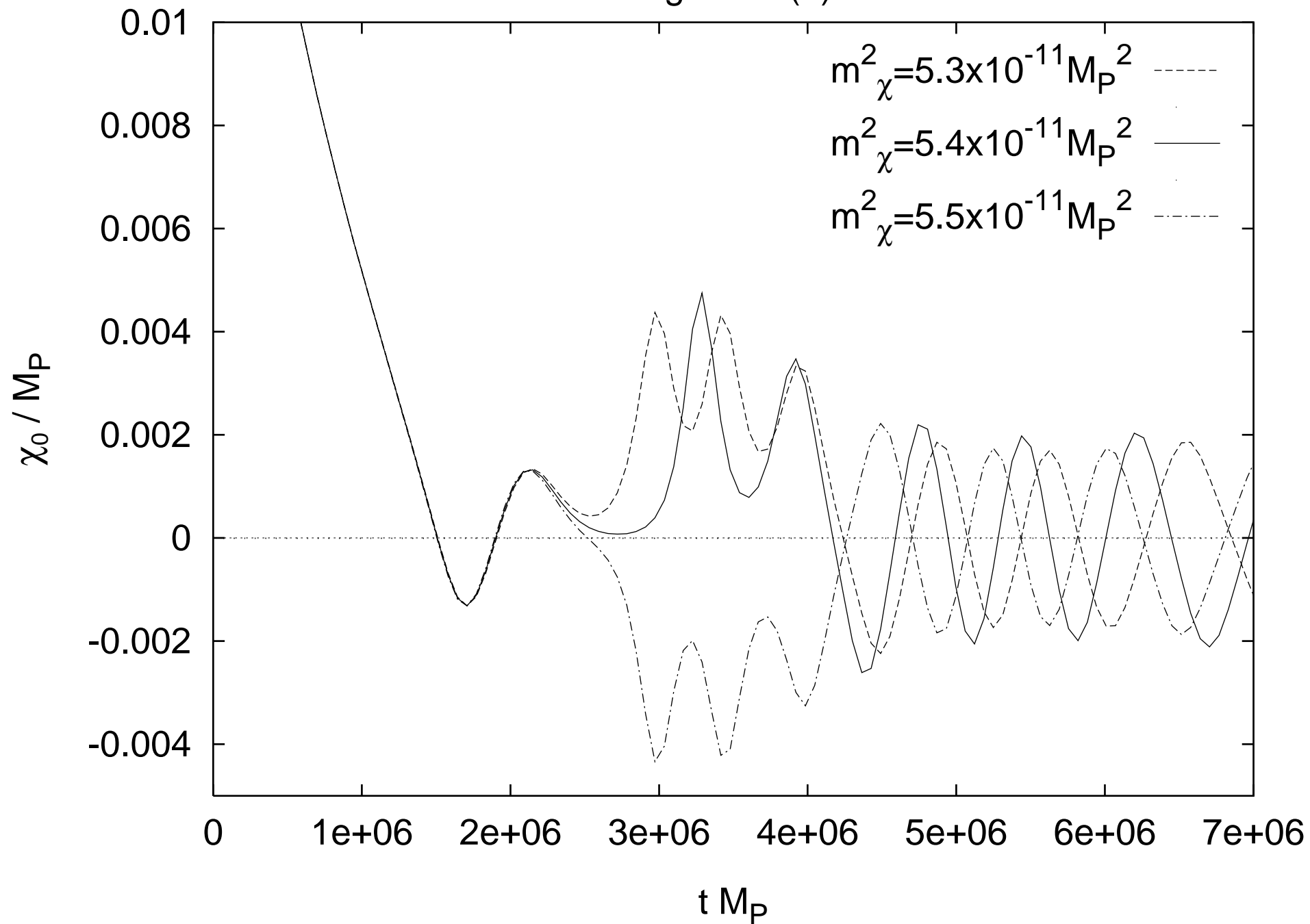


Figure 12(a)

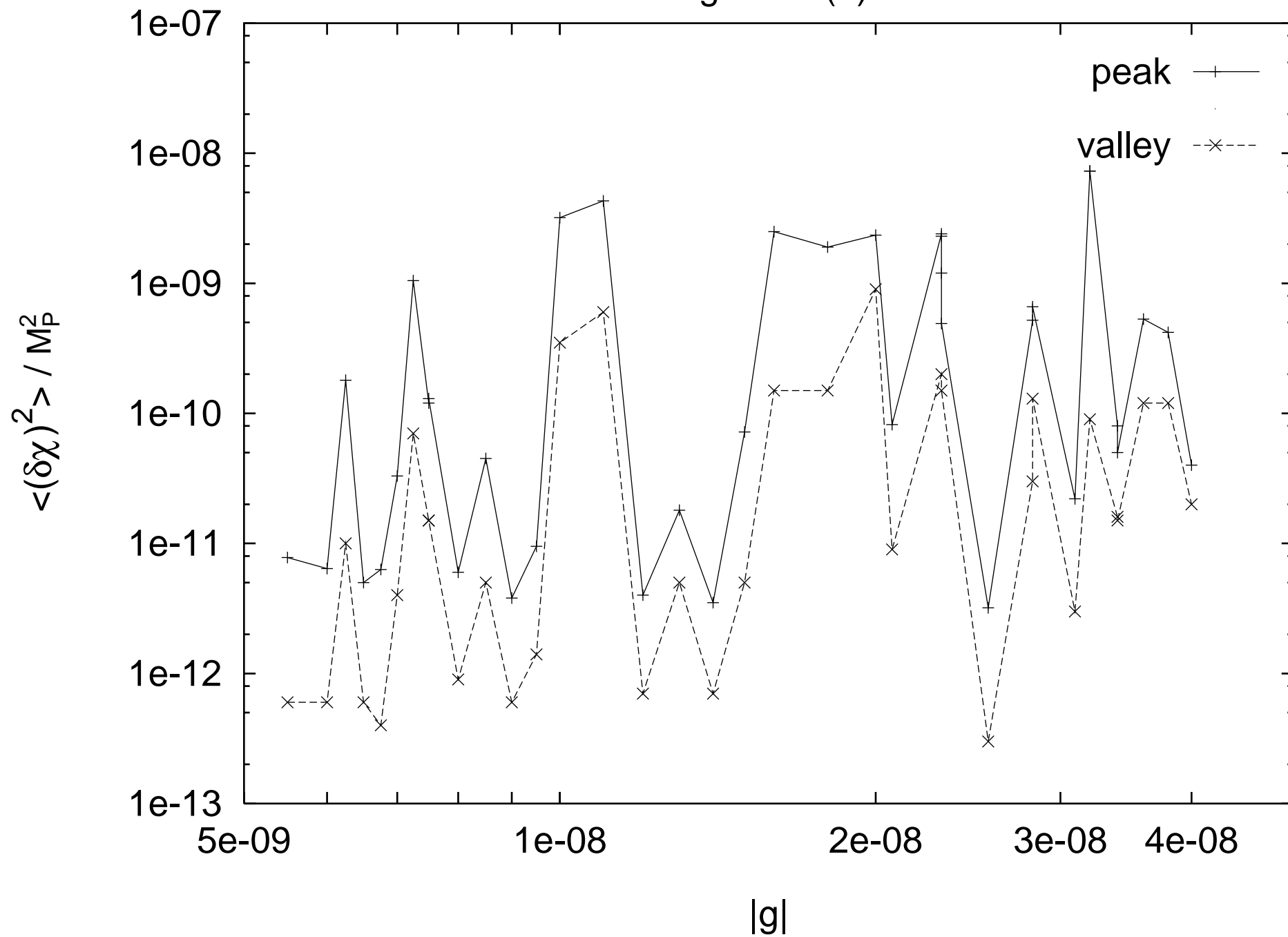


Figure 12(b)

